Challenges and opportunities of vertical flows in long-screened and open borehole wells for quantitative groundwater investigation

David Poulsen

Thesis
Submitted to Flinders University
for the degree of

Doctor of Philosophy

College of Science and Engineering
22 November 2019

Flinders
UNIVERSITY

Declaration

I certify that this thesis does not incorporate without acknowledgment any material previously submitted for a degree or diploma in any other university; and that to the best of my knowledge and belief it does not contain any material previously published or written by another person except where due reference is made in the text.

I am the primary author of this thesis and all manuscripts submitted for publication. I have been primarily responsible for conceptualisation, realisation and documentation of the work. The co-authors on the published papers provided intellectual supervision, editorial content and/or specific technical assistance.

David Poulsen

Acknowledgements

This PhD was undertaken as part of a collaborative project between the National Centre for Groundwater Research and Training (NCGRT) at Flinders University in Adelaide and Rio Tinto Iron Ore (RTIO) in Perth, with a focus on the Pilbara region of Western Australia. Funding was provided by an Australian Government Research Training Program Scholarship, Adelaide and Mount Lofty Ranges Natural Resources Management Board, the Australian Research Council (Linkage Grant LP150100395) and by RTIO.

I am most grateful for the mentoring, valuable advice and important contributions of my supervisor Peter Cook (NCGRT) and co-supervisors Craig Simmons (NCGRT) and Shawan Dogramaci (RTIO). I am also grateful for the specific technical assistance of my colleagues Jim McCallum, Saskia Noorduijn and Daniel Partington, which helped make this research possible. I acknowledge the constructive comments and input from the reviewers engaged during the journal submissions, and thesis examination, which helped to improve the clarity of each manuscript, and the thesis as a whole.

I appreciate the help of NCGRT and RTIO field staff in collecting the data reported in this thesis, in particular Lawrence Burk and Nick White at Flinders University, Dane Upchurch and Mark Dowler at RTIO and Derek Pool of Kinetic (borehole geophysical logging services). In addition, the historical borehole flowmeter data included in Chapter 3 were helpfully provided by Kent Inverarity at the South Australian Department of Environment and Water.

Finally, on a personal note, I am grateful for the moral support and encouragement of my family, friends and colleagues, which helped make the three and a half years of this PhD an enjoyable and positive experience.

Summary

Most of Earths available fresh water is underground, and this groundwater supports diverse natural processes and life forms, including the many needs of humans. Effective evaluation, use and management of groundwater relies on the knowledge developed by interpreting data obtained from boreholes and wells installed into an aquifer system. The degree to which such data are fit-for-purpose depends on the length of the well screen or open interval relative to the aim of investigation. In many real-world situations there is financial and practical incentive to make the most of existing wells, which have a longer-than-ideal screen length (e.g. supply wells). The three bodies of work presented in this thesis extend the knowledge base and approaches available to obtain maximum information from long-screened and open borehole wells in groundwater investigations. The specific contributions are 1) an improved understanding of ambient intraborehole flow in relation to purging and sampling; 2) a novel approach to determine the pumped flow profile in a well using a tracer; and 3) an innovative new way to determine depth-resolved aquifer chemistry by combining knowledge of ambient flows with depth-specific sampling within a well. Each piece of work is placed in the context of the existing literature and offers knowledge that has wide applicability.

Depth-resolved chemistry samples are critical to a wide range of groundwater investigations. If a well intersects zones of variable concentrations, the pumped sample is a composite of the inflows, which mix in the well. Where discrete concentrations are required, excessive mixing makes samples less useful and potentially misleading. An additional risk with sampling such wells that have been left un-pumped is that intraborehole flow, driven by vertical hydraulic head differences, invades part of the aquifer. Three dimensional numerical modelling (Chapter 2) is used to quantify sample bias caused by this ambient flow through a hypothetical un-pumped high-yield well, and the influence of pumping rate and heterogeneity on the volume of pumpage required to purge an invading plume of ambient flow. The modelling shows how sample bias can occur due to an insufficient pumping rate and/or, due to native groundwater displacement by ambient flow invading part of the aquifer when a well is left un-pumped. In particular, the results show that (1) the pumping rate must be at least an order of magnitude greater than the ambient flow rate to achieve permeability-weighted yield, (2) purge volume was 2.2 - 20.6 times larger

than the plume volume, with the ratio depending on plume location relative to hydraulic conductivity and head distributions, and (3) after an example 1,000-day un-pumped period, purging required removal of at least three orders of magnitude more water than the common practice of three to five well volumes. This work demonstrates that it is not feasible to purge the ambient flow plume from around a long-screened well, so samples of pumped discharge will inevitably be biased. It is therefore critical to know the in-well flow regime in ambient conditions and at the pumping rate used for sampling to inform a strategic sampling approach.

In ambient conditions, the in-well vertical flow profile shows the producing and receiving zones of flow driven by the natural vertical head gradient, and thus the relative vertical head gradient in the aquifer system, and potential bias in chemistry samples. A flow profile while pumping can be used to quantify aquifer heterogeneity and the sources of the pumped water mixture. Chapter 3 presents a novel approach to a single-well tracer test to quantify the flow regime in a pumped well, which is unique in its utility over a wide range of discharge rates. During constant pumping, a tracer is injected at the opposite end of the well and, as it is drawn towards the pump, the tracer is diluted in proportion to each inflow. A dilution model using the advection-dispersion equation is used to visually fit a flow profile that explains all tracer profiles (pre-injection, transient phase and steady-state). Results compare favourably to borehole electromagnetic flowmeter data, particularly if tracer density issues are correctly interpreted and head-loss in the flowmeter is avoided. A dimensionless Froude number is provided to assist both with understanding and minimising the role of free convection when planning all types of in-well tracer tests involving a density contrast. Like the flowmeter, this method is particularly suited to screened wells, where packers are ineffective. Used together or separately in existing wells, these in-well methods can provide considerable information on aquifer-well hydraulics.

To avoid the excessive mixing effects and bias caused by ambient flows in long-screened or open borehole wells, Chapter 4 presents an innovative new approach to reliably estimate the chemistry of depth-resolved groundwater inflows. Knowledge of the ambient flow regime is combined with depth-specific samples taken from within a well during ambient and/or pumped conditions. The ambient flow regime is shown to be particularly useful to sample groundwater native to defined inflow zones (head in the zone $>$ head in the well), and avoid zones impacted by the invasion of intraborehole flow (head in the zone $<$ head in the well). Depth-specific samples are interpreted as either native groundwater from a discrete source, subject only to analytical error, or a mixture from multiple sources that can be deconvolved, incorporating error in both flow and concentration measurement. Depth-resolved age tracers (CFCs, ^{14}C and He) in groundwater from three supply wells in the Pilbara region of Western Australia are verified with samples from a multi-depth nest

of piezometers. Results show old groundwater at all depths and the simultaneous occurrence of young water at shallower depths in undisturbed dual-porosity fractured aquifers.

This thesis brings into clear focus the opportunity offered by working with the flow regime within a well to resolve the depth and chemistry of specific inflows, in addition to characterising the intersected aquifer heterogeneity and distribution of hydraulic heads. This approach greatly improves the resolution of the derived information compared to the common practice of only measuring the standing water level, the drawdown induced by pumping and sampling pumped discharge. This is a valuable outcome in many real-world situations, where developing the knowledge to effectively manage groundwater resources is time consuming and expensive.

Contents

List of Figures

List of Tables

Chapter 1

Introduction

1.1 Research problem

The vast majority of Earths available fresh water exists within the pore space of sediment and rocks near the surface. This groundwater supports the flow of rivers and springs and diverse natural ecosystems, and it hosts unique life forms. People around the world interact with groundwater in many ways, from essential water supply for towns and cities, to irrigated agriculture and the needs of mining. Effective evaluation, use and management of groundwater resources rely on investigations beneath the land surface. Although subsurface investigations can be done with remote sensing like airborne or land-based geophysics (e.g. Robinson et al., 2008) or even satellite data (e.g. Lakshmi et al., 2018), invariably ground truthing is required, and most real-world problems need to be investigated in more detail. Physical study of the sub-surface environment requires drilling boreholes, and installation of wells for groundwater investigation. Material properties are directly sampled in drill cuttings or core, and a range of physical characteristics can be inferred over the entire depth of a borehole with geophysical techniques (e.g. Kobr et al., 2005). Some of these are relevant for hydrogeological studies – for example porosity and hydraulic conductivity profiles estimated with nuclear magnetic resonance imaging (Dlubac et al., 2013; Walsh et al., 2013; Behroozmand et al., 2015; Knight et al., 2016).

Once a well is installed in a borehole, or the borehole is left open below a surface casing, it interacts with the surrounding aquifer system over the length of the screened or open interval. Typical hydrogeological measurements – like the standing water level, transmissivity derived from an aquifer pumping test, or water chemistry sampled by pumping a well – are a composite (average) value over this interval. The degree to which such data are fit-for-purpose depends on the length of the well screen relative to the objective of investigation. For example, the classic pumping test analysis to assess aquifer capacity and the extent of induced drawdown uses wells that fully or partially penetrate the aquifer (Freeze and Cherry, 1979; Kruseman and de Ridder, 2000); an investigation of groundwater contamination must use

very short screens (e.g. 1 m) to characterise the extent of the plume and determine flow directions both horizontally and vertically (Einarson, 2006); seawater intrusion is best monitored with multi-depth sampling (Colombani et al., 2016); while studies of groundwater recharge rate assess environmental tracer concentrations at different depths in an aquifer system (Cook and Herczeg, 2000; Cartwright et al., 2017).

Clearly, appropriately designed wells are critical for the success of groundwater investigations. Contamination studies are usually at shallow depths and the cost of properly designed monitoring wells is relatively economical and absolutely necessary. However, for studies at the scale of natural groundwater systems, drilling and installing dedicated monitoring wells is a major expense and effort, particularly when a large vertical interval of an aquifer system needs to be investigated. The cost and effort is magnified in remote areas where access and logistics are more difficult. Therefore, there is a real financial and practical incentive to make the most of available existing groundwater infrastructure. Often this means using wells designed for other purposes (e.g. supply, dewatering, or monitoring whole-of-system effects) that have a longer-than-ideal screen length for groundwater investigations.

Although the straddle packer is an established system to isolate specific depth intervals within a well or borehole (e.g. Holloway and Waddell, 2008; Quinn et al., 2012), it is only effective where an interval can actually be isolated. Packers are mainly used to do hydraulic testing and sampling in smooth walled boreholes or wells that have multiple screens separated by grouted blank casing. Continuous gravel packed screen (common in supply wells) or a rough borehole wall allows vertical flow to bypass a packer, rendering it ineffective or at least causing bias in the results (e.g. Taylor et al., 1990; Nilsson et al., 1995b). In such cases, instead of trying to isolate intervals an alternative approach is to maintain the entire well or borehole as the vertical conduit that it is, and instead work with the vertical flow regime in ambient (un-pumped) and pumped conditions. Changes of flow rate with depth in a well are related to the intersected distribution of hydraulic conductivity and heads (Paillet, 1998, 2000, 2001; Day-Lewis et al., 2011; Sawdey and Reeve, 2012; Halford, 2009). This analysis can be particularly valuable when combined with other geophysical data and standard aquifer pumping tests (e.g. Paillet and Reese, 2000).

Accurate sampling is a particular challenge in wells that intersect stratified water chemistry. At best a normal pumped sample is a composite of aquifer concentrations intersected by a well (McCallum et al., 2017), while at worst the sample could be biased such that a parameter of interest is underestimated, overestimated or missed entirely (McIlvride and Rector, 1988; Einarson, 2006). This bias is known to be caused both by mixing of individual inflows in the well, and because groundwater native to the lowest head zone intersected by the well is often not sampled. This occurs because, when a well is left un-pumped, head-driven vertical flow invades

the lowest head zone, displacing the native groundwater (Reilly et al., 1989; Lacombe et al., 1995; Konikow and Hornberger, 2006; Mayo, 2010). So when the well is pumped, inflows from that lowest head zone actually originate from the highest head zone. Although this ambient intraborehole flow problem is known, its effect on purging and sampling a well had not been systematically explored in the literature prior to this work. Even if packers can be used for discrete depth sampling in a well, it is still necessary to measure the ambient vertical flow regime so that zones impacted by invading intraborehole flow can be identified and purged or avoided in sampling. For situations where the effectiveness of packers is compromised, a range of alternative depth-resolved sampling approaches have been explored (Jones and Lerner, 1995; Lerner and Teutsch, 1995; Nilsson et al., 1995b,a; Collar and Mock, 1997; Izbicki et al., 1999; Sukop, 2000; Izbicki, 2004; Harte, 2013). The most practical, reliable and widely used the approach first reported by Collar and Mock (1997), in which depth-specific samples and measurements of vertical flow rate before and after inflowing zones are combined in a mass balance to identify the concentration of inflowing groundwater. This approach has been applied almost exclusively in operational supply wells, where all inflows were groundwater native to the source intervals. Prior to the research presented in this thesis the literature lacked a paper presenting the benefits of depth-resolved sampling in, and with consideration to, the ambient flow regime in wells that are not always pumped.

The head differences between intervals of an aquifer system connected by a well commonly drive vertical flow through the well when it is not being pumped. Even small differences of head can drive significant flow, so ambient vertical flows are very common (Elçi et al., 2003, 2001). Wells usually intersect a much greater range of heads vertically over their screen length than horizontally across their diameter. This, together with the fact that the hydraulic conductivity of the well itself is effectively infinite compared to any aquifer material, means that vertical flow in a well usually completely overwhelms any horizontal flow (Gailey, 2017). For this reason attempts to measure horizontal flows (aquifer pore velocity) have largely been ineffective (Wilson et al., 2001), unless the well has a short screen and vertical head differences are minimal (Pitrak et al., 2007; Brouyère et al., 2008).

A borehole flowmeter is the most direct, practical and widely used tool for measuring vertical flow rates within a well. These instruments (impeller, heat pulse or electromagnetic (EM)) are operated on a braided stainless steel cable containing power and communication wires connecting the controller at the surface to the sensor in the well (known as a wireline). A flowmeter is a specialised piece of equipment, usually mounted on a dedicated logging vehicle, and as such they are not always financially or practically accessible. Flowmeters also suffer a range of issues including lack of sensitivity to low flows, high flows or an inability to measure a wide range of flow rates in a single pass (Arnold and Molz, 2000; Zlotnik and Zurbuchen,

2003; Paillet, 2004a; Newhouse et al., 2005; Clemo et al., 2009).

An alternative to the borehole flowmeter involves using a solute or heat tracer to observe the flow regime in the well. This requires inversion of measured tracer concentrations into flow rate by tracking the movement of a concentration or temperature interface, or by explaining tracer dilution in terms of flow rate. A range of single-well tracer tests exist, using either a solute (e.g. Tsang et al., 1990; Izbicki et al., 1999; Brainerd and Robbins, 2004; Maurice et al., 2011; Paillet, 2012; Chlebica and Robbins, 2013; Libby and Robbins, 2014) or heat (e.g. Banks et al., 2014; Leaf et al., 2012; Sellwood et al., 2015) as a tracer. But prior to this research there was a distinct lack of an efficient and accessible tracer method to reliably provide a profile of pumped flow rates in high yield supply wells, like those typical of our remote field site in the Pilbara region of Western Australia.

1.2 Research aim

The purpose of this research is to obtain more reliable and useful hydrogeological information from long-screened wells and long open borehole wells. This thesis explores the challenges and opportunities offered by working with the vertical flow regime within a well, with a particular focus on sampling chemistry from wells that have been left un-pumped. The aim was to address three specific knowledge gaps, identified after careful consideration of the existing literature and the practical challenges of using long-screened wells in groundwater investigations. The relevant existing knowledge base is summarised in the introduction to each of the three bodies of work.

The knowledge gaps and associated research aims addressed in this thesis are summarised as follows:

1. Although the problem caused by ambient vertical flows is clearly established, the effect on sample composition and the purge volume required to remove the invading plume remained uncertain. Therefore the first aim was to quantify the effect of intraborehole flow on purging and sampling long-screened and open borehole wells with a numerical simulation model. This provides a sound basis for using the vertical flow regime to inform a targeted sampling approach in such wells.

2. Borehole flowmeter is an established tool for measuring the vertical flow regime within a well. However, it is not without issues, and it is a specialised piece of equipment that is not necessarily available in all situations. So the second aim was to develop a method to identify the pumped flow regime in a well using a readily available tracer and downhole sonde combination. This provides an alternative to the borehole flowmeter that does not require expensive

specialised equipment (although it does require some specialised knowledge). It also provides a complementary line of evidence to improve resolution of the flow regime.

3. Finally, the ultimate aim of this research was to devise and verify a way to obtain reliable depth-resolved samples from wells with long screened or open intervals, particularly those that have been left un-pumped. This is directly relevant to the field site used for this research in the Pilbara region of northern Western Australia, where most available wells are long-screened, and environmental tracers are being used to study groundwater recharge rates and the structure of the flow systems.

These aims are addressed in order in Chapters 2, 3 and 4 of this thesis, and each is also a manuscript submitted for publication in respected international journals. At the time of writing, the first two papers are published and the third is in the peer review process, as identified at the start of each chapter. These main bodies of work were also the subject of three professional conference oral presentations, as detailed in Appendix A.

1.3 Contribution of this PhD

This PhD makes three related contributions towards doing better science with long-screened and open borehole wells. The modelling study described in Chapter 2 brings a more quantitative understanding of the effect of intraborehole flow on purging and sampling and it sets the scene for the second two contributions. Chapter 3 provides an alternative and complementary method to the borehole flowmeter for determining the vertical flow regime in a pumped well. While Chapter 4 brings into clear focus the opportunity offered by working with the flow regime within the well to resolve the depth and chemistry of specific inflows. These contributions directly improve the quality of hydrogeological knowledge derived from a unique research program in the Pilbara region of Western Australia. The concepts are also broadly applicable to all situations where heterogeneous aquifer properties, heads and/or water chemistry intersected by a well need to be better understood. Long-screened and open borehole wells are not a substitute for purpose-built monitoring wells but, where they already exist, they can provide valuable information with a little extra work and appropriate methods. The approaches presented in this thesis help to improve the return on investment of existing infrastructure and they also help to minimise the need for, and hence the cost, effort and impact of any new installations, required to target depth intervals that remain un-sampled.

Chapter 2

Effects of intraborehole flow on purging and sampling long-screened or open borehole wells

Published in *Groundwater*: Poulsen, D.L., P.G. Cook, C.T. Simmons, J.L. McCallum and S. Dogramaci (2018). Effects of intraborehole flow on purging and sampling long-screened or open wells. doi: 10.1111/gwat.12797.

2.1 Introduction

Vertical hydraulic head gradients are ubiquitous in groundwater systems. Thus, if a well has an appreciable screen length or open interval, the groundwater inflow distribution during pumping will be a function of the hydraulic head and conductivity distribution across the screened or open interval. A sample may not be drawn from the whole interval in proportion to the permeability distribution unless the pumping rate is high enough to overcome the influence of the head gradient (McMillan et al., 2014). Further, if the well is left un-pumped, it creates a short circuit for vertical flows between permeable zones connected by the well. This phenomenon is known as intraborehole flow (IBF) and it can significantly influence the flow system chemistry in the local area within and around a well. Over time, a plume of invading water (herein termed the "IBF plume") develops in zones with lower head, displacing native groundwater. When the well is pumped, water produced from zones at lower heads actually originated from zones with higher heads.

Previous work has established that IBF is an important factor to consider when sampling wells that have been left un-pumped, even in relatively homogeneous aquifers with small vertical head gradients (Church and Granato, 1996; Elçi et al., 2001; Lerner and Teutsch, 1995; Reilly et al., 1989). An indication of its prevalence

is given by Elçi et al. (2003), who reported measurable IBF (0.01 to 6.2 l/ min) in 73% of tested wells (142 monitoring wells at 16 sites across the USA).

Water sampled from a well is an inflow-weighted mixture from all contributing zones. Aside from the challenge of correctly apportioning water composition to each zone, the presence of an IBF plume around a well can further complicate interpretation of chemical analyses(Collar and Mock, 1997; Ma et al., 2011; Reilly and LeBlanc, 1998), either exacerbate or mask the presence of a contaminant (Hutchins and Acree, 2000; Konikow and Hornberger, 2006; Lacombe et al., 1995) and substantially alter the mix of groundwater ages sampled (Corcho Alvarado et al., 2009; Zinn and Konikow, 2007). If a long screened or open well is left un-pumped, it could take a long time to fully purge the resulting IBF plume so the well yields native groundwater from all contributing zones (Jones and Lerner, 1995; Mayo, 2010).

Although a nest of short-screened monitoring wells is preferred to secure accurate samples, this is an expensive installation. Despite potential complications arising from IBF, use of available infrastructure is the economical approach to study a groundwater system. Environmental tracer studies attempting to characterise groundwater flow systems may use wells that were installed for different purposes, which have a longer-than-ideal screen length (e.g. Cook et al., 2017). In such a situation, it would be helpful to assign tracer concentrations to specific depths in the aquifer. If the well has been left un-pumped, it is also important to properly consider the effects of the IBF regime on the sample. Failure to do so could result in erroneous conclusions and unrealised potential for better understanding of a groundwater flow system. Whether or not purging an IBF plume is feasible, it is important to understand the true origins of the water mixture being sampled, in addition to knowing the zones that contribute to the sample. However, there is little published literature on improving the quality of data and knowledge obtained from high-yield long-screened wells.

This paper characterises the effects of IBF on purging and sampling of a long-screened well, and provides insight that can be used to develop an informed sampling approach. A numerical model is used to highlight the importance of understanding the borehole flow regime, the location and extent of an IBF plume, and the sampled water mixture at the chosen pumping rate. The focus is on a homogeneous aquifer as a "base case", but the principles also apply to heterogeneous systems of porous media or fractured rock. An example of variability due to aquifer heterogeneity is included, as are some practical considerations for improving purging and sampling strategies.

2.2 Methods

2.2.1 Conceptual model

A three dimensional, synthetic regional groundwater flow system was used to investigate the effects of IBF on sampled groundwater mixtures from a long-screened, high-yield well in a recharge area (Figure 2.1). Groundwater age was used as a convenient way to identify water from different depths, with recharge assigned an age of zero and age naturally increasing with depth in the aquifer. However, with the non-zero, graduated background concentrations in the age simulation, the exact spatial extent of IBF in the aquifer and its subsequent contribution to well pumpage was not always clear. Therefore, IBF was also tracked explicitly in a separate simulation by setting the background concentration to zero and assigning a constant concentration (of one) to all water leaving the well. Thus, the fraction of IBF in each model cell and in water sampled from the well was quantified. The flow system was created by applying recharge across the top of the model and setting a constant-head boundary of 0 m on the right hand side, analogous to a spring or river at the land surface. Groundwater flows from left to right through the model. The land surface was assigned a 13.5 m elevation to ensure that the water table was completely within the model domain, allowing for unconfined conditions to occur. All lateral sides and the bottom of the model are no-flow boundaries. A long-screened well was positioned centrally 105 m from the left hand side of the model, in an area with a downward vertical flow component. With a 0.2-m diameter, 36-m-long screen (from -1.5 to -37.5 m), the well was similar in construction to production wells that may be co-opted for water chemistry sampling. The model grid was refined to 1.5 m horizontally near the well, geometrically increasing to a maximum size of 15 m. All 50 model layers are 1.5 m thick. Table 2.1 gives the model dimensions and parameters.

The model design is loosely based on that of Reilly et al. (1989) and Konikow and Hornberger (2006) with regard to the general model dimensions, position of the multi-node well, constant-head boundary, amount of recharge, and anisotropy ratio. Differences include simulation of the water table, a longer well screen, slightly less grid refinement (as explained below), and reduced overall hydraulic conductivity (K). Another significant difference is that the previous studies did not pump the well except to obtain a sample, whereas in this study the well was pumped with the goal of purging the IBF plume. As a consequence, small boundary effects were observed in the model during pumping. For example in the homogenous system, at the completion of purging there was 0.8 m head drawdown at the lateral and up-gradient boundaries. This resulted in relatively more water being drawn from the down-gradient area, in which most of the IBF plume resided. Although purge volume to remove the IBF plume was slightly less than a no-boundary-effect situation, the key concepts and outcomes demonstrated in this paper are unaffected.

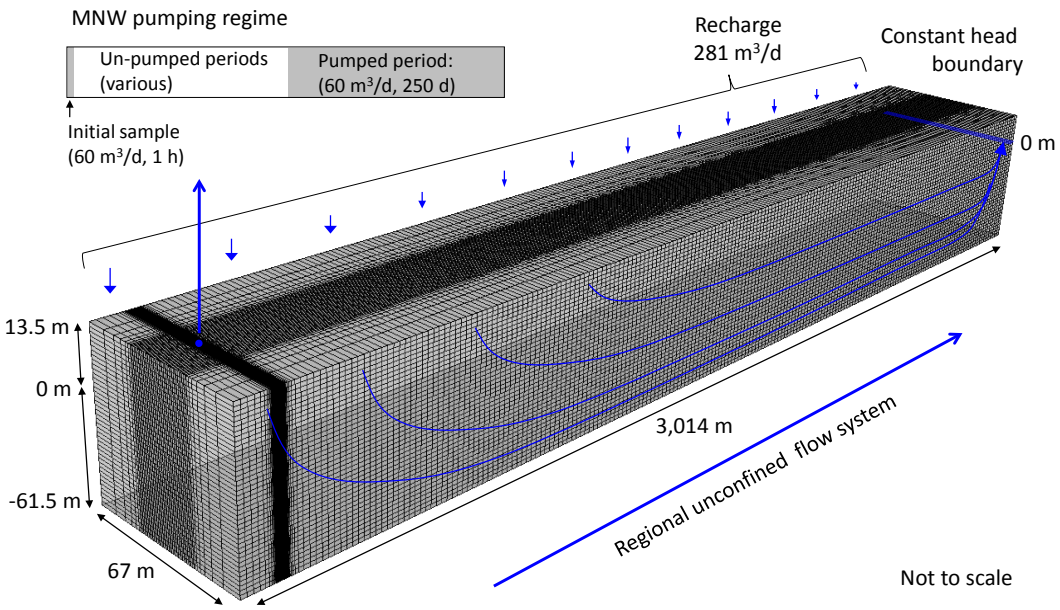

Figure 2.1: Diagram of model dimensions, sources and sinks and the multi-node well pumping regime over the duration of the simulation.

Parameter	Value
MODFLOW	
Refined grid size (m)	1.5
Default grid size (m)	15
Layer thickness (m)	1.5
Anisotropy ratio (Kh/Kv)	5
Well radius (m)	0.1
Well skin radius (m)	0.3
Well skin hydraulic conductivity (m/d)	6
Storativity	1×10^{-5}
Specific yield	0.15
Recharge rate (m/d)	0.00139
MT3DMS	
Effective porosity	0.25
Zero order reaction rate	1/365.25
Longitudinal dispersivity (m)	1.5
Horizontal transverse dispersivity ratio	0.1
Vertical transverse dispersivity ratio	0.01
Self-diffusion coefficient, water (m^2/d)	1×10^{-4}

Table 2.1: Model dimensions and universal parameters for MODFLOW to simulate intraborehole flow using the MNW2 multi-node well package, and MT3DMS to directly simulate groundwater age.

2.2.2 Numerical simulation

Steady-state and transient flow was simulated in three dimensions using the MODFLOW 2005 (Harbaugh, 2005) computer code, with a long-screened well represented by the Multi-Node Well Package (MNW2) (Konikow et al., 2009). Groundwater movement was tracked in two ways using MT3DMS (Zheng, 2010; Zheng and Wang, 1999): (1) direct simulation of groundwater age with a zero order reaction was used to examine the effects of IBF on groundwater age, and (2) the code was modified to assign a constant concentration of one to all water leaving the well, thereby identifying the fraction of IBF in each model cell and in the resulting pumped discharge. MT3D assigns a single composite solute concentration for the well, based on the flux-weighted concentrations of inflows, so differential solute movement through the well was not simulated. The flow and transport models were developed, executed and post-processed with the Python FloPy package (Bakker et al., 2016).

Steady-state groundwater head and age distribution (without the well) were used as initial conditions for transient simulations. Transient simulations included stress periods for sampling the well immediately after installation (pumping for 1 hr at $60\,m^3/d$), an un-pumped period (nominally 1000 days), followed by pumping at $60\,m^3/d$ until the IBF plume was fully purged (Figure 2.1). Full purging was taken to be the point when the composite age of the sample was again equal to the age immediately after well installation.

The flow equations were solved using the Preconditioned Conjugate Gradient solver, achieving a 1×10^{-5} m head change and residual convergence criterion. A limit on model convergence was a function of the cell-to-well conductance (CWC) term calculated by the MNW2 package. This term governs interaction of a well node with the local model cell because the volumetric flux between the two is a multiple of CWC and head difference. All else being equal, CWC increases as model cell size decreases, and MODFLOW can become numerically unstable when cell size approaches the specified well diameter (Halford and Hanson, 2002). Konikow and Hornberger (2006) used 0.75 m cells near the well, but here it was increased to 1.5 m to improve numerical stability for the heterogeneous systems. This change did not significantly affect model results, but it illustrates a limitation of the MNW2 package when simulating a long-screened well. The CWC value is also a function of the K of the well skin (K_{skin}), an assessment of which is provided below in the context of IBF.

The standard finite difference method in MT3DMS was used for solute transport simulation. With a longitudinal dispersivity of 1.5 m and characteristic length of 1.5 m (grid Peclet number = 1), numerical dispersion was not an issue (Anderson and Woessner, 2002; Zheng and Wang, 1999). This longitudinal dispersivity value is appropriate for an observation scale of tens to hundreds of metres (Gelhar et al., 1992), which is consistent with the extent of the simulated IBF plumes.

2.2.3 Hydraulic conductivity

The "base-case" model was assigned a homogeneous K distribution of 10 m/d. Vertical K was assigned to be five times lower than horizontal K. To test the effect of aquifer heterogeneity on the development and purging of an IBF plume, two horizontal model layers (1.5 m thick) intersecting the well were systematically assigned various higher K combinations over three orders of magnitude. The layers were positioned near the extremities of the range of aquifer hydraulic heads intersected by the well. Each layer extended throughout the model domain. This simple approach allowed an exploratory study of factors controlling potential variability in IBF plume extent and purge times, without requiring exhaustive stochastic modelling of a fully heterogeneous aquifer, which was beyond the scope of this paper.

2.2.4 Well skin

The well skin parameter in the MNW2 package allows the influence of the well screen, borehole annulus and surrounding disturbed zone to be simulated. The well skin can be a reduced K zone due to aquifer disturbance and/or a restrictive well screen (well losses), or an enhanced K zone where a gravel pack effectively increases the well diameter and/or fines are washed out of the surrounding aquifer during well development. A negligible skin zone was intended in this modelling exercise (K_{skin} =K), but the model would not converge when Kskin was more than 60% of K due to excessive cell-to-well conductance. Thus, for all modelled scenarios, K_{skin} = 6 m/d. The effect of the well skin on IBF rate was tested by applying a range of K_{skin} values in models with different homogeneous K (Figure 2.2). IBF is driven by the vertical head gradient, which is governed by K and recharge, and it approaches an upper limit as K_{skin} approaches K (0.68 m^3/d in the homogeneous system). For a given K_{skin} , increasing K reduces the vertical hydraulic gradient, and thus reduces IBF. However, the primary concern here was not the factors controlling IBF, but rather its influence on purging and sampling a well. Therefore, it was sufficient that a range of IBF rates were generated.

2.3 Results

The homogeneous regional flow system had an overall horizontal hydraulic gradient of 0.0036 toward the constant head boundary "at the surface" on the right hand side. Vertical gradients were downward on the left hand side of the model, negligible through the central area, and upward to the discharge feature. At the location of the well, the downward vertical gradient was 0.00014 over the 36 m screened interval. The standing water level in the well was 10.465 m. In comparison, aquifer head at the top of the well was 10.469 m and at the bottom of the well it was 10.464 m. That

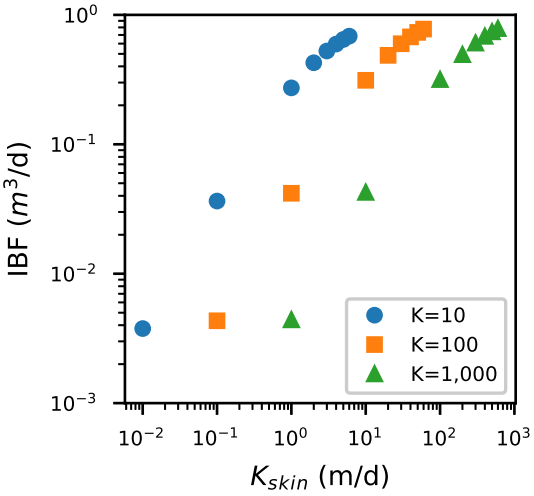

Figure 2.2: Relationship between well skin hydraulic conductivity (K_{skin}) and IBF for three different aquifer hydraulic conductivities (K).

is, aquifer head was greater than well head in the top half of the well, and vice versa in the lower half, and this downward vertical head gradient drove IBF through the well. During pumping (60 m^3/d) there was minimal water level difference between aquifer and well (0.05 m), which showed that well losses were minimal. Drawdown in the well was 0.86 m at the completion of purging.

2.3.1 Intraborehole flow

If the well is left un-pumped, a plume of IBF develops in the zone with lower head, driven by the vertical hydraulic gradient. For example, in the homogeneous system a head difference of just 5 mm between the top and bottom of the screen was sufficient to drive downward IBF of 0.68 m^3/d (0.47 l/min). These results are shown in Figure 2.3a, as the borehole flow profile in the well – negative values denote downward flow, increasingly negative values with depth indicate inflow and decreasingly negative values with depth indicate outflow to the aquifer. The IBF rate is given as the maximum absolute value reached on the x-axis. Flow in the well is zero at the top and bottom of the screen because it is not being pumped.

Figure 2.3b shows groundwater age after a 1000-day (2.7-year) un-pumped period, during which 680 m^3 of IBF has occurred. This longitudinal cross-section at the well location shows the IBF plume extending several tens of metres into the aquifer. A plume of younger (shallower) water was introduced into a zone with otherwise older (deeper) groundwater. The composite age of IBF is 12.1 years, compared to native groundwater in the receiving zone of 30 to 50 years. The extent of the IBF plume (indicated by the black polygon in Figures 2.3b and 2.4b) was defined by the model cells containing at least 1% IBF by volume. The full extent of the IBF plume is not apparent in the groundwater age distribution mainly because of the limited ability of a graduated colour-map to show subtle age changes as the IBF water is increasingly diluted.

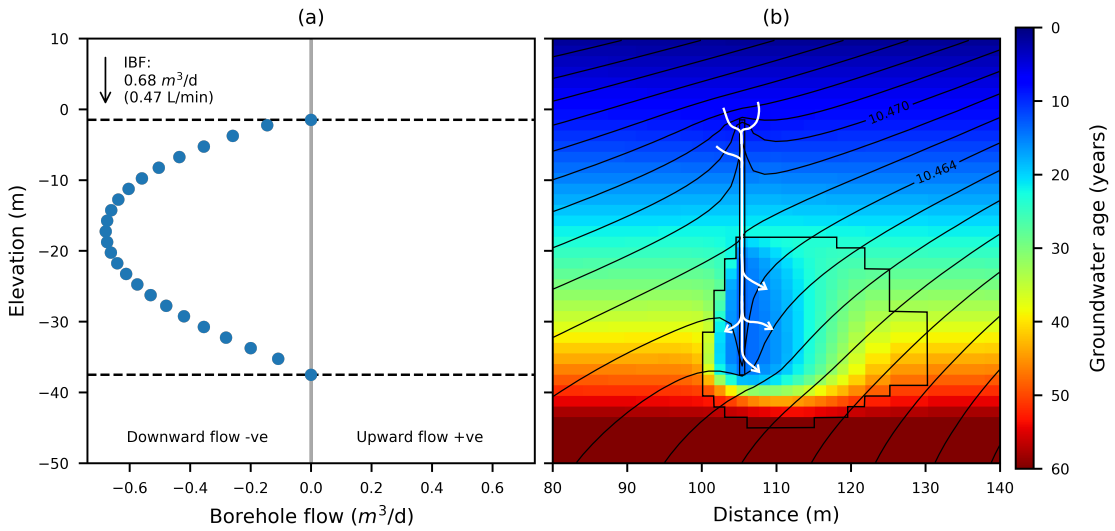

Figure 2.3: (a) Borehole flow profile and (b) longitudinal cross-section at the well showing head contours (interval = 0.002 m), flow lines through the well (white arrows), groundwater age, and extent of the IBF plume (black polygon) after a 1000-day un-pumped period (homogeneous system). Dashed lines indicate the screened interval.

2.3.2 Pumping rate

When a well is pumped, inflow is a function of K and the local head gradient between aquifer and well. In this homogeneous aquifer, there is potential for uniform inflow over the whole screened interval. But to achieve this, the pumping rate must be high enough to overcome the vertical head gradient and make K the limiting factor. For example, Figure 2.4a shows a permeability-weighted borehole flow profile, with flow increasing almost linearly from zero at the bottom to the pumping rate (60 m^3/d) at the top of the screen. But as the pumping rate was reduced the flow profile became increasingly non-linear as it was increasingly influenced by the vertical head gradient in the aquifer (Figure 2.5). The threshold for negligible head influence in the inflow profile was at a pumping rate of about 14.4 m^3/d (10 l/min) in this model. When the pumping rate was similar to the IBF rate (0.68 m^3/d), all flow was sourced from the higher head zone in the upper part of the screen, while at the same time some downward IBF continued. For reference, Figure 2.5 includes the un-pumped profile, when the natural head gradient fully controlled flow in the well.

2.3.3 Purging an intraborehole flow plume

The volume of water forming a plume in the zone of lower hydraulic head is given by multiplying the IBF rate by the length of time the well is un-pumped. However, Figure 2.4 illustrates two key reasons why purging an IBF plume requires pumping a much larger volume of water than the volume of the plume itself. First, some parts of the screen still yield native groundwater, so IBF is only a fraction of pumped water. Second, the IBF plume is skewed in the direction of regional groundwater

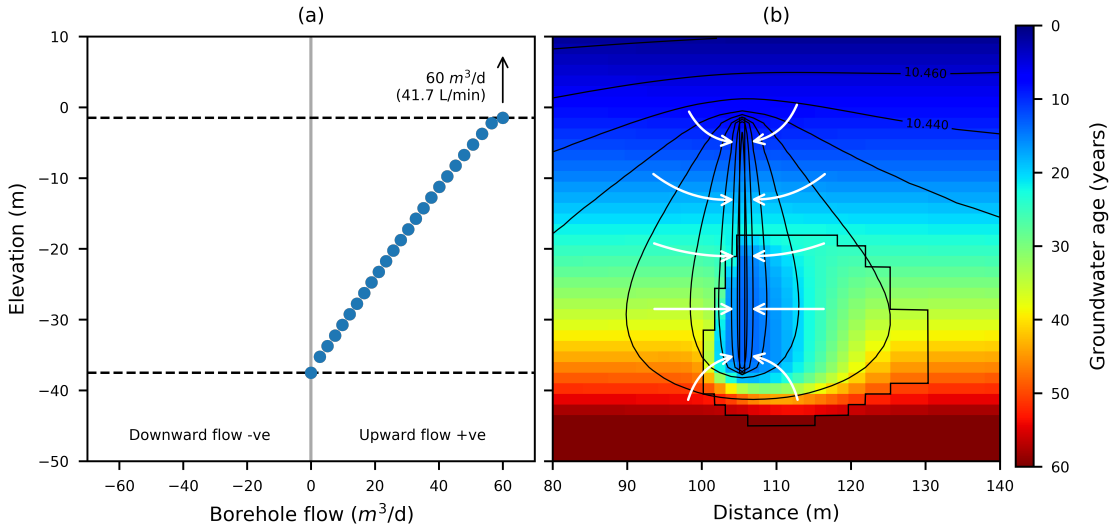

Figure 2.4: Figure 4: (a) Borehole flow profile and (b) longitudinal cross-section at the well showing head contours (interval = 0.02 m), flow lines to the well (white arrows), groundwater age, and extent of the IBF plume (black polygon), upon commencement of pumping after a 1000-day un-pumped period (homogeneous system). Dashed lines indicate the screened interval.

flow, so the up-gradient area will purge sooner than down gradient.

Figure 2.6 shows the evolution of IBF in pumpage, as a fraction of sample volume, and the composite age of the sample during purging after the well is left un-pumped. With no un-pumped period, there is no IBF fraction and the sampled age is the same as the initial age for a few hundred well volumes, after which it slowly increases, as pumping alters the flow field in the area around the well and draws in more older water. With a 1000-day un-pumped period, the sample initially contains just under 50% IBF and sample age is reduced by 40%. Purging of about 3000 well volumes (4500 m^3) is required for sample age to return to the initial age, at which point about 4% IBF remains in the sample. This apparent contradiction simply illustrates that the composite age mixture is not unique, and a slightly higher proportion of older water in pumpage causes the sample age to equal the initial age before the IBF plume is completely removed. This purge volume is 6.6 times the actual volume of IBF of 680 m^3 (0.68 m^3/d for 1,000 days).

2.3.4 Sampled mixtures

The presence of an IBF plume around a well causes significant sample bias because it replaces the contribution of native groundwater, and associated solutes or contaminants, from some parts of the well screen. In this case the well is in a recharge area and downward IBF forms a plume of anomalously young water surrounding the bottom half of the well screen. The reverse would occur in a discharge area where an upward hydraulic gradient would drive an IBF plume to develop around the upper part of the screen.

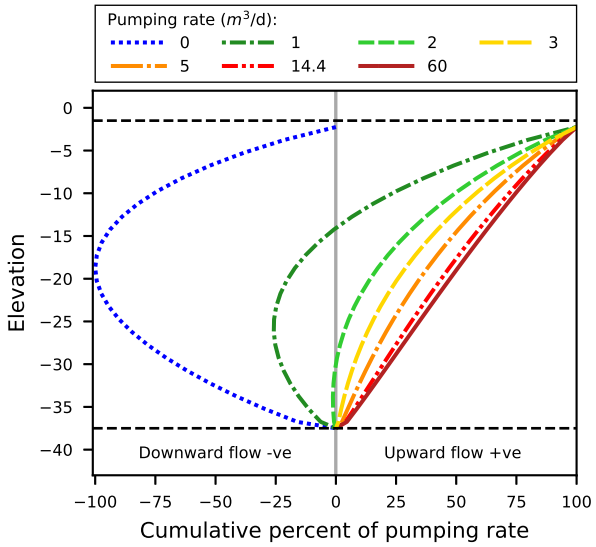

Figure 2.5: Borehole flow profiles in un-pumped conditions (pumping rate = 0) and while pumping at different rates (homogeneous system). Cumulative flow normalised to the percentage of pumping rate, or IBF rate for the un-pumped profile. Dashed lines indicate the screened interval.

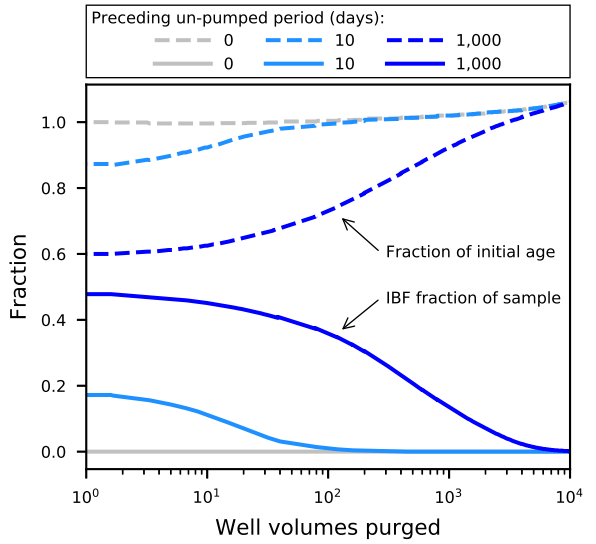

Figure 2.6: Purging after an un-pumped period (homogeneous system): solid curves are fraction of IBF in the sample; dashed curves are sample age as a fraction of the initial composite age, both shown as a function of well volumes pumped (well vol. = 1.5 m^3). For reference, pumping the well without a preceding un-pumped period (0 days) is also shown.

To illustrate sample bias due to IBF, Figure 2.7 shows how the proportion of different groundwater ages in the pumped sample changes with time – immediately after installation, after a 1000-day un-pumped period, and at increasing purge volumes. In this example, if the well is sampled immediately (initial), composite age is 24.4 years, with a fairly even distribution of 9 to 47 years due to the stratified system. However, if the well is un-pumped for 1000-days before pumping commences, the fraction of younger water is much higher, with a reduced age range of 8 to 23 years and just over half the composite sample age. As purging progresses, younger water is gradually removed, with the sampled age mixture returning to that of native groundwater after about 3000 well volumes have been pumped.

2.3.5 Effect of heterogeneity

In a heterogeneous aquifer, well fluxes occur more in zones with higher K, in response to natural or induced head gradients. To examine the effect of K contrasts on the

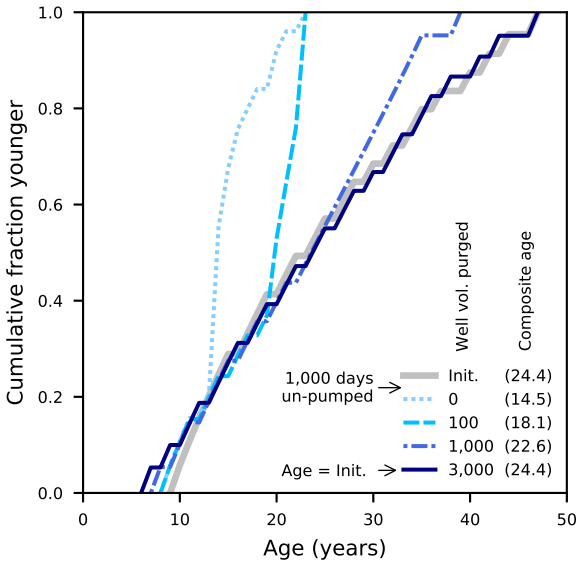

Figure 2.7: Proportion of different groundwater ages in the sample, as a cumulative fraction younger (homogeneous system). "Init." represents groundwater sampled immediately after well installation (no preceding un-pumped period), "0" shows the sampled mixture after a 1000-day un-pumped period, and the other curves indicate the sampled mixture after different well volumes purged (well vol. = 1.5 m^3), with composite age of each sample in brackets.

development and purging of an IBF plume, two model layers were assigned various combinations of higher K (50-5,000 m/d) compared to the homogeneous K of 10 m/d everywhere else. Figure 2.8 shows the range of effects on the flow system at the location of the un-pumped long-screened well. Figure 2.9 shows key relationships drawn from this exercise using results from all combinations of K, expressed as a ratio (K1/K2), with values greater than one indicating higher K in the upper layer than the lower layer and vice versa.

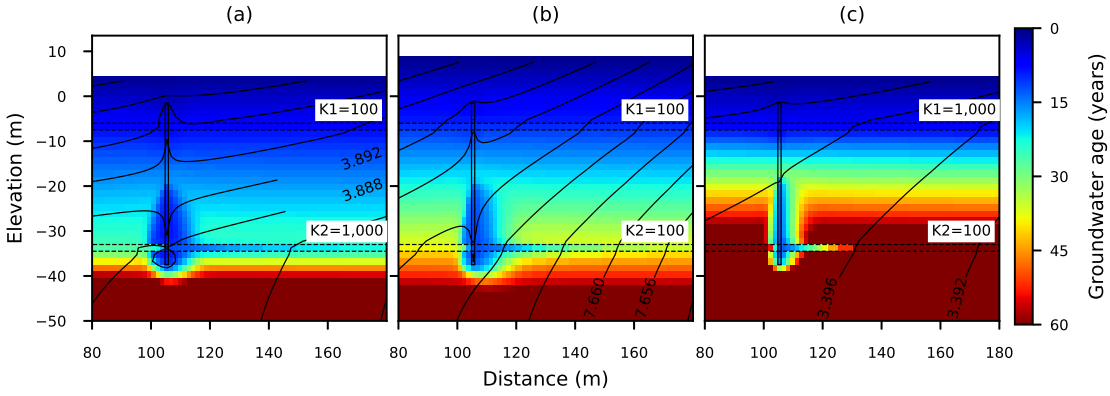

Figure 2.8: Influence of IBF, driven by a vertical head gradient (black contours), on groundwater age in the vicinity of a well (black rectangle) after a 1000-day un-pumped period, for three different combinations of higher K in two layers in an otherwise homogeneous aquifer with K of 10 m/d.

In all cases, the modelled water table was lower than the homogeneous system because the average aquifer K was increased without changing any other boundary conditions. For the range of K combinations tested, the vertical head gradient was steepest when the highest K layer coincided with the lowest head intersected by the well (Figures 2.8a and 2.9a), and this translated to a maximum IBF rate (1.3 m^3/d, Figure 2.9b). In this situation, the wellbore provided a path of less resistance than

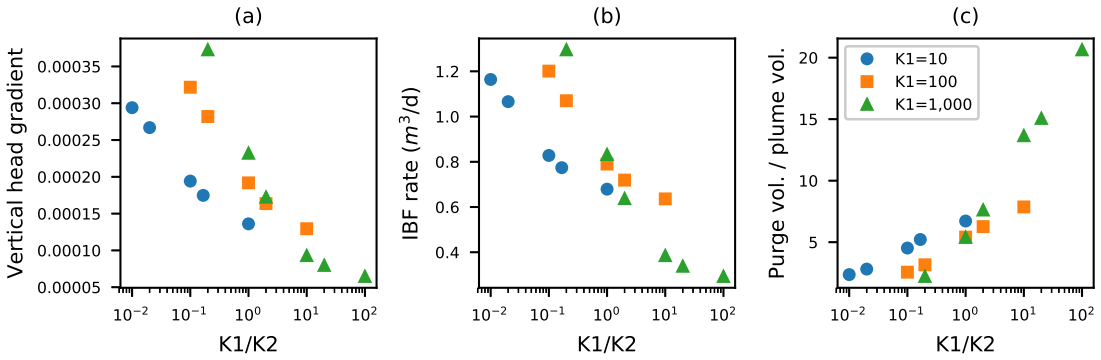

Figure 2.9: Results of testing the effect of two higher K layers intersecting the well (positions indicated in Figure 2.8) in an otherwise homogeneous aquifer with K of 10 m/d: relationship of (a) vertical head gradient, (b) IBF rate and (c) the ratio of purge volume to plume volume, for the range of K combinations tested, plotted against the ratio of K in the upper layer (K1) to K in the lower layer (K2).

the surrounding aquifer for recharging water to reach the higher K layer. Despite the larger IBF plume, the purge volume was minimised because IBF was a large fraction of well pumpage (Figure 2.8a, purge vol. / plume vol. ratio = 2.2). Conversely, the minimum IBF rate occurred when the highest K layer coincided with the highest head (Figures 2.8c and 2.9b). This was because more inflowing IBF simply exited the well at the same level, to continue flowing in the high K layer, rather than taking a downward path of more resistance. A gentler downward vertical gradient in the system (Figure 2.9a) generated a lower IBF rate (0.3 m^3/d) and a smaller IBF plume. However, a smaller IBF plume did not equate to a smaller purge volume. The reason is that IBF is a smaller fraction of pumpage – well influx comes from all permeable zones whereas the IBF plume resides only in the zone with lower head. Thus, it is evident that purge volume can be exceedingly large (Figure 2.8c, purge vol. / plume vol. ratio = 20.6) if the high K zone and IBF plume location do not coincide.

2.4 Discussion

This paper uses example models to examine the relationship between pumping rate, purge time and sample composition (age and IBF fraction) from a long-screened well that has been left un-pumped for varying periods of time up to 1,000 days. The well is in the recharge area of a groundwater system and is subject to downward IBF. The modelled IBF rates of 0.3-1.3 m^3/d (0.2-0.9 l/min) are a conservative example of commonly measured rates (e.g. 0.01-6.3 l/min, Elçi et al., 2003). In this work, aquifer geometry was simple and K variance was limited by numerical stability issues with the MNW2 package. Real-world aquifers can be more structurally complex, with larger K contrasts and different boundary conditions resulting in larger vertical head gradients driving higher IBF rates. These factors all influence the extent and

position of an IBF plume, and hence the specifics of purging and sampling.

The results clearly cast the concept of "purging" in a new light when IBF is present. It is not so much about removing stagnant water in the well as it is about removing a plume around the well. For example, to remove the 3000 well volumes required to purge the IBF plume in the homogeneous system, the well would need to be pumped for about 5 days at 10 l/s. Clearly, this is an entirely different paradigm than the common well-purging practice of removing three to five casing volumes (Neilsen and Neilsen, 2007). The cost and logistics of pumping such a large volume of water could be prohibitive, so the sampling objectives and strategy need to be carefully considered.

To optimize sampling of long-screened or open wells, it is important to measure the flow profile in un-pumped conditions and at the pumping rate used for sampling. Methods to measure flow profiles include borehole flowmeter (Boman et al., 1997; Molz et al., 1994; Newhouse et al., 2005), tracer-dilution tests in un-pumped conditions (Maurice et al., 2011), tracer-pulse tests while pumping (Izbicki et al., 1999) and tracer-dilution tests while pumping. The latter can be performed with a constant injection of tracer (Brainerd and Robbins, 2004) or with single replacement of the borehole fluid column (e.g. Doughty and Tsang, 2005; Paillet, 2012). In un-pumped conditions the flow profile shows the inflow and outflow zones, which are the high and low head zones respectively, and the IBF rate(s) between them. In pumped conditions the flow profile shows the inflow distribution in the well at the applied pumping rate. These data enable informed decisions to be made about whether or not to attempt purging an IBF plume, how best to sample a well and how to interpret the sample.

Once the IBF rate and outflow zone(s) are established, the plume volume can be estimated if the pumping history is known. It is difficult to accurately determine the purge volume without knowing the specific structure and hydraulic properties of the aquifer system. However, this paper shows that purge volume is a multiple of the plume volume, depending on the position of the plume relative to the K distribution across the well (Figure 2.9c). To reduce the purge volume it is necessary to increase the fraction of pumped water that is derived from the plume. One way to do this is to isolate the interval containing an IBF plume with packers. Another solution is to insert a flexible, impermeable, water filled liner into the well to prevent IBF from occurring (e.g. Keller et al., 2014). This would not prevent IBF within the gravel pack of a cased well, but it would greatly reduce the overall volume. The liner is removed for sampling and native groundwater is pumped from all depths after a modest purge.

It is also worth noting that well influx from the IBF plume (lower head) zone is not optimised unless the pumping rate is sufficient to overcome the head related influence. For example, in this model the pumping rate needed to be at least $\sim$14.4 m^3/d

to fully overcome an IBF rate of 0.68 m^3/d (Figure 2.5). This is about the maximum rate achievable with the commonly used Grundfos MP1 sampling pump. In practice IBF rates can be orders of magnitude higher (e.g. Bexfield and Jurgens, 2014), so purging an IBF plume would require a commensurately higher pumping rate, and may often be infeasible.

Whether or not purging an IBF plume is feasible, the IBF regime in a well can be used to advantage when sampling. That is, the high head (IBF inflow) zones produce native groundwater without purging, so it could be beneficial to sample these specifically. This has been alluded to previously (e.g. Paillet, 2004b), but the practice is not widely reported. A single IBF inflow zone may be sampled with a "grab sampler", or by pumping the well more slowly than the IBF rate. In principle, this would produce an accurate groundwater sample from a known depth interval. For example, in this model, when pumping at a rate of 1 m^3/d (Figure 2.5), all inflow was sourced from the IBF inflow zone in the top one third of the well.

If an IBF plume is purged, a well provides a composite mixture of native groundwater from all depths according to the inflow distribution at the pumping rate used for sampling. However, the remaining challenge is to identify water composition at specific depths, in addition to the IBF inflow zones. Packers are an established method of sampling specific depth intervals, where they can be isolated. However, this is not always possible (e.g. due to gravel pack in a cased well or an irregular borehole wall) so an alternative that works in the open wellbore is necessary. In such cases, the borehole flow and solute mass-balance method (Collar and Mock, 1997; Gossell et al., 1999; Izbicki, 2004; Sukop, 2000) could be an effective solution.

2.5 Conclusion

A long-screened well was simulated in the recharge area of a synthetic groundwater flow system to quantify the effects of vertical hydraulic head gradient, and IBF in particular, on the sampled water mixture for different pumping rates and un-pumped periods. The modelling results show that:

- The pumping rate must be at least an order of magnitude higher than the IBF rate to minimise hydraulic head bias in the sample and minimise the purge volume.
- After an example 1000-day un-pumped period in a homogeneous system, purging an IBF plume required removal of at least three orders of magnitude more water than the common practice of three to five well volumes.
- A basic assessment of heterogeneity showed that purge volume depends both on the proportion of well influx drawn from the IBF plume location and the volume of the plume itself. Purge volume ranged from 2.2 - 20.6 times the

volume of the IBF plume for the range of K combinations tested (10 - 5000 m/d), and was at a maximum when the IBF plume location did not coincide with the high K zone.

- An IBF plume resides only in lower head zones so, even if purging is not feasible, native groundwater samples can be obtained from high to intermediate head (IBF inflow) zones.

These results highlight the importance of knowing the borehole flow regime in unpumped conditions and at the pumping rate used for sampling, to enable proper understanding of the water mixture sampled from wells in which IBF is active.

Chapter 3

A constant rate salt tracer injection method to quantify pumped flows in long-screened or open borehole wells

Published in *Journal of Hydrology*: Poulsen, D.L., P.G. Cook, C.T. Simmons, J.L. McCallum, S.L. Noorduijn and S. Dogramaci (2019). A constant rate salt tracer injection method to quantify pumped flows in long-screened or open borehole wells. doi: 10.1016/j.jhydrol.2019.04.051.

3.1 Introduction

Installation of wells or piezometers for groundwater investigations is expensive, particularly in remote areas, so the economical approach is to use available infrastructure where possible. However, wells designed for purposes such as water production have much longer screened or open intervals than those for collecting data from discrete depths. This means that traditional methods average hydraulic properties, water levels and chemistry over an unhelpfully large interval of the aquifer system. Although straddle packers can be used to obtain depth-specific data, they rely on isolating specific intervals of the well. This is not possible if bypass flow occurs in the gravel pack around the screen or between the packer and an uneven borehole wall. In such situations it can be more effective to maintain the well as the path of lowest hydraulic resistance and work with the in-well flow regime in both ambient (un-pumped) and pumped conditions. Specifically, this approach enables the vertical distribution of hydraulic conductivity and head to be derived (e.g. Day-Lewis et al., 2011; Sawdey and Reeve, 2012) and water samples to be properly interpreted (e.g. Poulsen et al., 2018).

Borehole flowmeters are established and commercially available geophysical tools

for measuring in-well flow profiles – they are relatively efficient to operate and can be used in ambient and pumped conditions. There are three types of flowmeter (Newhouse et al., 2005; Young and Pearson, 1995): heat-pulse (mainly suited to low flows), electromagnetic (EM) (suited to a wide range of flows), and the impeller/spinner (best suited to higher flows). These wireline instruments measure fluid velocity past a sensor as function of depth in the well, in stationary or trolling mode. Tracer dilution tests within a well can be used instead of, or complementary to, a borehole flowmeter to improve resolution of in-well flows with multiple lines of evidence.

For ambient conditions and low pumping rates, a tracer is introduced to the fluid column in the well, uniformly or at a point, or the entire water column is replaced. Then, successive tracer profiles in the well over time show the "moving front" of inflowing aquifer water displacing and/or diluting the tracer. Evolution of the tracer profile over time can be converted into borehole flow using a mass balance (Paillet, 2012) or the advection-dispersion equation in a spreadsheet model (Maurice et al., 2011) or a numerical code (Doughty and Tsang, 2005).

For higher pumping rates, when there is a shorter residence time of water in the well, a tracer pulse test can be used (Goldrath et al., 2015; Izbicki et al., 1999) or the constant rate tracer dilution approach reported here. The tracer pulse test is time-consuming because, for each point measurement of in-well flow rate the tracer must travel from the injection point to the sensor at the surface, and many point measurements are required to generate a flow profile.

In comparison, the constant rate tracer dilution method is more efficient because it requires little more than a single tracer travel time from injection point to the pump. Aside from the tracer pulse test, the objective of existing single-well pumped tracer tests were mainly to characterise individual fractures in low-yield bedrock wells with weak ambient flow regimes (e.g. Brainerd and Robbins, 2004; Chlebica and Robbins, 2013; Libby and Robbins, 2014; Tsang et al., 1990).

Transient methods are problematic in high yield wells because a slug test would recover far too quickly for tracer profiles to be measured, a low pumping rate would cause insufficient drawdown to overcome ambient flows, while a high pumping rate may flush the single fluid column of tracer out of the well before multiple concentration profiles could be collected, and a strong ambient flow regime would complicate the uniform emplacement of tracer in the water column in the first place. In contrast, our constant rate method is suited to high-yield wells and particularly situations where a higher pumping rate is needed to overcome ambient flows and generate inflow from all aquifer zones intersected.

In this paper we present a combined field and numerical method that is unique in its efficacy and applicability over a wide range of pumping rates in both screened and open wells. A constant rate approach, with simultaneous pumping and injection

of tracer is used in a similar manner to Brainerd and Robbins (2004). However, we use common salt as the tracer (instead of a dye), due to its availability and ease of measurement, and collect continuous fluid column electrical conductivity logs before and during the transient phase of the test and at steady-state. Analysis using the advection-dispersion equation enables flow rate to be quantified at all depths in the well. Field data from two high-yield, long-screened wells and an uncased bedrock well are used to demonstrate the utility of the method. We compare the results with borehole EM flowmeter data from the same wells at similar pumping rates, and provide some important considerations for the use of both methods.

3.2 Theory

At a pumping rate sufficient to overcome the ambient flow regime (see section 3.8.4), a well can be conceptualised as a linear network with monotonically increasing flow in one direction (Figure 3.1a), analogous to a gaining river. Water enters the well according to the hydraulic conductivity and head distribution in the surrounding aquifer and the hydraulic stress induced by pumping. If a tracer is injected continually at a constant rate near the distal end of the well, it is drawn towards the pump and diluted in proportion to each of the inflows. Movement of the tracer front during the initial transient phase indicates velocity in the well, and its shape is determined by the degree of dispersion, mixing and aquifer inflows. Once the tracer has reached the pump, a steady-state situation arises where there is no further change in the tracer concentration profile, assuming that all fluxes are constant, and dispersion becomes insignificant, which is a key advantage of this approach. At this point, the shape of the tracer concentration profile (Figure 3.1b) is primarily determined by the distribution of inflows from the aquifer, and (with or without the transient profiles) it can be inverted to give the inflow profile by quantifying the tracer mass balance to each element in the network (Figures 3.1c and 3.1d).

Flow velocities along the length of a well range from zero to the applied pumping rate, with increases resulting from lateral inflows from the aquifer. Flow varies across the well diameter according to the type of flow regime, from a minimum at its wall to a maximum at its centre. We considered it impractical to explicitly quantify the full flow velocity field, so we made some simplifying choices to model tracer dilution in a well: 1) we neglect radial variations in flow velocity and solute concentration and simply consider the averages at each depth, 2) we assume that the advection-dispersion equation (commonly used for porous media) is a reasonable approximation of transport in a well over the range of flows we encountered (mostly laminar, tending to turbulent), 3) we approximate dispersion as the product of average velocity, a dispersivity constant and diffusion (Eq. (2)), and 4) we assume monotonically increasing flow between the injection point and the pump. On this

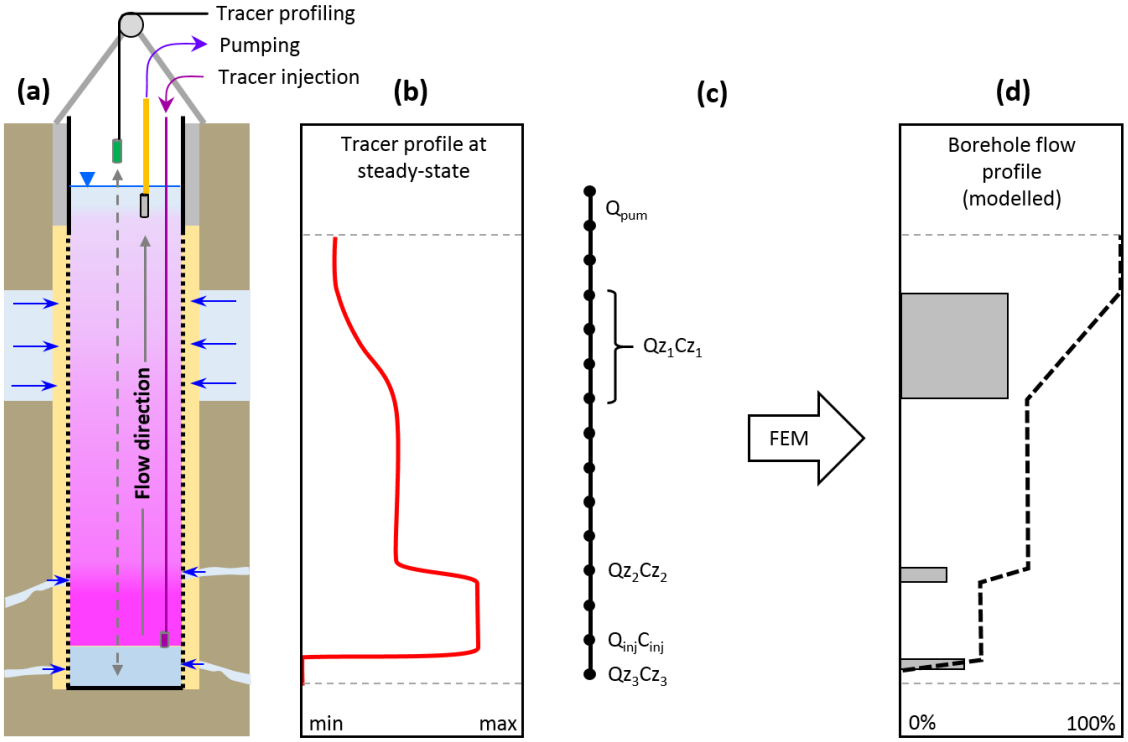

Figure 3.1: Conceptual diagram of (a) test setup in a long-screened well illustrating pumping, tracer injection, tracer profiling over the test interval and discrete vs. distributed aquifer inflows, (b) measured steady-state tracer concentration profile in response to dilution by aquifer inflows at the applied pumping rate, (c) fluxes translated into a finite element network, and (d) the inflow zones and cumulative borehole flow profile interpreted with the finite element model (FEM).

basis, the rate of change of mass in the well with depth (z) and time (t) is expressed with a one-dimensional form of the advection-dispersion equation (Maurice et al., 2011):

$$A\frac{\partial C(z,t)}{\partial t} + \frac{\partial Q(z)C(z,t)}{\partial z} = A\frac{\partial}{\partial z}\left[D_z\frac{\partial C(z,t)}{\partial z}\right] + q_iC_i \tag{3.1}$$

where A is the cross-sectional area of the well (L^2), Q is flow rate in the well ($L^3/L/T$), q_i is the groundwater inflow rate ($L^3/L/T$), C and C_i are the concentrations in the well and the groundwater inflow respectively, z is the vertical position in the well (L) and D_z is the dispersion coefficient (L^2/T). By adjusting q_iC_i at each depth to fit the measured $\partial C/\partial z$ profile, the inflow profile to the well can be obtained for the known pumping rate, tracer injection rate and tracer concentration. Since q_i and C_i are both unknowns, this method is limited to situations where $C_i(z) = 0$, where $C_i(z)$ is assumed to equal the concentration of pumped discharge from the well, or where $C_i(z)$ can be estimated for each inflowing zone. The shape of the tracer front is governed by the longitudinal dispersion coefficient:

$$D_z = \alpha v_z + Dm \tag{3.2}$$

where α is the dispersivity (L), v_z is the average flow velocity (L/T), and Dm is the molecular diffusion coefficient (L^2/T). This form of the advection-dispersion equation is appropriate when dispersivity is constant in laminar flow conditions. Dispersivity is reduced in turbulent flow because eddies and random motion homogenise the flow velocities (Hart et al., 2013). In addition to dispersion, a certain distance along the well is required for complete mixing of flow with tracer at the injection point and with each inflow from the aquifer. This 'mixing length' is much shorter in turbulent flow than in laminar flow. An example from the water treatment industry gives a mixing length of 10 times the pipe diameter where chlorine is introduced mid-stream in turbulent pipe flow (Pizzi, 2009, p. 186). This translates to a length of 2 m for the 0.2 m diameter wells used in this work. Although flows are usually laminar in the vicinity of the tracer injection point, lateral inflow from the aquifer causes small eddies and enhances tracer mixing (Martin-Hayden et al., 2014; Martin-Hayden and Wolfe, 2000).

For pipe flow, the type of flow regime is assessed with the dimensionless Reynolds number (Re):

$$Re = \frac{\rho v_z d}{\mu} \tag{3.3}$$

where ρ is the density (M/L^3) and μ is the dynamic viscosity of water ($M/L.T$) (both depend on water temperature), vz is the average flow velocity (L/T), and d is the diameter of the pipe (L). Indicatively, laminar flow prevails for Re<2000 and turbulent flow occurs where Re>4000, with the intervening flows in the transitional range, where either flow type may occur (e.g. Avila et al., 2011). Reynolds number calculations for the 0.2 m diameter wells used in this work indicate laminar flow up to 0.51 m/min (16 l/min) and turbulent flow above 0.95 m/min(30 l/min).

Where a tracer test involves fluids with contrasting density (e.g. different salinity), tracer movement occurs by two mechanisms: forced convection and free convection(Ataie-Ashtiani et al., 2018) (Ataie-Ashtiani et al. 2018). Forced convection is due to an external pressure gradient (e.g. pumping or the natural head difference between depths of the aquifer system connected by the well), and is often referred to as advection, whereas free convection is the buoyant fluid movement driven by a density contrast. If there is a density contrast between the tracer and water in the well, free convection may affect tracer mixing and initial transport. In the case of a dense tracer injected into an upward flow regime, the mixing zone may extend below the injection point to a depth depending on the strength of the pumping induced flow relative to the density contrast (van Sommeren et al., 2013) (van Sommeren et al. 2013). The assisting or opposing effect of free convection in tracer transport is not explicitly included in our model, but we do explore and discuss ways to assess its role in the test.

A characteristic of dilution is that the change in concentration is relative to the concentration difference between the two fluids. So the change of tracer concen-

Table 3.1: Well and test details.

Parameter	**LHRP4**		**WB11AH001**		**6628-21204**	
Well type	Machine slotted PVC		Machine slotted PVC		Uncased	
Aquifer media	Dolomite/gravel/sand		Gravel/fault gouge		Siltstone, fractured	
Screen/open interval, m ToC	65.9-141.8		35.2-143		6-55.7	
Diameter, m	0.195		0.203		0.204	
Transmissivity, m^2/d	12917[a]		2690-6360[b]		-	
Intraborehole flow[c], l/ min	-6		-5 and +7		-0.07	
Test/flow direction	Up	Down	Up	Down	Up	Down
Standing water level, m ToC	27.36	27.36	26.97	26.99	10.32	10.15
Pump depth, m ToC	60	139	30	70	15	45
Pumping rate, av. l/ min	48.3	66.3	44.5	51.2	12	10
Water level drawdown, max. m	0.05	0.09	0.03	0.04	2.14	1.91
Injection depth, m ToC	139	66	60,70,90,110	38	50	20
Injection rate, l/ min	0.56	0.55	0.53	0.64	0.51	0.61
Tracer EC, mS/cm	40.0	40.0	20.0	30.8	17.38	22.5
Ratio of injection/pumping rate	0.012	0.008	0.012	0.013	0.043	0.061
Pumped EC (compos.), mS/cm	1.007	1.038	0.993	0.995	2.290	2.190

[a](Aquaterra 2007); [b](Aquaterra 2011); [c]downward flow –ve, upward flow +ve

Top of Casing (ToC) $\sim$ 0.5 m above ground level.

tration in the well for equal aquifer inflow becomes exponentially less as dilution progresses, if the concentration of aquifer inflow is constant. Thus the method is sensitive to small inflows only when tracer concentration is increased significantly above background over the entire tested interval of the well. To help choose an appropriate tracer concentration, the maximum extent of dilution expected in pumped discharge (C_{pss}), is given with a simple steady-state mass balance:

$$C_{pss} = \frac{Q_{inj}(C_{inj} - C_{p0})}{Q_p} + C_{p0} \tag{3.4}$$

where Q_{inj} is the tracer injection rate (L^3/T), Q_p is the pumping rate (L^3/T), C_{inj} is the undiluted tracer concentration and C_{p0} is the tracer concentration of pumped water before the test (which is readily measured). Tracer concentrations can be in units of M/L^3 or an analogue such as electrical conductivity ($Siemens/L$).

3.3 Site description

The method was initially tested in an open well in the fractured bedrock of the Adelaide Hills, South Australia. It was then applied in two long-screened wells in the remote Pilbara region of Western Australia, with one providing a relatively straightforward example, and the other illustrating a more challenging situation. Table 3.1 gives details of these three wells.

3.3.1 Adelaide Hills

Well 6628-21204 is one of several wells installed in fractured Adelaidean sedimentary rock at a research site near the town of Balhannah in the western Mount Lofty Ranges (Harrington et al., 2004). The aquifer media is compact laminated metasiltstone tending to sandstone, with quartzite in places, and groundwater flowing exclusively in fractures. A borehole camera was used to establish that this 0.204 m diameter well is uncased below 6 m and it appears to be open to near the full drilled depth of 55.7 m (timber/steel debris lodged below 53.7 m). The borehole is generally competent, but the wall is variably rough and enlarged in places. Airlift yield at the time of drilling was recorded at 1.9 l/s. In our testing, pumping rates of up to 0.2 l/s induced about 2 m drawdown in the well. With a pumping water level of 12 m this well had a 43.7 m effective open interval.

3.3.2 Pilbara

The Pilbara is known for its globally significant iron ore deposits, which are mined in open pits, and for its unique natural environment, including groundwater dependent ecosystems (Rojas et al., 2018). The competing interests of maintaining dry mining conditions (dewatering) and maintaining groundwater levels to support surface ecosystems are driving research to characterise groundwater ages and recharge rates in the region's aquifers (e.g. Cook et al., 2017; McCallum et al., 2017). However, virtually all available wells have long screens designed to maximise discharge capacity or to monitor overall responses to dewatering. This means that pumped samples are a mixture of groundwater from a wide range of depths, which limits the utility of any chemical analyses. Thus, the purpose of applying this method of measuring in-well flows in the Pilbara is to enable better informed sampling by quantifying specific inflow zones. The two test wells (LHRP4 and WB11AH001) used in this work are in the Hope Downs area of the southern Hamersley Basin. They were installed as supply wells for railway construction and, as such, they are remote from the mining areas and they have been disused for several years.

Well LHRP4 is screened in variably weathered and fractured dolomite of the Wittenoom Formation and the overlying gravelly detrital sediments. A borehole camera was used to establish that the PVC casing of this 0.195 m diameter well is machine slotted below 66 m and, although a total depth of 144 m was originally logged, it is now silted up to 142 m, giving a 78 m long screened interval. Gravel pack is recorded for the entire borehole annulus except for a cemented surface collar, with telescoping hole diameters of 0.45 m (3-70 m), 0.32 m (70-134 m) and 0.27 m (134-144 m). A previous aquifer test indicates the well has a high transmissivity (12900 m^2/d) and it was pumped at 25 l/s with 2.6 m drawdown (Aquaterra, 2007). In our tests, pumping rates of up to 1 l/s induced up to 0.09 m drawdown.

Well WB11AH001 is in a particularly complex geological setting, with logged material ranging from clayey gravel to gravel and then 'fault gouge' with depth, the latter containing fragments of crystalline dolomite, shale, banded iron formation and chert. A borehole camera was used to establish that the PVC casing of this 0.203 m diameter well is machine slotted below 35.2 m and the total open depth of 142.8 m, giving a 107.6 m long screened interval. Gravel pack is recorded for the entire borehole annulus (consistently 0.3 m diameter), except for a 2 m bentonite seal above the screen (24-26 m) and a cemented surface collar. A previous aquifer test gave transmissivity in the range 2690-6360 m^2/d with pumping at 25 l/s and just 0.64 m drawdown (Aquaterra, 2011). In our tests, pumping rates of up to 0.85 l/s induced up to 0.04 m drawdown.

3.4 Field methods

As illustrated in Figure 3.1a, this test involves collecting a sequence of tracer profiles in the well, while simultaneously pumping from one end of the screen and injecting tracer at the other end. In each case, the test was repeated with the pumping and injection locations reversed, to provide a check on the uniqueness of the interpreted flow profile, and to assess whether the test worked better in one orientation than the other due to the distribution of inflows. This resulted in the six tests summarised in Table 3.1.

Electrical conductivity (EC) as specific conductance at 25 °C was used as the tracer, with sodium chloride (cooking salt without anti-caking agent) used to create the tracer solution. As others have shown (e.g. Tsang et al., 1990), EC is linearly related to salt concentration in water at relatively dilute concentrations (EC<7 mS/cm) so we used it directly in our inversion model as an analogue for concentration, with the focus being on relative differences. The initial tracer EC and pumped discharge EC were measured with a calibrated field meter (WTW, model Multi 3420, accuracy ±0.5% of measured value). EC profiles were recorded with a multi-parameter sonde (YSI, model 600XLM-DEEP, depth accuracy ±0.3 m; EC accuracy ±0.5% of reading), lowered and raised using a hand operated winch. The sonde recorded EC and pressure (depth) at one second intervals, giving measurements with a median spacing of 0.1-0.2 m throughout the water column. Trolling in the downward direction was preferable because the EC sensor, located on the bottom of the instrument, was first to contact undisturbed water. In the upward direction, passage of the instrument body (0.042 m diameter, 0.54 m length) ahead of the sensor caused a smearing effect in the EC profiles. Ideally the tracer measuring instruments should be calibrated together. Here the difference between the surface meter reading of pumped discharge and the (flow weighted) average of background EC determined from the tracer profiles was subtracted from the profiles to bring

them into line with the meter reading.

Field logistics dictated a manageable volume of tracer solution, so the tracer injection rates were a small percentage (0.8-6.1%) of the pumping discharge rates. With the low volume injection, relatively high tracer concentrations (17-40 mS/cm) were used so that dilution was measurable throughout the test intervals (initial mixing in the well rapidly reduced EC to more dilute levels).

After measuring the standing water level, an ambient EC profile was collected before the well was disturbed by pumping. Then the ¼ inch nylon tracer injection tubing and submersible pump (Grundfos, model MP1 or SQEN3) were placed near the top or bottom of the well, depending on the orientation of the test. Pumping commenced (10-66.3 l/ min) and while water level drawdown was stabilising (10-60 min) the tracer solution was prepared in a 200 L drum using aquifer water and pre-mixed salt concentrate. Before starting the test one or more EC profiles were collected during pumping to establish the initial conditions. The test began when tracer entered the well at the injection point, which occurred once the injection tube filled with tracer a few minutes after the injection pump started. Tracer was injected at a constant low rate (0.51-0.61 l/ min) using a peristaltic pump (Pegasus, model Athena). A diffuser, consisting of a short length (0.15 m) of perforated pipe with an end cap, was used to help direct the tracer radially into the well. The diffuser was not centralised, so the well's vertical alignment was probably the main control on the position of the tracer injection point and the EC sonde each time it was lowered and raised. During the test, regular EC profiles were collected and downloaded from the sonde to give real time tracking of tracer migration in the well, and to assess when the steady-state condition was reached (later checked with model simulations). Regular measurements of injection rate and pumping rate (volume/time method) and EC of pumped discharge were also made. The test was complete when the tracer had reached the pump, EC in pumped discharge had stabilised, and successive tracer profiles had the same shape.

3.4.1 Borehole flowmeter

Vertical flow measurements were made with a borehole EM flowmeter (Century Geophysical LLC, model 9721) in well LHRP4 and well WB11AH001 and historical data were obtained for well 6628-21204, for comparison with the pumped tracer dilution test results. In all cases, the instrument was used in stationary mode at regular intervals while the well was being pumped at a similar rate to that used in the tracer dilution test. Ambient flow profiles were also collected.

According to the manufacturer, the response range for the flowmeter is 0.05-40 l/ min, with an accuracy of ± 0.02 l/ min. The product description also indicates *"When using the tool to measure low velocity flow rates a rubber skirt is attached to the outside of the sensor to block off the bore hole and force the fluid to pass*

through the 1 inch diameter opening inside the sensor coil... When measuring faster flow rates the rubber skirt is typically removed and the tool is run in either the static station or dynamic mode". We include this statement because it has a strong bearing on the results. We used such a rubber skirt (flow diverter) in all profiles and maintained flow through the sensor below the stated upper end of the response range (40 l/ min). For example on well LHRP4, flow through the sensor was limited to 29 l/ min when pumping at 50 l/ min by using an under-sized flow diverter (0.188 m) compared to the well diameter (0.195 m). However, according to Arnold and Molz (2000) head loss across the meter becomes significant when flow through the sensor exceeds 10 l/ min (see discussion for details).

At each well, a two point calibration procedure was used with the instrument positioned in the water column above the top of the screen. In ambient conditions this comprised a stationary zero-point followed by trolling the instrument at a known rate and using the well diameter to calculate flow rate through the sensor. In pumped conditions the second point was recalibrated to the known pumping rate with the instrument held stationary. Because the calibrations were done with the flow diverter in place, any bypass flow was built-in, assuming the well diameter remained constant.

3.5 Numerical methods

To quantify the vertical profile of flow in the well, the measured tracer profiles were modelled with a finite-element formulation of the one-dimensional advection-dispersion equation (Eq. 3.1). The well was discretised into a network of nodes and elements (e.g. Figure 3.1c) and aquifer inflows were visually identified in the tracer dilution profiles at the resolution of the node spacing. Grid convergence was achieved with node spacing of 0.05 m, which was near the minimum numerically practical spacing (for solution time). This fine discretisation was necessary to represent strong gradients of tracer concentration, particularly around the injection point. According to the Peclet number constraint, node spacing did not exceed the dispersivity length so that dispersion characteristics of the model were not unduly affected. Discrete inflows can be assigned to individual elements, or inflow zones can span many elements, with the proportion of total inflow distributed evenly over the zone. Tracer injection and pumped discharge were assigned per element, so the fluxes were split between two nodes. When the pump was placed below the injection point, an adjusted cross-sectional area of the well was used in the model, given by subtracting the pump hose cross-sectional area from that of the well. The area of the injection hose was negligible.

The Laplace Transform Galerkin method (Sudicky, 1989) was used to generate a time-continuous solution for the measured pre-test, transient and steady-state tracer

profiles simultaneously. This was advantageous because the collection time for each profile (i.e. the time taken to troll the length of the well, ∼10 minutes) was non-negligible relative to flow velocities in the well ($\leq 2\,\mathrm{m/min}$). The time-continuous solution was inverted back to real time values using the de Hoog et al. (1982) algorithm at the time of each measurement in the tracer profiles. The Laplace transform provides a time-continuous solution so the usual Courant number constraint, that solute mass must not move more than the node spacing per time step, was unnecessary. The model was implemented as a Python class and a graphical user interface was developed to assist with the iterative fitting process.

A 'best-fit' of the modelled tracer concentration profiles to their measured equivalents was achieved by manually adjusting the fraction of discharge and background tracer concentration for each inflow zone. The background tracer concentrations in aquifer inflows were estimated by including the pre-test tracer profile, obtained while pumping the well but before commencing tracer injection, in the model fitting process. Dispersivity was adjusted to fit the shape of the tracer dilution front in the transient profiles. For all simulations, dispersion included molecular diffusion at a rate of 9.7×10^{-8} $\mathrm{m^2/min}$, a value appropriate for sodium chloride in water (Cook and Herczeg, 2000). The field steady-state tracer concentration profile was verified theoretically by modelling a profile at a large time (1440 min) compared to the test duration (<420 min).

3.6 Results

The three field examples illustrate the general utility (and some challenges) of the method in both uncased bedrock wells and long-screened wells in a range of hydrogeological situations. Table 3.1 provides summary information including ambient flow rates and pumping induced drawdown for each test. Figure 3.2 shows the EC of pumped discharge from each well before and during the tests, mainly to help interpret the results. In all cases, the (composite) background EC is clearly identified (first horizontal line). When this was used in Eq. 3.4 with the applied pumping and tracer injection rates we could estimate the expected steady-state concentration of discharge (second horizontal line). Deviations from these predictions are explained in each case. The time elapsed between first arrival of tracer at the pump and the observed steady-state concentration indicates the effect of dispersion, and this is also seen as the "S" shaped curve in the transient tracer profiles presented below. In Figures 3.3, 3.4 and 3.6, panels (a) and (c) show the tracer profiles (these look different for each orientation of the test because of the different position of the injection and pumping locations with respect to the inflows to the well), while panels (b) and (d) give the interpreted inflow zones and resulting flow profiles, for direct comparison with each other and with the flowmeter data shown in panel (e). In the-

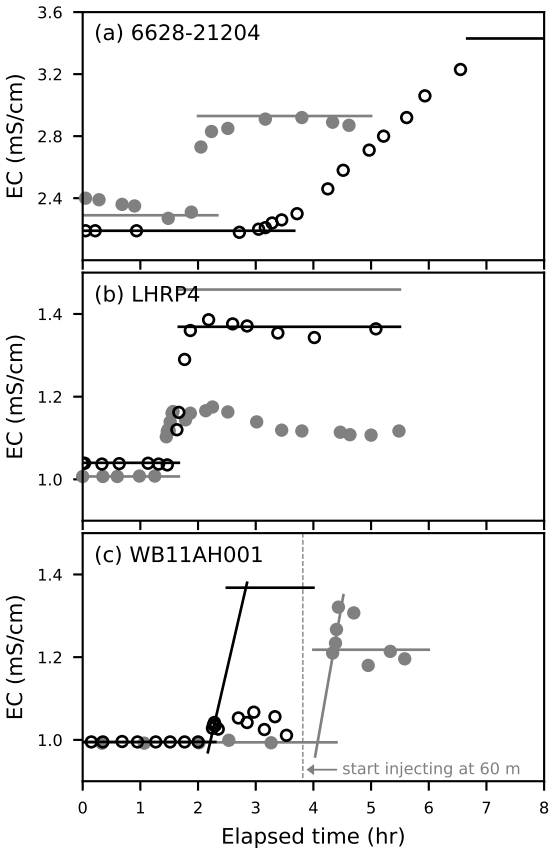

Figure 3.2: Tracer concentration in pumped discharge over the duration of each test, with injection at the top (open black circles) and injection at the bottom (closed grey circles) in (a) 6628-21204, (b) LHRP4 and (c) WB11AH001. For each test, the first (lower) horizontal line indicates the background EC of pumped discharge and the second (upper) shows the expected EC at steady-state calculated using Eq. (4).

ory, these three independent interpretations of the inflows should be identical, while the resulting flow profiles are cumulative in the direction of flow so they depend on the position of the pump in the well.

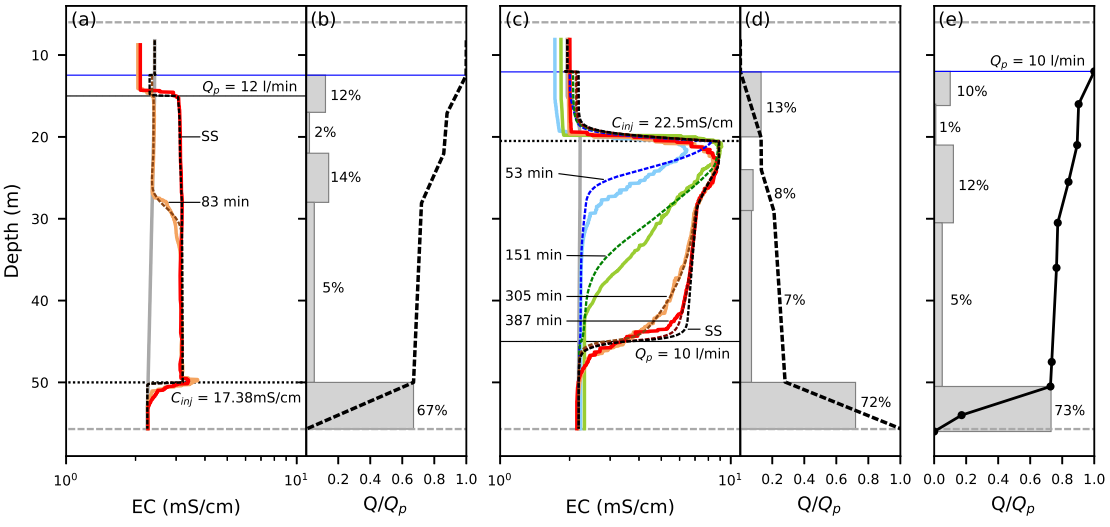

Figure 3.3: 6628-21204: (a) and (c) measured (solid lines) and modelled (dashed lines) tracer profiles, with injection at bottom and top respectively. Red line is the last measured profile, black dashed line is modelled steady-state; (b) and (d) modelled inflow zones (grey bars indicating % of discharge) and cumulative borehole flow profile (black dashed line); and (e) EM flowmeter data for direct comparison of inflow zones and percentages (Q normalised by Qp). Also shown: open interval (grey dashed lines), pumping water level (blue line), pump location (solid black line) and injection location (dotted black line).

3.6.1 Well 6628-21204

In the first test (Figure 3.3c), a downward flow regime was created by placing the pump at 45 m, and tracer was injected at 20 m, to provide opportunity for enough flow from above to drive transport. The tracer profiles showed a large concentration increase at the injection point and slow downward transport, indicating a small fraction of flow was sourced from above the pump, and even less from above the injection point. First tracer arrival at the pump occurred after 183 min, but concentration was still approaching the predicted steady-state by the end of the day (Figure 3.2a). This is consistent with the modelling (Figure 3.3c), which indicated the last measured concentration profile was short of the theoretical steady-state profile. The test in the reverse orientation (Figure 3.3a) clearly showed that the majority of inflow was from below the injection point at 50 m. There was large dilution at the injection point and rapid transport of the tracer to the pump, with first arrival at 113 min and steady state a short time later (Figure 3.2a). The best fits of the model to each dataset show similar flow distributions, with 72% and 67% of flow from the lower zone (50-55.7 m) for the tests with injection at the top and bottom respectively (Figure 3.3b and 3.3d). The good agreement between the dilution tests and the EM flowmeter data (Figure 3.3e) suggests that the main features of the flow profile are correctly identified.

In fitting the model to the measured data, dispersivity was (unexpectedly) found to differ by an order of magnitude between the two tracer tests, despite flows in both tests being laminar (Re=100-1000). A dispersivity of 0.5 m was obtained with tracer injection at the top, when flow rates in the tested interval were slow (0.04-0.09 m/ min). This large value is clearly manifest in the EC of pumped discharge (Figure 3.2a) with a very disperse tracer front, the time between first arrival and steady-state concentration being 53% of the total test duration. In the reverse direction, with faster flow rates in the tested interval (0.25-0.34 m/ min), the best-fit dispersivity was 0.05 m and the time between first arrival and steady-state was just 16% of the test duration. The exact reason for this difference in dispersivity is unclear, but we note that this bedrock well had very rough walls. So perhaps the effect of wall roughness on dispersivity is actually non-negligible in laminar flows (e.g. Gloss and Herwig, 2010) and tracer transport was impeded more in the slower flow regime, particularly if the injection point was against the borehole wall.

3.6.2 Well LHRP4

In the first test on LHRP4, tracer injection was at 139 m, the pump was above the screen and pumping induced in-well flow rates were up to 1.48 m/ min. Tracer arrival at the surface took 75 min and steady-state was established after 96 min (Figure 3.2b), with the difference being 22% of the test duration. The amount of

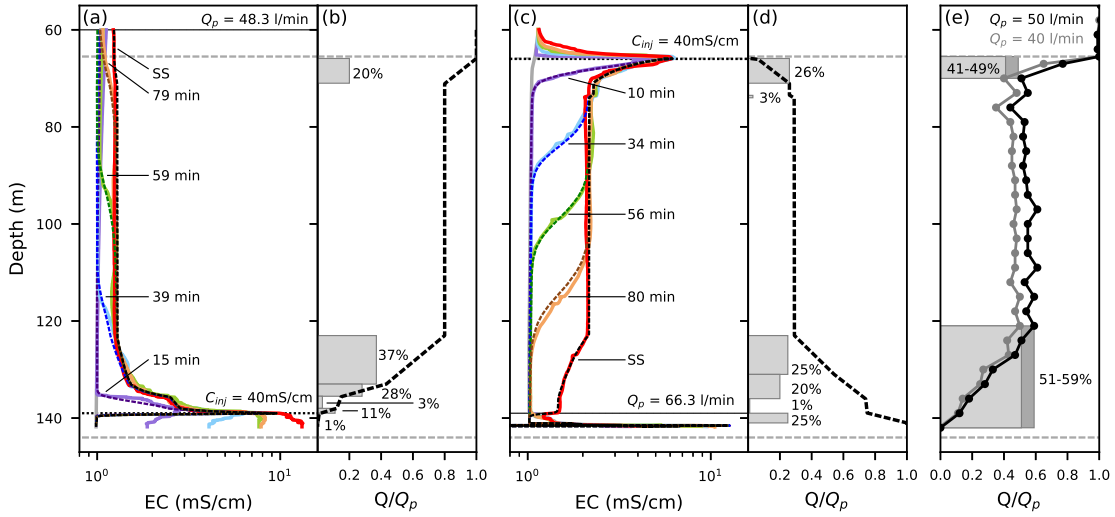

Figure 3.4: LHRP4: (a) and (c) measured (solid lines) and modelled (dashed lines) tracer profiles, with injection at bottom and top respectively. Red line is the last measured profile, black dashed line is modelled steady-state; (b) and (d) modelled inflow zones (grey bars indicating % of total discharge) and cumulative borehole flow profile (black dashed line); and (e) EM flowmeter data for direct comparison of inflow zones and percentages (Q normalised by Qp). Also shown: screened interval (grey dashed lines), pump location (solid black line) and injection location (dotted black line).

dilution was much more than expected at the applied pumping rate (Figure 3.2b), and the measured EC profiles clearly show loss of tracer into a stagnant zone below the injection point (Figure 3.4a). This discrepancy was due to free convection of tracer in the slow upward flow (<0.17 m/ min) at the injection point. In fitting the dilution model, the only way to match both the moving tracer front in the transient phase and the steady-state profile was to assign an effective injection rate less than the actual injection rate. A good model fit was achieved with an effective injection rate of 0.31 l/ min travelling upwards, giving 0.25 l/ min of tracer lost to density convection. Over the duration of the test to steady-state, this loss rate is consistent with the amount of tracer mass required to generate the observed concentrations below the injection point. In contrast, with injection at the top, the pump placed at 139 m and pumping induced in-well flow rates up to 1.87 m/ min, it took slightly longer for tracer to arrive at the surface (92 min) and to establish steady state conditions (118 min), but the proportion of the test duration was the same (22%) and the amount of dilution was as expected (Figure 3.2b).The steady-state tracer profiles in both orientations (Figure 3.4a and 3.4c) clearly show two producing zones separated by an interval with no inflow. The interpreted flow profiles (Figure 3.4b and 3.4d) have very similar inflow zones, generally consistent with those identified in the EM flowmeter data (Figure 3.4e). However, the proportions of inflow were different, with the tracer tests indicating more flow from the lower zone (71-80%) than the flowmeter (51-59%).

Estimated dispersivity was 0.2 and 0.1 m for the downward and upward flow

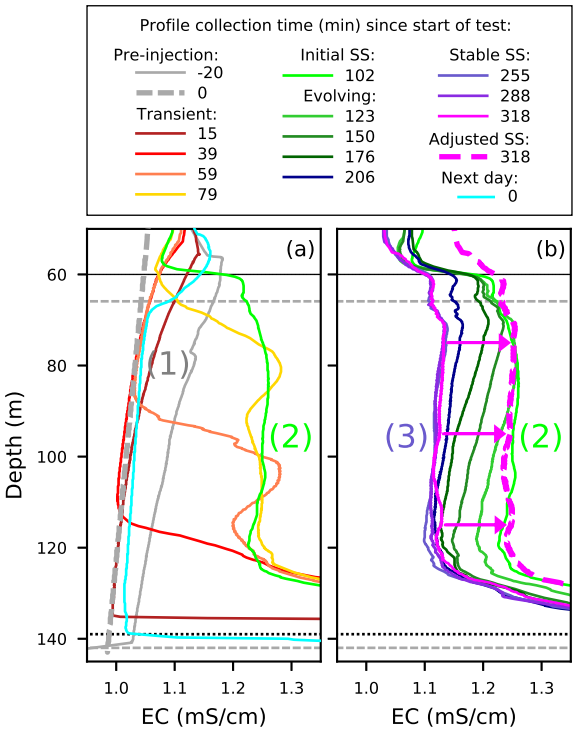

Figure 3.5: Tracer profiles from LHRP4 during the test with injection at the bottom and pumping at the top: a) pre-test to 102 minutes (tracer arrival at pump) and (b) 102 minutes to end of test, showing (1) shift of the pre-injection (background) EC profile, (2) the initial dilution profile and (3) the eventual steady-state dilution profile.

regimes respectively. The difference between the two is likely due to differing flow regimes through the middle part of this well. That is, flow in the downward direction (19 l/ min) was laminar to transitional, whereas flow in the upward direction (39 l/ min) was above the turbulent threshold (30 l/ min). Turbulence homogenises flow velocities and causes turbulent diffusion, which reduces dispersivity.

Intraborehole flow in this well was a complicating factor in the first test. Borehole flowmeter data collected in ambient conditions showed downwards head-driven flow from the upper aquifer zone into the lower zone (data not shown). So, EC in the well prior to pumping was dominated by the upper zone. Whereas during pumping (from above the screen) EC in the well was that of water drawn upwards from the lower zone. However, the water produced from the lower zone was actually (in part) the intraborehole flow plume (i.e. water from the upper zone!), until such time as the plume was purged.

In analysing the data from the first tracer test we identified that the upper zone had an EC of approximately 0.12 mS/cm higher than the lower zone. This manifested in the tracer test in three distinct stages, indicated by the numbering on Figure 3.5: (1) there was an initial period during pumping, prior to starting the test, where EC in the well decreased as water from the lower zone was drawn upwards, replacing the water from the upper zone. This is shown in Figure 3.5a by the difference in the profiles at -20 mins and 0 mins; (2) after the transient phase of the test, once the tracer had reached the pump, theory dictates that the tracer profile should remain steady, which should have occurred at around the 102 min profile (Figure 3.5a). Prior to this time, inflow from the lower zone was of consistent

EC (note 39, 59, 79 and 102 min profiles plotting over each other at approximately 1.25 mS/cm), interpreted to be from the intraborehole flow plume; (3) but, rather than remaining steady in the 102 min position, the profile then shifted leftwards on Figure 3.5b, starting with a decrease at the lower inflow zone, which propagated upwards until a steady-state was reached, with multiple identical profiles obtained (255, 288 and 318 min, Figure 3.5b). This is interpreted to be the period during which there was a decreasing fraction of intraborehole flow plume water inflowing to the well, before the plume was fully purged (176 min profile). But it wasn't until the consistent EC of native groundwater had travelled the length of the well that a stable tracer profile was established (255 min profile).

On completing this test, pumping continued (67 l/ min at 139 m, maximum pump insertion depth) for 20 min after tracer injection ceased, to remove as much of the tracer as possible ahead of the next test, with injection and pumping in reverse positions. The next day, prior to starting the test, pumping continued for 138 min (67 l/ min at 139 m) and multiple EC profiles were collected to confirm a stable initial EC profile. This stable profile (cyan curve in Figure 3.5a) is similar to the pre-injection profile used for analysis of the first test. It also shows residual high concentration of tracer in the bottom of the well, even after considerable purging. This together with the high EC at the injection point (139 m) indicates very little flow from beneath, and places the base of the lower producing zone at approximately 140 m.

The dataset used in the tracer dilution analysis of the first test (Figure 3.4a) is essentially that shown in Figure 3.5a, except that the 102 min profile was replaced with the 318 min profile (as shown by the arrows in Figure 3.5b) because it provided better resolution of the inflow features. The test also relies on a stable background tracer concentration, so we estimated this from the parts of the transient profiles where the tracer front had not yet reached, as indicated by the dashed profile (0 mins) in Figure 3.5a.

With the first test showing the majority of tracer dilution was caused by inflow from the lower zone, it seemed clear that a lesser proportion of inflow was sourced from the upper zone. Thus, the tracer would travel more slowly downward through the test interval when the pump was placed at the bottom. So the second test was done at a higher pumping rate (66.3 l/ min) to ensure it could be completed in a day. The injection point was at a similar depth as the top of screen (66 m), and the smaller tracer spike (6.5 mS/cm) indicates immediate inflow at this depth. Presence of tracer above the injection point (Figure 3.4c) is attributed to repeated upward passage of the EC sonde, which dragged tracer into the stagnant zone above the screen. Integration of tracer mass associated with this concentration increase above the screen gave 2.9% of total mass lost. So an effective injection rate of 0.54 l/ min was used in model fitting to account for this loss. At all other points in the well this

"mechanical dispersion" effect was overwhelmed by advection.

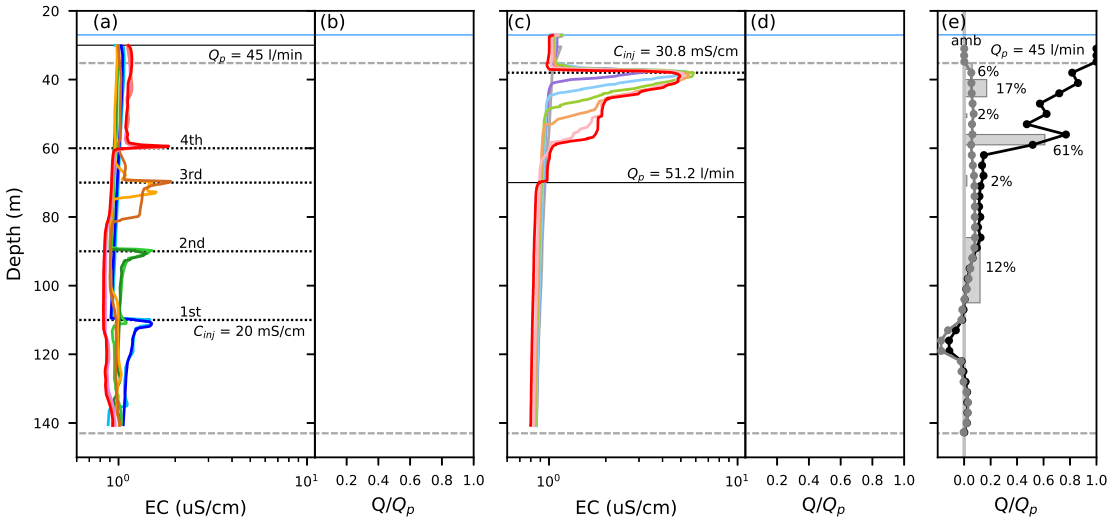

Figure 3.6: WB11AH001: (a) measured tracer profiles with pumping above the screen and the 1st, 2nd, 3rd and 4th injection locations indicated; (b) and (d) tracer dilution data insufficienrt to model flow; (c) measured tracer profiles with injection at the top and pumping at 70 m. Red line is the measured steady-state profile; (e) EM flowmeter data for un-pumped (amb) and pumped conditions (Q normalised by Qp): positive values represent upward flow, negative values represent downward flow, increasing absolute values represent water entering the well, and decreasing absolute values represent water leaving the well back into the aquifer. Also shown: screened interval (grey dashed lines), pumping water level (blue line), pump location (solid black line) and injection location (dotted black line).

3.6.3 Well WB11AH001

Applying the tracer dilution test in well WB11AH001 was problematic because of the low proportion of inflow sourced from below about 60 m, and the strong head-driven intraborehole flow regime that was not overcome by pumping. However, the EM flowmeter readily measured the in-well flow regimes in ambient and pumped conditions, so these results are described first to illustrate the situation (Figure 3.6e). An interesting feature of the ambient flow regime is that upward and downward flow occurred simultaneously over different intervals. Specifically, upward flow of 3.7 l/ min was produced from a zone between 85-105 m and exited the well near the top of the screen. Meanwhile, downward flow of 7.9 l/ min occurred in the zone between 110-125 m. This downward flow regime continued when the well was pumped from above the screen at the maximum achievable rate (45 l/ min). Yield to the pump was mainly sourced from above 60 m, with a small portion from 68-71 m (2%) and 85-105 m (12%).

To test the finding of downward flow below 105 m during pumping, tracer was injected at 110 m (Figure 3.6a, "1st" injection). The tracer indeed travelled downwards. However, when the injection point was raised to 90 m the same downward

transport occurred, at a point where the flowmeter data indicate slow up-flow of around 0.12 m/ min. The injection point was then raised to 70 m and downward transport again occurred, with evidence of a small component of upward transport (flowmeter: up-flow of 0.19 m/ min). Finally, the injection point was raised to 60 m and tracer travelled upwards to the pump (flowmeter: up-flow of 0.22 m/ min at 62 m and 0.71 m/ min at 59 m), with total dilution as expected (Figure 3.2c). The downward transport of tracer in an upward flow field must be due to free convection of the higher density salt tracer (EC: 20 mS/cm) in the relatively slow advective flow of fresher aquifer water (EC: 1 mS/cm) below the main inflow zone. The spike of tracer at 60 m followed by such rapid and near complete dilution indicates that the injection point was right on the base of the major flow zone.

The test was repeated with pumping from 70 m and tracer injected at 38 m, just below the top of the screen (Figure 3.6c). A clear dilution profile was obtained, from a peak concentration of around 5 mS/cm to near full dilution at the pump. The steady-state dilution profile indicates fairly discrete zones of inflow that match those in the borehole flowmeter profile (Figure 3.6e), even providing greater resolution of flowing features. However, the dilution model could not be applied because an excessive amount of dilution was observed. A calculation using Eq. (4) suggests that at least five times the applied pumping rate would be required to explain the observed dilution in pumped discharge (Figure 3.2c, open black circles). But interestingly, the observed first arrival of tracer at the pump can be reproduced if the inflow profile from the flowmeter is used to directly model flow velocities (not shown).

3.7 Sensitivity analysis

The sensitivity of the dilution model to the fitting parameters was assessed using the dataset from well LHRP4 with injection at the top. The results (Figure 3.7) show the effect of varying the individual model parameters by ±10% from the best-fit to the measured data shown in Figure 3.4c. Although the model was insensitive to dispersivity over this range of variation (Figure 3.7a), dispersivity does control the shape of the tracer front when varied over a larger range. To illustrate this, the effect of varying dispersivity by ±50% is also shown (blue lines). A larger dispersivity value increases the time/distance between the leading edge of the tracer front and the steady-state concentration, and vice versa. The model is insensitive to all values of dispersivity at steady-state because the tracer front is no longer in the well. Varying tracer injection rate (Figure 3.7b) and concentration (Figure 3.7c) shifts the position of the steady-state concentration profile without changing the tracer velocity indicated by the transient profiles. In contrast, varying the pumping rate changes both the tracer velocity and the overall amount of dilution indicated

by the steady-state profile (Figure 3.7d). Finally, shifting the background tracer concentration profile has a similar effect on the steady-state profile and a smaller effect on the transient profiles (Figure 3.7e). The pumping rate, injection rate and injected tracer concentration were carefully and regularly measured during the test, and there is little scope for more than 1-2% error. The background tracer concentrations are constrained by the pre-injection profile measured while pumping but before commencing tracer injection, and uncertainty is less than used in this sensitivity analysis.

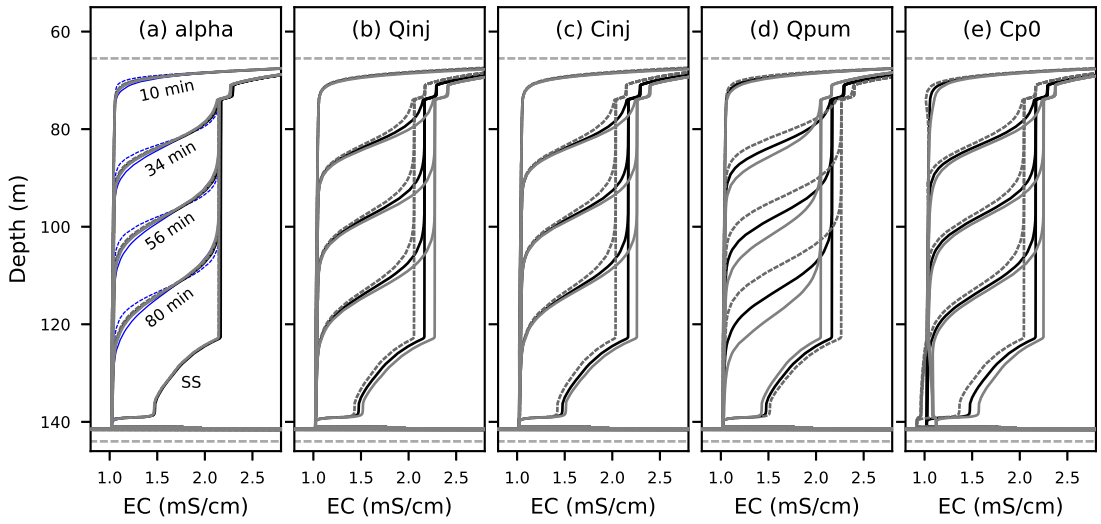

Figure 3.7: Sensitivity analysis of modelled tracer concentration profiles during the transient period (10, 34, 56 and 80 min) and at steady-state (SS). The base-case (black lines) is the model best-fit to the measured tracer profiles shown in Figure 3.5c. Model parameters are varied by +10% (solid grey lines) and -10% (dashed grey lines) for (a) dispersivity (blue lines show ±50%), (b) tracer injection rate, (c) tracer concentration, (d) pumping rate and (e) background tracer concentration.

3.8 Discussion

Successful use of this constant rate pumped tracer dilution test requires that (1) drawdown in the well stabilises so that the inflow profile is consistent (this also applies with the borehole flowmeter), (2) the in-well flow rate increases monotonically between the injection point and pump so that tracer mass is conserved (i.e. pumping must overcome the ambient flow regime so that water/tracer are not lost back into the aquifer), (3) tracer concentration remains sufficiently above background over the test interval, and (4) flow velocity at the injection point is sufficient to overcome tracer density issues (or the loss of tracer to free convection is resolved). These conditions appear to have been met in the tests on well 6628-21204, with very similar flow profiles in both orientations, no evidence of tracer density issues and good agreement with the EM flowmeter data. This indicates that the theoretical

basis of our modelling approach (e.g. laminar flow, no density-driven transport) is sufficiently robust. For well LHRP4, these conditions were also met once we identified the effective injection rates. Here the key to solving the effective injection rate issue (due to partial free convection of injected tracer) was recognising that the correct inflow profile must explain both the transient profiles (tracer front progress indicating flow velocities) and the steady-state profile (overall dilutions). That is, reducing the injection rate allowed the model to fit the steady-state profile without altering the fit to the transient profiles, as illustrated in the sensitivity analysis (Figure 3.7b). By identifying in-well flow velocities, and thus $q_i(z)$, the transient profiles also helped constrain the other unknown, $C_i(z)$, for each aquifer inflow. Thus, while the method can be used with just the steady-state profile, these points highlight how good transient profiles can improve confidence in the results. For LHRP4 the interpreted inflow zones were similar between the two tracer test orientations and the flowmeter, but the flowmeter gave significantly different proportions from each zone. For well WB11AH001 the situation was complicated by heterogeneity and a strong ambient flow regime. Here we examine each of these important issues – tracer density, potential inflow bias with the flowmeter, and issues with strong ambient flows and heterogeneity.

3.8.1 Tracer density issues

The relative importance of forced convection and free convection in a mixed flow regime can be assessed with a mixed convection ratio. Although both forms of convection are always active, for practical purposes mixed convection is considered where free and forced convection are roughly of commensurate strength. A mixed convection ratio, or dimensionless number, allows thresholds to be established, beyond which one type of convection dominates over the other. This has been done for porous media in the groundwater literature (e.g. Massmann et al., 2006), while the fluid mechanics literature provides an analogue for mixed convective flow within a well. van Sommeren et al. (2013) describe experiments in which a dense solute was injected into upward flow in a vertical (square) pipe, for different combinations of flow rate and density contrast each characterised by a densiometric Froude number. Although it is found in a range of forms for different applications, the dimensionless Froude number (Fr) for this purpose is defined as (van Sommeren et al., 2013):

$$Fr = \frac{u_u d^{1/3}}{{B_s}^{1/3}} \tag{3.5}$$

where u_u is the advective flow velocity (L/T) in the well at the point of interest, d is the well diameter (L) and B_s is the buoyant source term, which accounts for the

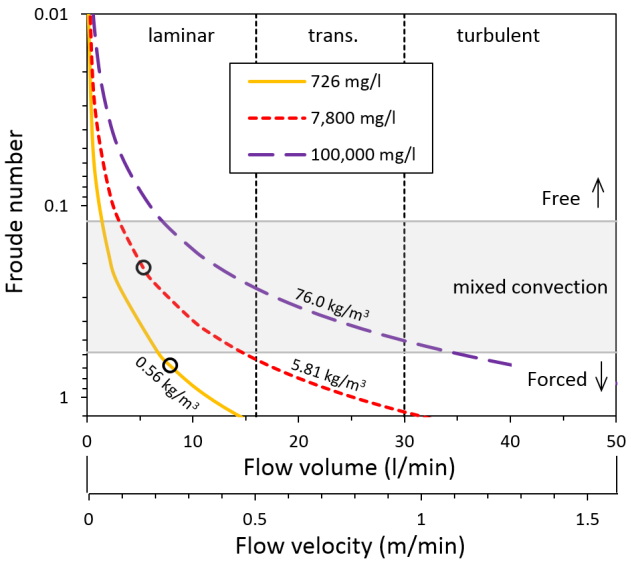

Figure 3.8: Froude number as a function of flow velocity (volumetric flow also indicated for a 0.2 m diameter pipe) for a range of density contrasts between tracer and aquifer water (density difference annotated on plot; salt concentration difference shown in legend). Open black circles indicate the situation at the injection point for the two extremes of density contrast in our tests. Vertical dashed lines show the transition from laminar to turbulent advective flow, and the horizontal grey area shows the zone of balanced mixed convection.

density difference between the two fluids using the Boussinesq approximation as:

$$B_s = g\frac{\rho - \rho_0}{\rho_0}Q_s \tag{3.6}$$

where g is acceleration due to gravity ($L/T.T$), ρ and ρ_0 are the density (M/L^3) of the source (tracer) and background (aquifer water) respectively and Q_s is the source injection rate or inflow rate (L^3/T).

We interpreted their results on the depth of the buoyant mixing zone as a function of Froude number to indicate a threshold for considering tracer density issues (Figure 3.8). At about Fr <0.1 free convection dominated and the mixing zone was large or did not stabilise, while at Fr >0.6 forced convection dominated and the mixing zone was small to negligible, meaning that all of the solute was transported upwards. A region of mixed convection occurred within these bounds (0.1< Fr <0.6) in which a steady depth of mixing developed. Although not tested, we can infer that buoyancy assists rather than opposes transport of a dense tracer in a downward flow regime. The strength of this effect is uncertain, but based on our results from well 6628-21204, which showed very good agreement of both test orientations, we infer that the effect is probably small over the timeframe of this test.

With a threshold established (i.e. Fr >0.6) we can assess the role of free convection in our tracer tests, and provide a tool for planning all types of in-well tracer tests involving a density contrast. This includes those where de-ionised water is used to contrast with the natural salinity of groundwater (e.g. Doughty and Tsang, 2005). For example, if the salt concentration is zero in a well and 726 mg/l in inflowing aquifer water (15 °C), the flow velocity in the well would need to be at least 0.21 m/min for buoyancy not to affect how that water moves. In Figure 3.8 this point is where the orange line drops below the grey mixed convection zone.

With the tracer test described in this paper, the large initial contrast between tracer solution and aquifer water quickly reduces as the low volume injection mixes

with the high volume of water in the well. So it is perhaps more realistic to consider the peak density difference measured in the well during the test. For the purpose of calculating the density difference, solute concentration was estimated as total dissolved solids from the measured EC (TDS mg/l = 0.6 x EC µS/cm). In well 6628-21204 we measured a maximum density contrast of 0.56 kg/m^3 (15 °C) and an upward flow velocity of 0.25 m/min at the injection point. This gives $Fr = 0.68$, which is above the threshold for balanced mixed convection (Figure 3.8), indicating that forced convection dominates, and indeed we did not observe any buoyancy effects. In contrast, in well LHRP4, we measured a maximum density contrast of 5.81 kg/m^3 (30 °C) and an upward flow velocity of 0.17 m/min at the injection point. This gives $Fr = 0.21$, which is within the balanced mixed convection zone, tending towards dominance of free convection (Figure 3.8). This is consistent with our experience of nearly half of the injected tracer sinking downwards instead of moving upwards as intended. While in well WB11AH001, with a density contrast of just 0.45 kg/m^3 (30 °C) the upwards flow needed to be at least 0.21 m/min (Fr ≥0.6) to fully overcome buoyancy issues. This was only achieved at the final injection location at 60 m according to the flowmeter data. Below that, with injection at 70 m ($Fr = 0.56$) and 90 m ($Fr = 0.35$) the tracer moved downwards instead of upwards as intended.

Buoyancy flows can enhance or retard transport (in the vertical dimension) depending on whether the advective flow is moving with gravity or against it (Jackson et al., 1989; Nield and Bejan, 2017). Here the tracer was denser than aquifer water, so it would tend to sink downwards under free convection. Thus, tracer transport would be enhanced when free convection assists forced convection (downward flow), and retarded when it opposes forced convection (upward flow). In well LHRP4, this would cause the proportion of flow from the upper zone to be underestimated in both test orientations. However, in well LHRP4 the first arrival of tracer at the pump was slower with injection at the top than with injection at the bottom despite a higher pumping rate and the assisting downward flow (with gravity). This clearly indicates a smaller proportion of yield from the upper zone. Therefore, we can say that opposing/assisting free convection is not the main reason that the tracer test and flowmeter results differ, although it may in part explain the difference between the two tracer test orientations.

3.8.2 Inflow bias with the flowmeter

The unexpected small-scale vertical fluctuations in the flowmeter measurements at the higher flow rates are repeatable. Two flow profiles are shown in Figure 3.4e, but others were collected at different pumping rates on both well LHRP4 and well WB11AH001, and all show similar fluctuations at consistent depths. This repeatability suggests a physical basis for the phenomenon (e.g. voids existing in the gravel

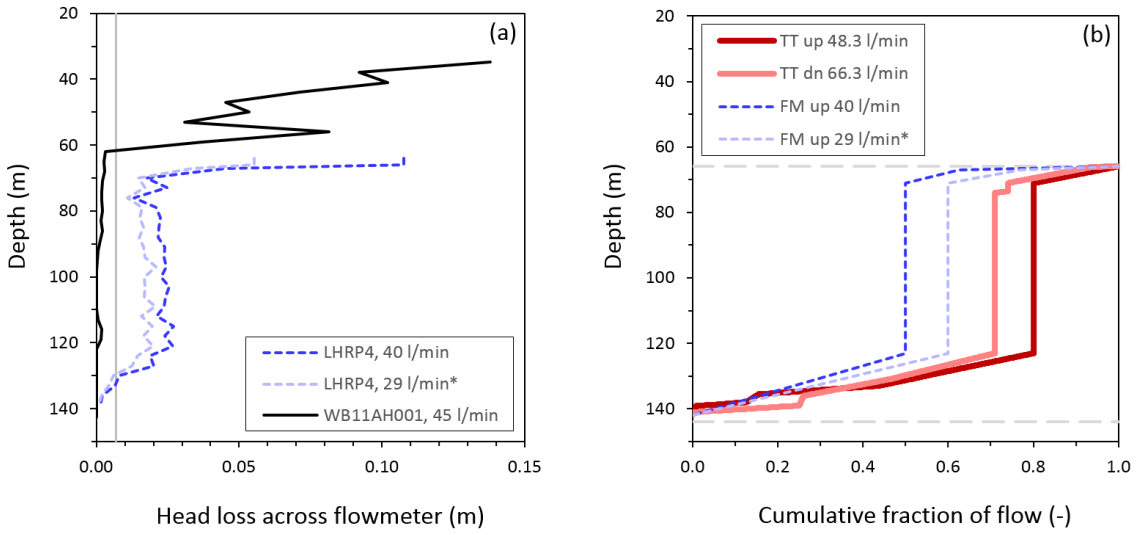

Figure 3.9: (a) Profiles of head loss across the flowmeter calculated with the nozzle equation given in Arnold and Molz (2000). Vertical grey line indicates the 10 l/min threshold below which head loss is considered negligible. (b) Comparison of flow profiles derived from the tracer test (TT) and the flowmeter (FM) in well LHRP4 for the indicated flow orientations and pumping rates. In both legends the asterisk (*) indicates the pumping rate was 50 l/min, but an undersized flow diverter limited maximum flow through the meter to 29 l/min.

pack within the borehole annulus), and hints at a potential issue with the data. When using the flowmeter with the flow diverter, the effective diameter of the well is the 0.025 m instrument annulus. In this situation, Arnold and Molz (2000) showed that head loss across the instrument is increasingly significant at flows >10 l/min. Using the nozzle equation verified by their work, we calculated head loss profiles for our flowmeter data (Figure 3.9a). For reference, the 10 l/min threshold equates to a head loss of 0.007 m. With the major inflow zone near the bottom of well LHRP4, flow rates quickly increased above the head loss threshold, whereas in well WB11AH001 head loss was negligible until the major inflow zone in the upper part of the well. In the upper part of both wells the head loss through the meter exceeded the drawdown (<0.05 m) induced by pumping. Thus it seems clear that the flowmeter was not the lowest resistance pathway to flow at these higher flow rates. Zlotnik and Zurbuchen (2003) clearly show the problem in this situation, with more inflow drawn from the interval between the pump and flowmeter, and the proportion of flow sourced from below (i.e. passing through the meter) being underestimated relative to the unimpeded inflow profile. When we compare the flowmeter profiles to the flow profiles derived from the tracer test (Figure 3.9b), which did not obstruct the wellbore, we can clearly see enhanced inflow from the upper zone in the flowmeter profiles, which converged on the top of the screen. This is also evident in the different positions of the vertical section of the profile (70-120 m in Figure 3.9b): the fraction of flow from the lower inflow zone (i.e. below the flowmeter) was less in both flowmeter profiles than in the tracer tests, particularly at the higher

pumping rate. Thus we conclude that the flowmeter data are impacted by head losses, whereas the tracer test is not, and the correct flow profile is probably an average of the two tracer test orientations.

To avoid head loss issues with the flowmeter, the flow diverter can be under-sized (more than we did) or removed entirely and used with a centraliser (Clemo et al., 2009) or even without one if flows are strong enough (i.e. turbulent) and the trolling mode is used (Newhouse et al., 2005). A bypass flow factor is then included in the instrument calibration or in post-processing the data (e.g. Paillet, 2004a). Newhouse et al. (2005) demonstrate that the EM flowmeter is actually capable of measuring much higher flows than stated by the manufacturer. However, the trade-off is a reduced sensitivity to slower flows because only a fraction passes through the sensor. While a spinner meter could have measured the upper end of the flow regime in our wells (>30 l/min), it would not be sensitive the majority of flow rates encountered. Thus, it is challenging to accurately sense a wide range of in-well flow rates in a single flowmeter profile. A practical solution might be to combine the results of two separate profiles, one with the full flow diverter and another with an under-sized flow diverter to measure the higher flow rates.

3.8.3 Issues with strong ambient flows and heterogeneity

Our attempts to do the pumped tracer dilution test on well WB11AH001 were complicated bystrong ambient flows, heterogeneity and buoyancy issues with the EC tracer at low flow velocities. In the simple theoretical modelling of Poulsen et al. (2018), a weak ambient flow regime (0.5 l/min) was overcome with pumping at 4-5 times the ambient flow rate. However, this field example shows that the ambient regime is not so easily overcome in a heterogeneous environment with strong head gradients. Our pumping at 45 l/min from above the screen only slightly reduced the downward ambient flow occurring in the lower part of the well, while slightly enhancing the overlying upward flow rate (Figure 3.6e). We believe the maximum upward and downward flow rates within this ambient flow regime would be additive when considering a pumping rate to overcome the ambient flow. Thus, while our pumping rate was 3.9 times the total ambient flow rate (11.6 l/min), it seems a significantly higher rate would be needed to reverse the downward flow in the lower part of the well (i.e. to drawdown the water level in the well below the head in the aquifer). We were unable to cause more than 0.04 m of drawdown in this high transmissivity well (Table 3.1), which limited our ability to influence the ambient flow regime.

Although the flowmeter is undoubtedly a practical solution to measure flows in wells like WB11AH001, a carefully designed tracer test could be applied in the interval over which flow can be induced towards the pump. With a highly productive zone near the top, it was difficult to generate flow lower in the well by pumping above

the screen. Our tracer test could have been improved by using a neutrally buoyant tracer in the upward flow orientation, or by placing the pump much lower in the downward flow orientation. For the latter, inflow from the upper producing zone would rapidly transport tracer downwards to the pump. Fitting the dilution model then requires an effective pumping rate. The difference from the actual pumping rate would give the fraction of inflow from the "un-tested" interval of the well below the pump.

3.8.4 Prognosis

Tracer dilution tests are of particular value to assess in-well flows when a borehole flowmeter is not available, but also to provide a complimentary line of evidence. A good starting point is an un-pumped tracer test (e.g. Maurice et al., 2011; Paillet, 2012) to identify the ambient flow regime in the well, to help with designing the pumped tracer test (orientation, injection depth, pumping rate). The ambient flow profile shows the actively outflowing zones, which need to be reversed to inflowing to use the method reported here (successful reversal would be evidenced by tracer dilution in those zones). Without some knowledge of vertical head gradients in the groundwater system the amount of pumping induced drawdown in the well necessary to cause inflow from all aquifer zones is uncertain. However, our experience suggests it would be prudent for the pumping rate to be at least an order of magnitude more than the ambient flow rate. Our method and that of Brainerd and Robbins (2004) is particularly suited to high discharge rates (where water disposal is not an issue) when there is a short tracer travel time in the well, and turbulent flows actually assist with mixing tracer and aquifer inflows in the well. There are practical limitations with long travel times so it is best to design the test to be completed in a single day. Simple calculations of velocities, travel times and Froude numbers for a range of potential scenarios can be used to assist with planning a test. The choice of tracer type should be made with consideration to the potentially competing interests of achieving measurable concentration in pumped discharge and avoiding buoyancy issues at the injection point, which may be subject to low flows even at high pumping rates. Thus, any prior knowledge of flow zones gained from an ambient flow test would be valuable in positioning the injection point so that there is some driving flow. In practice, one must be prepared to do the tracer test in both orientations and/or refine the configuration to optimise the results. If there is a tracer buoyancy issue, an unresolved effective injection rate is problematic for the test (e.g. our first test on well WB11AH001), although it can still provide useful qualitative information about the flow regime. An ideal tracer has zero background concentration and thus provides a wider range of detection, but we believe there is merit in using a salt (EC) tracer because of its ready availability and ease of measurement. Obviously it is limited to situations where EC can be made significantly different than the

background EC over the whole test interval, which could mean using a low EC tracer in saline environments.

The utility of this method could be improved by 1) refining the theoretical basis of the model to properly deal with turbulent flow, 2) experimentally assessing the role of free convection in the upwards and downwards orientations, and 3) testing the utility of the dimensionless Froude number reported here. Alternatively, it would be advantageous to explore the use of a more neutrally buoyant tracer that can be measured at high resolution with a wireline sonde. Examples of such tracers that could be adapted for use in this test include fluorescent dye (e.g. Libby and Robbins, 2014), artificially increased dissolved oxygen (e.g. Chlebica and Robbins, 2013) or artificially altered temperature (e.g. Klepikova et al., 2011; Read et al., 2014).

3.9 Conclusion

This paper presents a combined field method and numerical model for a single-well tracer dilution test to quantify the pumped flow regime in long-screened or open wells. Controlled boundary conditions are established by pumping to create a monotonically increasing flow regime in the well and simultaneously injecting a tracer at the opposite end of the interval to be characterised. The test is unique in its efficacy to characterise the entire length of a well over a wide range of flow rates, requiring little more than the time taken for tracer to travel from the injection point to the pump. Sequentially measured tracer concentration profiles are modelled with the advection-dispersion equation by specifying for each inflow zone: depth interval, background tracer concentration and fraction of total yield. The test results are consistent with EM flowmeter data, especially if density issues with the tracer are avoided or correctly interpreted. The main challenges with EC as a tracer are determining the background concentration for each flowing zone and managing density related issues that arise at low flow rates. This test not only provides an accessible alternative to a borehole flowmeter, but it also provides a complimentary line of evidence to improve resolution of the in-well flow regime over a wide range of pumping rates. It has the potential to provide a wider dynamic range of flow rate sensitivity, particularly in situations where using a flow diverter with the flowmeter is problematic, such as screened and gravel packed wells. This approach, using existing wells, can provide considerable information on aquifer hydraulics and chemistry without the cost of additional drilling.

Chapter 4

Depth-resolved groundwater chemistry by longitudinal sampling of ambient and pumped flows within long-screened and open borehole wells

Published in *Water Resources Research*: Poulsen, D.L., P.G. Cook, C.T. Simmons, D.K. Solomon and S. Dogramaci (2019). Depth-resolved groundwater chemistry by longitudinal sampling of ambient and pumped flows within long-screened and open borehole wells. doi: 10.1029/2019WR025713.

4.1 Introduction

Groundwater chemistry sampled from wells is used to define contaminant plumes (e.g. Einarson, 2006), determine sources of nutrient pollution (e.g. Kendall and Aravena, 2000; Widory et al., 2005) and to assess the timescales of groundwater flow and solute transport using environmental tracers (e.g. Cartwright et al., 2017; Cook and Herczeg, 2000), among many other types of investigation. If the screened or open interval of a well intersects different concentrations, a pumped sample will be an inflow-weighted mixture from all contributing intervals. The chemical composition of a sample is affected by the position and length of the well screen with respect to the intersected distribution of hydraulic conductivity and head (Einarson, 2006; Brassington, 1992), the pumping rate at which the sample was obtained (McMillan et al., 2014; Poulsen et al., 2018), and the history of ambient vertical flow through the well prior to sampling if it has been left un-pumped (Elçi et al., 2001; Mayo, 2010; McDonald and Smith, 2009; McIlvride and Rector, 1988; Poulsen et al., 2018; Reilly et al., 1989; Silliman and Higgins, 1990; Shapiro, 2002). These

factors could cause a constituent of interest to be overestimated, underestimated or missed entirely if the composite sample is not correctly interpreted.

The representativeness of a sample depends on the aims and scale of investigation (Claasen, 1982; Neilsen and Neilsen, 2007). High-resolution contaminant monitoring requires samples from very discrete depth intervals (e.g. < 1 m), whereas regional scale environmental tracer studies can use data from somewhat larger intervals. Although groundwater usually contains a range of ages at any depth simply due to the tortuosity of flow paths through porous media (e.g. McCallum et al., 2015), the value of age tracers is diminished by excessive mixing in wells (Cook et al., 2017; McCallum et al., 2014; Müller et al., 2016), and bias caused by recovery of ambient flows (Poulsen et al., 2018; Zinn and Konikow, 2007).

The ideal approach for reliable depth-resolved sampling is to use a multi-depth nest of piezometers or an engineered multi-port system. These installations are necessary for contaminated sites (usually shallow depths) and detailed investigations, to ensure accuracy of samples and avoid aquifer cross-contamination. However, their cost escalates for more regional scale studies, particularly when a large vertical interval of an aquifer system needs to be investigated. There is therefore a financial and practical incentive to make the most of existing infrastructure, including supply or dewatering wells that have long screened or open intervals. The challenge with such wells is to identify the depth interval and chemistry of specific inflows. Although straddle packers can be used in some situations, they are compromised where flow can bypass the packer through the gravel pack around the well screen, between a packer and a rough borehole wall or even in the formation adjacent to the packer (Nilsson et al., 1995b; Taylor et al., 1990). A range of alternative methods to identify the composition of inflows have been reported. Baffle systems and separation pumping (Harte, 2013; Lerner and Teutsch, 1995) are complicated, equipment- and labour-intensive, and uncertain. An approach that has found more wide practical application uses the flow regime in the well while it is being pumped. Depth-specific samples and measurements of vertical flow rate before and after inflowing zones are combined in a mass balance to identify the concentration of inflowing groundwater. Collar and Mock (1997) appear to be the first to report this method, but it was subsequently adopted by the US Geological Survey (Izbicki et al., 1999; Izbicki, 2004) and used to identify water quality issues (arsenic and salinity) in operational supply wells (Goldrath et al., 2015; Halford et al., 2010; Izbicki et al., 2008, 2010, 2006, 2005; Jurgens et al., 2014; Landon et al., 2010; O'Leary et al., 2012, 2015; Smith, 2005). Where such wells are regularly pumped at a high rate, the effect of ambient flows will be minimised and inflows at all depths are likely to be groundwater native to the source interval. However, where such wells are left un-pumped, the vertical flow regime driven by a natural vertical head gradient is highly relevant, presenting both a problem and an opportunity.

Ambient flow is very common in un-pumped wells (Elçi et al., 2003), and over time a plume develops in the aquifer zone(s) with lower head, displacing the native groundwater. These ambient flows can be large (e.g. 800 L/min, Bexfield and Jurgens, 2014), but even low flow rates can have significant implications for sampling (e.g. 0.5 L/min, Poulsen et al., 2018). The problem is that a pumped sample is then biased towards the chemistry of the zone with higher head until such time as the plume is removed, which is often prohibitively large (e.g. Mayo, 2010; Poulsen et al., 2018, 10^3 well volumes). The opportunity offered by an ambient flow regime is that the higher head zone(s), constantly producing native groundwater, can be directly sampled without purging or pumping. This was suggested in discussion by Shapiro (2002), and by Paillet (2004b) with reference to one field application (Paillet and Thomas, 1996), but the concept does not appear to have been explicitly presented in the literature.

To this end, in this paper we comprehensively show how the groundwater chemistry of discrete intervals within a long-screened well can be determined from depth-specific sampling in the ambient and/or pumped flow regimes. A key point of difference from previous studies is the focus on the ambient flow regime, which can actually provide better sampling conditions than while pumping. We verify the approach with discrete samples from a nest of piezometers, and in doing so provide insight into the range of ages present in an undisturbed groundwater system in the Pilbara region of Western Australia.

4.2 Theory

Figure 4.1 shows a conceptual diagram of a groundwater system including three aquifers separated by aquitard material. An ideal sampling installation provides representative samples from short screens isolated in each aquifer (Figure 4.1a). In contrast, a long-screened well connects these aquifers and provides some mixture of the inflows, which mix in the well when it is pumped (Figure 4.1b). If the well is left un-pumped, intraborehole flow redistributes water between aquifers (Figure 4.1c). Aquifer-well fluxes depend on the hydraulic head in the well (h_{av}) relative to head (and transmissivity) in the intersected aquifer intervals (h_1, h_2, $h_3 \ldots$ h_z). Figure 4.1a shows the head in each of the three hypothetical aquifers, indicating a downward vertical gradient. When pumped, drawdown in a well may or may not be sufficient to create inflow at all depths (McMillan et al., 2014; Poulsen et al., 2018). In Figure 4.1b the pumping water level in the well is below the head in all three aquifers, so all are inflowing. But, when the well is not being pumped (Figure 4.1c) its water level is some average of the three aquifers, according to the intersected hydraulic conductivity and head distribution (sometimes referred to as the blended water level (e.g. Quinn et al., 2015)). In this example, water inflowing

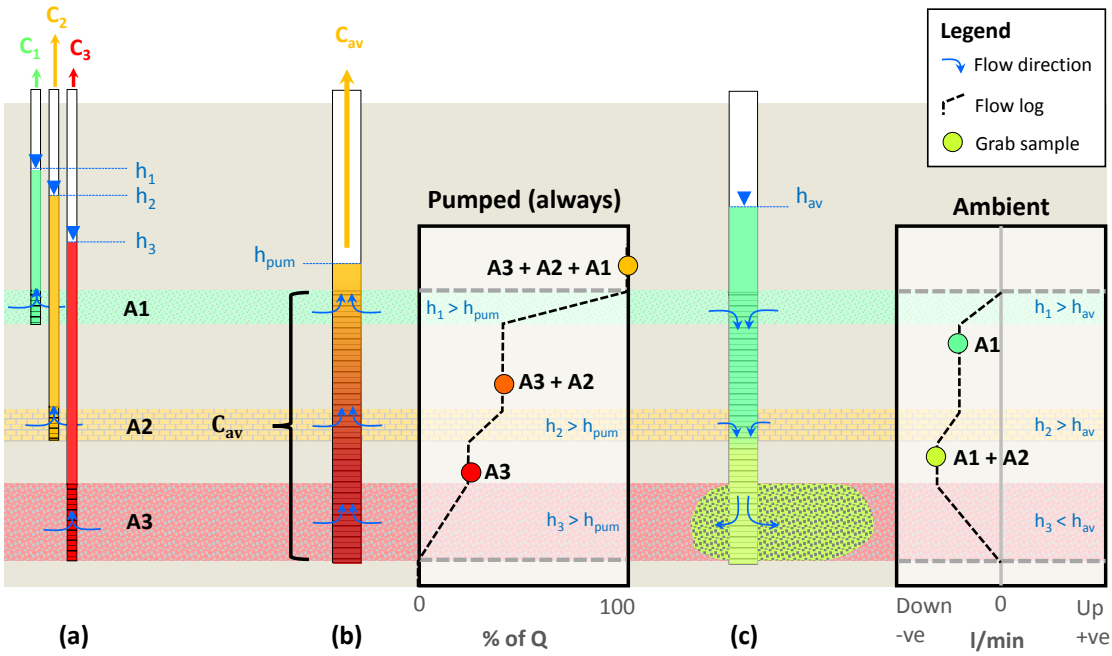

Figure 4.1: Hypothetical three-aquifer system (each aquifer is assigned a colour to help visualise water movement and intermixing). (a) Nest of piezometers providing representative heads and chemistry for each aquifer. (b) Long-screened well providing an inflow-weighted mixture of the chemistries from each aquifer (always pumped such that water level in the well is below all three aquifers). (c) When un-pumped, the long-screened well is a conduit for vertical flow between the aquifers. Also shown for (b) and (c) is the associated profile of vertical flow rates in the well as a function of depth (as either a fraction of the pumping rate or as volumetric flow). The coloured dots on the flow logs illustrate the composition of water in the well at key depths in these two flow regimes, either from a discrete source or a mixture of two or more sources.

from the first two aquifers (A1 and A2) moves vertically downwards in the well and outflows into the third aquifer (A3), displacing the native groundwater. A subsequent pumped sample would be biased towards the chemistries of the first two aquifers, and the third aquifer is not sampled until the intraborehole flow plume is purged. Purge volumes can be excessively large because plume volumes are large (ambient flow rate multiplied by length of un-pumped period), only a fraction of pumped discharge is sourced from the affected zone (unless packers are used), and matrix diffusive processes may delay recovery of some invading water.

For a well affected by intraborehole flow, we contend that a clearly defined ambient flow regime actually provides better sampling conditions than the pumped regime (potentially making the latter unnecessary). This is because the in-well chemistry at all depths is the product of an established flow regime, and inflows are exclusively from zones that produce native groundwater. In contrast, pumping alters the pre-existing flows and a certain time is required for the chemistry at all depths in the well to be representative of the new flow regime. Although a hydraulically steady flow regime occurs as soon as drawdown stabilises, a chemically steady regime is not reached until the inflow located furthest from the pump reaches the pump (Reilly and LeBlanc, 1998; Martin-Hayden, 2000; Martin-Hayden et al.,

2014) and inflow compositions stabilise (e.g. following purging of an intraborehole flow plume). This travel time is a function of the inflow distribution to the well, and in particular it is inversely related to the fraction sourced from the inflowing zone most distant from the pump.

In a clearly defined and chemically steady flow regime, the chemistry at any depth in a well is a mixture of all upstream inflows (indicated by the grab samples in Figure 4.1b and 4.1c). If concentration and flow rate are measured before and after an inflow zone, then the concentration of the inflow is given by (Collar and Mock, 1997):

$$C_i = \frac{Q_a C_a - Q_b C_b}{Q_a - Q_b} \tag{4.1}$$

where the concentration (C) from a given aquifer interval (i) is calculated to explain the observed concentration change in the well at the measured flow rates (Q) before (b) and after (a) the producing interval. This assumes all significant inflows are accurately identified, complete mixing of inflow with flow already in the well, no loss of flow between the samples and that chemical alterations within the well are negligible. The resulting concentration is averaged either over a unique inflowing interval identified in the flow profile, or simply the spacing between the depth-specific samples. This approach is similar in many ways to using longitudinal sampling in a river to estimate the chemistry of groundwater inflows to the river (Batlle-Aguilar et al., 2014). As such, there is a minimum distance required for mixing of inflows with flow already in the well, which is much greater in laminar flows than turbulent flows. In either case the cross-sectional area of a well is usually small enough that the sampling process itself, even with low-rate pumping, will likely introduce convergent flow at the pump intake depth, thereby effectively sampling all flow lines in the well, even in an otherwise laminar flow regime.

4.3 Site Description

We applied this sampling approach in three inactive supply wells in the Pilbara iron ore mining region of Western Australia (Figure 4.2, Table 4.1). The wells are in the southeastern Hamersley Basin situated on relatively wide plains, which are surrounded by hills of banded iron formation and intersected by dykes and faults. Further information on the physiography, climate, geology and general hydrogeology of the area is available in existing publications (Cook et al., 2017; Dogramaci et al., 2012; Dogramaci and Skrzypek, 2015; Rojas et al., 2018). This paper mainly demonstrates the sampling concept and method, so we focus on the immediate borehole environment more than the broader hydrogeological context that would inform a particular avenue of investigation.

Lithological logs for the wells (Figure 4.3) indicate that the regional aquifer is mainly the Paraburdoo Member of the Wittenoom Formation, which is part of the

Hamersley Group. This was logged as dolomite, but it is more widely known to include interbedded shale, dolomite, sandstone and mudstone. Groundwater flows mainly in weathered and fractured zones within this variably competent formation. The overlying Tertiary Detritals also variably form aquifers or aquitards depending on the amount of silt and clay matrix filling pore space in the sand and gravel. WB11AH001 intersected material logged as fault gouge, indicating a geological complexity at this location, which has deformed and smeared different formations together.

Well LHRP4 was installed in 2006 and is located on Pebble Mouse Creek, a tributary to Welli Wolli Creek (Aquaterra, 2007). Although relatively close to mining (∼2 km, Figure 4.2b), it is unaffected by dewatering induced drawdown because an intervening dolerite dyke forms a hydraulic barrier (Figure 4.2c). Upstream of the dyke a modest hydraulic gradient (0.00015 m/m) prevailed, while across the dyke there was a 40 m drop in groundwater level. Records show that a water level drop across the dyke was present before mine dewatering commenced, but it was about half as much. Wells WB11AH001 and WB11HD6001 were installed in 2011 and they are remote from mining or notable surface water features (Aquaterra, 2011). Drilling was completed with mud rotary (LHRP4) or air percussion (WB11AH001 and WB11HD6001) methods. The wells are constructed of machine slotted (1 mm aperture) PVC pipe with a nominal 0.2 m internal diameter, packed with graded (3.2 - 6.4mm) clean gravel, and completed at the surface with a concrete pad and cover (Figure 4.3). In LHRP4, telescoping borehole diameters were used (0.45, 0.32 and 0.27 m), while for WB11HD6001 and WB11AH001 the holes were consistently 0.3 m, giving a nominal gravel pack thickness of 50 mm. The gravel pack has much higher conductivity than the native geology (e.g. gravel: ∼250 m/d, dolomite: ∼0.5 m/d, Freeze and Cherry (1979)), except perhaps in the most productive aquifer zones, and as such it could act as a conduit for vertical flow outside the well casing. In LHRP4 the gravel pack above the screen may enable water from shallower depths to contribute to inflow at the top of the screen.

Table 4.1: Details of the long-screened wells.

Parameter	LHRP4	WB11HD6001	WB11AH001
Elevation, m AHD	621	669	665
Easting, m MGA Zone 50	715628	738339	741389
Northing, m MGA Zone 50	7452508	7442083	7441794
Screen interval, m ToC[a]	65.9-141.8	34.5-155	35.2-143
Diameter, m	0.195	0.203	0.203
Transmissivity, m^2/d	12,917[b]	2690-6360[c]	2030[c]
Intraborehole flow[d], l/ min	-6	-5 and +7	+1
Blended water level, m ToC	27.54	27.20	22.60
Drawdown @ 40 l/min, m	<0.05	<0.03	0.01
Well vol. (water filled casing and screen), litre	3420	3748	4285
Purged vol. (start-end sampling), well vol.	4.6-6.5	3.0-5.0	2.8-4.1

[a]Top of Casing (ToC) ∼ 0.5 m above ground level; [b](Aquaterra 2007); [c](Aquaterra 2011)
[d]downward flow –ve, upward flow +ve

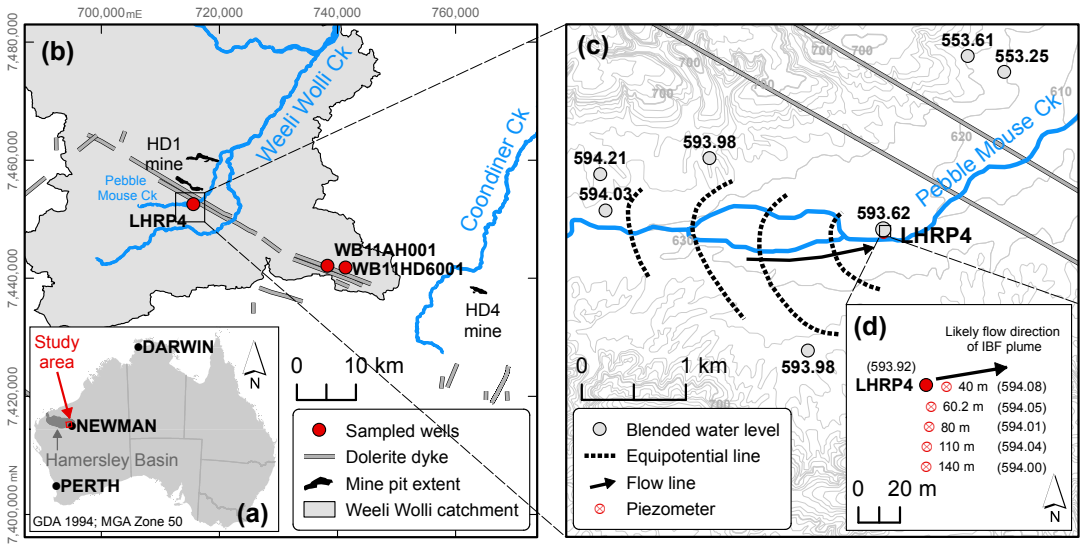

Figure 4.2: (a) Location of the study area in the Hamersley Basin, Western Australia; (b) location of the sampled wells in the study area, showing their proximity to the Hope Downs 1 (HD1) and Hope Downs 4 (HD4) mines; (c) locality of LHRP4 showing topographic elevation contours relative to the Australian Height Datum (m AHD), groundwater hydraulic head contours based on the blended water levels shown next to the symbols (m AHD, taken Jun-Aug 2016) and interpreted groundwater flow direction; (d) position of the multi-depth nest of piezometers adjacent to LHRP4, indicating the likely flow direction of the intraborehole flow (IBF) plume from LHRP4 at 130-140 m depth. Piezometer completion depths are indicated, with groundwater elevations in brackets (m AHD, taken 30 Apr 2017).

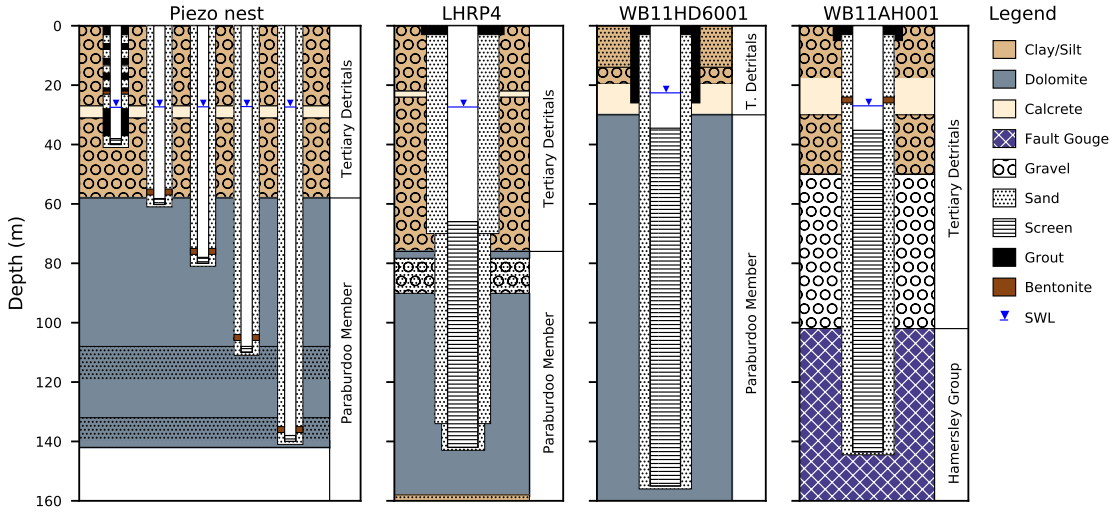

Figure 4.3: Lithological logs, construction details and measured standing water levels (SWL) for the long-screened wells and piezometers adjacent to LHRP4. Diagrams not to scale. Piezometers are spaced approximately 10 m apart as shown in Figure 4.2d.

4.4 Methods

4.4.1 Environmental Tracers

Environmental tracers that indicate groundwater age are used in this paper to demonstrate the utility of the sampling approach. Cook et al. (2017) describe the use of chlorofluorocarbons (CFCs) and radiocarbon (^{14}C) to characterise young and old groundwater respectively, in the context of this study area. In summary, CFCs are an event marker whose concentrations have increased from zero over the last 60 years due to anthropogenic release. The maximum expected concentration is approximately 180 pg/kg for CFC-12 in water that was recharged in the years 2003-2004. ^{14}C activity in groundwater decreases with time by radioactive decay at a known rate (half-life of 5730 yrs) and this can be related to the time since recharge, in the age range of 200-30000 yrs. Here we consider the reported percent modern carbon (pmC) as an indicator of groundwater age, without applying any corrections for rock-water interactions. We also measured noble gases (He, Ne, Ar, Kr and Xe) and specifically looked at helium because its concentration in groundwater is known to increase with time due to radiogenic release from aquifer materials, among other sources (Solomon, 2000). Prior to recharge, precipitation in equilibrium with the atmosphere at this site will contain about 4.07×10^{-8} cubic centimetres of He per gram of water at standard temperature and pressure (ccSTP/g). A measurable increase of He in groundwater is expected after a residence time on the order of 10^3 years for typical regional aquifers (Solomon, 2000).

4.4.2 In-Well Flow Measurement

The in-well flow regimes were measured with an electromagnetic (EM) borehole flowmeter (Century Geophysical LLC, model 9721, response range 0.05–40 $\pm$0.02 l/min). Measurements were made with the instrument held stationary at regular depths, and with a flow diverter (rubber gasket) in the space between the instrument body and well casing, aiming to force all flow through the sensor. While this maximises the sensitivity to low flow rates, it has been found that friction related head loss becomes increasingly significant when flow through the sensor increases above a threshold of about 10 l/min (Arnold and Molz, 2000). Specifically, the nozzle equation given by Arnold and Molz (2000) indicates head loss across the sensor (0.025 m inside diameter) of 0.007 m at 10 l/min and 0.11 m at 40 l/min, the maximum flow rate used in this work. In comparison, water level drawdown in the wells used in this study was $<$0.05 m when pumping at 40 l/min. Given the highly productive nature of these wells we expect resistance to flow through the meter could be greater than that for inflow from the overlying zone between the meter and the pump (Zlotnik and Zurbuchen, 2003; Ruud et al., 1999), causing the meter to under-measure borehole flow at rates above about 10 l/min. Flow may also bypass the meter in the gravel

pack (or void) around the well screen. This zone shrinks as the meter is raised in the well, and eventually all discharge is forced through the sensor at the top of the screen. Together theses effects can result in an over-estimate of the fraction of inflow sourced from near the top of the well. We have not attempted to account for this head loss related bias in the analysis, but the 10 l/min threshold is indicated on the borehole flow plots, and it is dealt with where relevant in the results. In addition to this systematic bias in flow measuring, practical uncertainties with measuring the flow profiles include an imperfect seal of the flow diverter, and turbulence, which can cause random noise in the measurements. We represented this uncertainty in the analysis by assigning an error of ±5%. This compares to the generally much lower manufacturer-stated error of ±0.02 l/min in ideal conditions.

The flowmeter was calibrated in the water-filled blank casing above the top of the screen in each well. A stationary zero-flow point was followed by raising the instrument at a known rate and using the well diameter to calculate flow rate through the sensor. In pumped conditions, the stationary meter was also calibrated to the known discharge rate. Assuming the well diameter remains constant, any bypass flow due to an imperfect seal of the diverter in the well is built into the calibration.

4.4.3 Sampling and Analysis

Depth-specific samples were obtained from the ambient and pumped flow regimes in each of the three wells in late April 2018 with an air operated submersible piston pump (Bennett Sample Pumps, Inc., model 1400-6 ¾ inch). A low flow rate (0.5–1 l/min) was used so that the prevailing in-well flow regime was altered as little as possible. We had *a priori* knowledge of the ambient flow regime to inform the choice of sampling depths, so sampling was done on arrival at each well, at progressively increasing depths, prior to any other disturbance. After sampling, the ambient flow regime was measured to establish the conditions prevailing at the time of sampling. Then a pumped flow regime (40 l/min) was created with a submersible pump (Grundfos, model SQEN3) placed above the screen. Sampling commenced after between 3 and 6.5 well volumes had been purged, which occurred while the pumped flow profile was being measured. In the pumped flow regime the procedure started with a sample from just above the screen, followed by progressively increasing depths, and ending with another sample from above the screen. The samples from above the screen represent the composite of all inflows to the well, and the difference between these samples indicates the degree to which the chemistry of inflows was stable during the sampling procedure. At each depth, for both ambient and pumped sampling, the sampling line was purged of its volume (15 litres) and field parameters (electrical conductivity, pH, and reduction-oxidation potential) were observed to be stable before to sampling. In total about 30 litres of water was

removed during sampling at each depth, which is approximately the same as the volume of water contained in 1 m of well casing, so the sample can be attributed to the intended depth even in a weak in-well flow regime.

Samples were collected for ^{14}C, CFCs, noble gases and major/minor ion chemistry in new and unused containers, rinsed with sample prior to filling. Samples for ^{14}C were collected in 500 ml High Density Polyethylene (HDPE) bottles and analysed at the GNS Science Rafter Radiocarbon Laboratory (New Zealand). Results are given as percent modern carbon (pMC) according to the convention described in Stuiver and Polach (1977), with a one standard deviation (1σ) analytical precision of between 0.3 and 0.4 pmC. Samples for CFC analysis were collected (bottom filled, zero headspace) in 125 ml clear glass bottles with metal screw lids and analysed for CFC-11, CFC-12 and CFC-113 concentrations at GNS Water Dating Laboratory (New Zealand). Only the CFC-12 values are included in this paper, as measured. The analytical precision (1σ) of these analyses was between 1.2 and 3.6 pg/kg for CFC-12, and the detection limit is approximately 5 pg/kg. However, sampling was done through nylon tubing, and this may introduce contamination of up to 5 pg/kg for CFC-12 (Cook et al., 1995). Together these errors mean that reported CFC-12 concentrations below about 10 pg/kg are generally indistinguishable from zero. We consider precision of the results by comparing duplicate samples, because this better represents variability due to common sampling issues with dissolved gases, as described by Cook et al. (2017). The difference between duplicate results was within 20% of the mean value for 75% of samples for CFC-12, suggesting that actual precision (2σ) is in the vicinity of $\pm$20% for this range of measured concentrations. Samples for noble gases were collected in clamped copper tubes and analysed by the Noble Gas Lab at the University of Utah (United States). The total helium concentrations included in this paper have an analytical precision of about $\pm$1%, but the absolute accuracy is $\pm$5% because the high helium concentrations required splitting prior to inlet into the mass spectrometer. Major and minor chemical constituents were collected in 500 ml HDPE bottles and analysed at Australian Laboratory Services (ALS) in Perth. This paper also includes results of composite samples obtained from these wells in June 2016 using the same methods and laboratories. On that occasion, the wells were pumped from above the screen at 180 l/min, with a longer duration of purging (8-10 well volumes) prior to sample acquisition.

4.4.4 Interpretation

The depth-specific samples are interpreted in the context of the flow regime from which they were taken. In each flow regime, the most upstream sample is representative of the average inflow concentration from a single inflow interval, and is subject only to the analytical error, reported here as the 95% confidence interval (2σ). Downstream samples are deconvoluted using Eq. (1), and the estimated inflow

concentration is subject to errors in both the concentrations and flows measured in the well (as given above). A Monte Carlo approach was used to include the error associated with each parameter in the mass balance. The 95% confidence interval from 10000 iterations of a normally distributed variation of each parameter about the measured value is reported.

The profiles of measured in-well flow rates are interpreted to identify inflowing zones, and the increase of flow rate between each pair of depth-specific samples. The minimum signficant inflow is relative to the magnitude of flow already in the well, and the concentration difference between inflows. A physical constraint on the combined interpretation of inflow rates and solute concentration is that concentrations cannot be negative, nor should they be unrealistically high. The practitioner must be alert to either of these situations, which indicate that either the flow profile is in error or that aquifer-well fluxes are more complex than conceived in this paper. We cover the difficulties with flow measurement and potential error in Section 4.4.2 and in the discussion (Section 4.6).

4.4.5 Multi-Depth Nest of Piezometers

As part of this study, five piezometers were installed (November 2016) in individual boreholes adjacent to LHRP4 (Figure 4.2d). Each piezometer has a single 2 m screen, the bottom of which was placed at depths ranging from 40 to 140 m . This enabled us to assess the effectiveness of the approach for identifying discrete aquifer concentrations using the long-screened well (potential interaction between LHRP4 and the piezometers is discussed in Section 4.6). In all cases, a similar lithology was encountered to that in LHRP4 (Figure 4.3) with 56–62 m of gravelly clays (Tertiary Detritals) overlying dolomite (Paraburdoo Member of the Whitenoom Formation), which included calcareous sand between 108–120 m and 132–140 m. Drilling was achieved with air percussion (0.1 m diameter borehole) and the 50 mm machine slotted PVC piezometers were gravel packed, except for a 2 m bentonite seal placed just above the screen and a concrete surface collar. Unfortunately, the intervals above the bentonite seals were gravel packed instead of grouted, and these may act as conduits for some vertical flow along the boreholes. We acknowledge that this may cause cross-contamination of water between depths, potentially impacting the depth-discrete nature of samples from these piezometers. Although this remains an area of uncertainty, the data presented in this paper show significant differences of tracer concentrations with depth, so any such impacts appear to be minimal. Five months after installation the piezometers were developed by pumping at least 10 casing volumes from above the screen at 10 l/min with a submersible pump (Grundfos, model MP1). Drawdown was small in all piezometers (<0.4 m, except 2.2 m in the 60 m piezometer), indicating productive aquifer material was intersected. Later (September 2017), each piezometer was further pumped of 10-20 casing volumes

before being sampled for the same suite of tracers as the adjacent long-screened well using the same methods. With dissolved gases being sampled (CFCs, noble gases), the large purge volumes, combined with the time elapsed since drilling, were aimed at removing any drilling related modern air contamination of the aquifer.

4.5 Results

Laboratory analysis of samples from the three long-screened wells (Table 4.2) returned in-well concentrations of CFC-12 ranging between 7.9 and 70.7 pg/kg, ^{14}C between 17.1 and 25.7 pmC, He between 9.2×10^{-8} and 4.9×10^{-6} ccSTP/g and TDS between 489 and 611 mg/l. CFCs showed the most evidence of stratification so we use CFC-12 to demonstrate how chemistry measured in each well can be related to the chemistry of defined depth intervals in the surrounding aquifer. We then provide depth profiles for all four of these tracers and compare the interpreted aquifer concentrations from LHRP4 with those measured in the adjacent piezometers. As a general theme, the ambient flow regimes provided good estimates of aquifer concentrations from defined inflowing zones, while the pumped regimes were complicated by returning intraborehole flow.

4.5.1 LHRP4

The ambient flow profile from LHRP4 shows a downwards vertical flow regime (Figure 4.4a). Figure 4.4b illustrates this, with inflow of native groundwater from two main zones, one at the top (66–70 m, 3.5 l/min) and the other near the bottom (123–130 m, 1.5 l/min), and smaller contributions from the intervening interval (1 l/min), all of which outflowed back into the aquifer at the bottom of the well (130–140 m, 6 l/min). This shows a downward vertical head gradient in the aquifer system, which was confirmed by head measurements from the nested piezometers, with a decrease of 0.08 m between 60 and 140 m depth (Figure 4.2d). The sample taken at 70 m depth in the ambient regime is representative of native groundwater from the upper inflowing zone (which may include a contribution from the interval above the screen, flowing in the gravel pack), with 70.7 ±14 pg/kg of CFC-12 (Figure 4.4a). Below this there were considerable decreases in CFC-12 concentration but little increase in measured flow rate. This caused the mass balance to give negative concentration values for inflowing groundwater, which is impossible. However, zero CFC-12 (reasonable for low permeability material) is given by slightly increasing the proportion of inflow from this intermediate interval (70–115 m), bringing its contribution to 27% of the total ambient flow (red line in Figure 4.4a). Although this flow profile is a slightly poorer fit to the flowmeter data it provides a plausible explanation for the measured CFC-12 concentrations. Beneath this, the measured difference of flow and concentration in the well before (115 m) and after (135 m) the distinct inflowing zone

Table 4.2: All data derived from the long-screened wells, indicating inflow concentrations in the ambient and pumped flow regimes, either from a single sample or calculated using the flow rates and tracer concentration measured in the well before and after an inflow in Eq. (1). Samples are an average of all upstream inflows. Inflow concentrations are averaged over the interpreted source depth interval. Black coloured font indicates inflows that are considered representative (also shown in Figures 4.4, 4.5 and 4.6 for CFC-12).

Source depth interval (m)	Flow rate[a] (l/min)		^{14}C (pmC)			CFC-12 (pg/kg)			He (ccSTP/g)			TDS (mg/l)		
	before	after	before	after	inflow	before	after	inflow	before	after	inflow	before	after	inflow
LHRP4					*ambient flow regime (downward)*									
66-70	0	-3.57	-	25.4	25.4	-	70.7	70.7	-	4.11e-6	4.11e-6	-	588	588
70-95	-3.57	-4.17	25.4	25.7	27.6	70.7	51.4	-64.4	4.11e-6	4.73e-6	8.43e-6	588	556	364
95-115	-4.17	-4.35	25.7	25.2	13.6	51.4	45.3	-97.0	4.73e-6	4.88e-6	8.44e-6	556	560	653
115-135	-4.35	-5.96	25.2	25.1	24.8	45.3	38.1	18.5	-	-	-	560	559	556
					pumped flow regime (upward)									
66-142[b]	0	180	-	24.8	24.8	-	9.0	9.0	-	-	-	-	611	611
66-142[c]	0	40	-	25.5	25.5	-	37.5	37.5	-	4.52e-6	-	-	568	568
66-142[d]	0	40	-	25.6	25.6	-	30.2	30.2	-	-	-	-	570	570
66-70	28.6	40	25.0	25.5	26.7	24.2	37.5	70.9	-	-	-	551	568	610
70-95	28.4	28.6	25.3	25.0	-17.5	30.2	24.2	-827	-	-	-	490	551	9201
95-115	28.2	28.4	25.6	25.3	-11.3	34.5	30.2	-575	4.43e-6	-	-	574	490	-11337
115-135	8.0	28.2	25.6	25.6	25.5	55.6	34.5	26.1	-	4.43e-6	-	578	574	572
135-142	0	8.0	-	25.6	25.6	-	55.6	55.6	-	-	-	-	578	578
WB11HD6001					*ambient flow regime (upward)*									
40-70	0.73	1.01	17.1	18.4	23.7	13.3	27.2	83.9	-	-	-	496	520	616
70-120	0.35	0.73	17.7	17.1	16.6	10.3	13.3	16.1	1.14e-7	1.02e-7	9.01e-8	489	496	502
137-140	0	0.35	-	17.6	17.6	-	13.3	13.3	-	1.16e-7	1.16e-7	-	500	500
					pumped flow regime (upward)									
34.5-155[b]	0	180	-	21.6	21.6	-	28.7	28.7	-	-	-	-	572	572
34.5-155[c]	0	40	-	20.8	20.8	-	17.5	17.5	-	-	-	-	508	508
34.5-155[d]	0	40	-	20.9	20.9	-	16.3	16.3	-	-	-	-	515	515
50-134	0.44	1.08	-	-	-	-	-	-	1.00e-7	1.00e-7	1.00e-7	-	-	-
34.5-50	1.08	40	18.2	20.8	20.8	18.7	17.5	17.5	1.00e-7	9.23e-8	9.21e-8	516	508	508
50-100	0.6	1.08	17.5	18.2	19.0	10.9	18.7	28.5	-	-	-	514	516	519
100-134	0.44	0.6	17.6	17.5	17.0	12.1	10.9	7.6	-	-	-	530	514	531
134-155	0	0.44	-	17.6	17.6	-	12.1	12.1	-	1.00e-7	1.00e-7	-	530	530
WB11AH001					*ambient flow regime (upward)*									
40-65	2.01	7.19	20.4	20.6	20.7	18.7	25.4	28.0	1.09e-7	1.13e-7	1.15e-7	511	522	526
90-104	0	2.01	-	20.6	20.6	-	14.5	14.5	-	1.09e-7	1.09e-7	-	491	491
					ambient flow regime (concurrently downward)									
110-116	0	-5.04	-	20.6	20.6	-	15.7	15.7	-	1.15e-7	1.15e-7	-	529	529
					pumped flow regime (upward)									
34.5-143.5[b]	0	180	-	20.5	20.5	-	28.5	28.5	-	-	-	-	558	558
34.5-143.5[c]	0	40	-	20.5	20.5	-	25.4	25.4	-	1.15e-7	1.15e-7	-	518	518
34.5-143.5[d]	0	40	-	21.0	21.0	-	8.5	8.5	-	-	-	-	528	528
35-40	32.6	40	20.8	20.5	19.4	16.3	25.4	67.2	-	-	-	532	518	456
35-65	2.2	40	-	-	-	-	-	-	1.10e-7	1.15e-7	1.15e-7	-	-	-
40-65	2.2	32.6	20.8	20.8	20.8	7.9	16.3	16.9	-	-	-	531	532	532
90-104	0	2.2	-	20.6	20.6	-	7.9	7.9	-	1.10e-7	1.10e-7	-	530	530
					pumped flow regime (concurrently downward)									
110-116	0	-2.8	-	21.1	21.1	-	7.9	7.9	-	1.19e-7	1.19e-7	-	527	527

[a]downward flow −ve, upward flow +ve; [b]composite sample taken in 2016; [c]start and [d]end of depth-specific sampling.

gave an inflow concentration of 18.2 ±39 pg/kg of CFC-12. This was only slightly affected (15.0 ±45 pg/kg) by the alternative flow profile fit in the overlying zone. The concentration of intraborehole flow invading the aquifer between 130–140 m is given by the sample from 135 m (38.1 ±8 pg/kg).

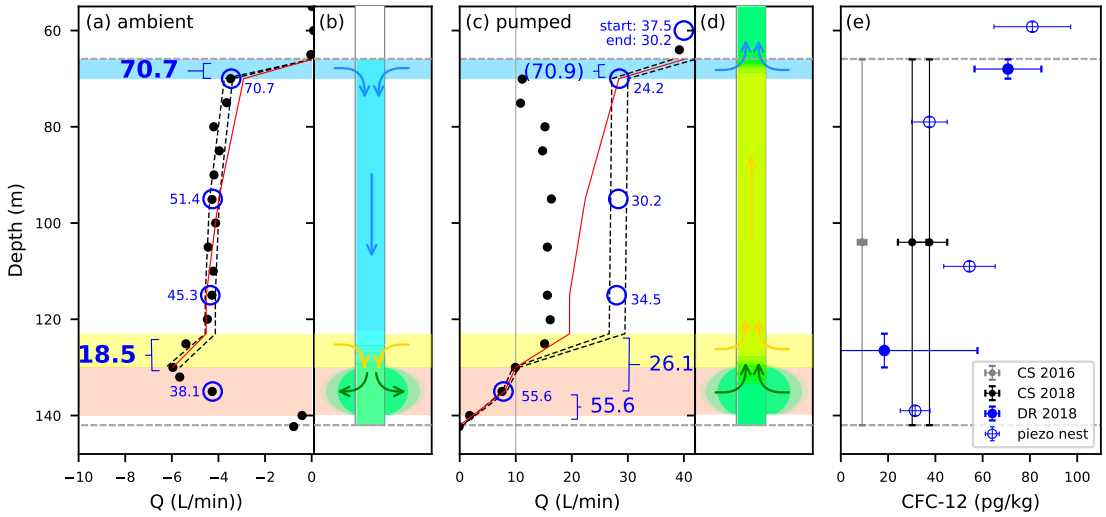

Figure 4.4: LHRP4. (a) Measured ambient flow regime (solid black circles) showing ±5% of measured flow (black dashed lines), depth and measured CFC-12 concentration of samples taken within the well (open blue circles) and interpreted flow profile that best explains the concentrations (red line, see text). Larger font indicates calculated inflow concentration from the aquifer, large bold font indicates where these are representative of groundwater native to the inflow interval. (b) Diagram illustrating the ambient flow regime. The colours in the diagrams and background are intended to help visualise flow and mixing of water from different intervals. (c) Measured flows while pumping at 40 l/min with CFC-12 samples shown on one version of the interpreted flow profile, accounting for bias in the flowmeter data above 10 l/min (threshold indicated by vertical grey line) (other symbology as per (a)). (d) Diagram illustrating the pumped flow regime. (e) Aquifer CFC-12 concentrations identified from depth-resolved (DR) interpretation (ambient regime) and the adjacent piezometer nest (described later), compared to composite samples (CS) pumped from the well. Vertical bars show the sample mixing interval (less than symbol size for piezometers), horizontal bars indicate the 95% confidence interval for the values.

When LHRP4 was pumped, the same flowing zones were observed both using a borehole flowmeter (Figures 4.4c and 4.4d) and a tracer dilution test (Poulsen et al., 2019). Thus, all possible opportunities to sample aquifer chemistry were already provided in the ambient flow regime. The lowermost zone, which was not sampled in ambient conditions, only provided the returning intraborehole flow when pumped. This was evidenced by the high concentration of the sample from 135 m (55.6 pg/kg ±11 CFC-12), a depth at which native groundwater should have been near zero CFC-12 concentration (i.e. less than the overlying zone, identified in ambient conditions Figure 4.4a). The fact that the returning concentration was not identical to that of the invading ambient flow (38.1 ±8 pg/kg CFC-12) is probably due to variable outflow concentration over time, mixing in the aquifer, or/and imprecision in CFC measurements.

The flowmeter's head-loss threshold (10 l/min, see Section 4.4.2 and Figure 4.4c) was exceeded above 130 m in the pumped regime, so flow was increasingly under-measured as it was raised in the well. This problem with flow measurement creates uncertainty with using the mass balance approach to calculate inflow concentrations from the in-well samples. Figure 4.4c shows two possible versions of the flow profile: one (black dashed lines) is consistent with the flow profile identified in the earlier tracer test (Poulsen et al., 2019) and allows the mass balance to give the inflow concentration from the 70–66 m zone identified in the ambient regime (i.e. a known concentration); while the other (red line) shows the flow required to explain the measured in-well concentrations in the 123–70 m interval by assigning the minimum possible concentration (i.e. 0 pg/kg CFC-12) to inflows. This 22% of total discharge is similar to the proportion of the ambient flow regime (27%) required to explain the same decreasing concentrations, but it is inconsistent with the flowmeter and tracer test, neither of which showed inflow from this interval. We provide further discussion of this situation in Section 4.6.

In terms of purging the intraborehole flow plume, we can look at the CFC-12 concentration of pumped discharge. Given that the invading plume contained more CFCs than native groundwater in that interval, we expect to see CFCs in discharge decrease with pumping, until the plume is fully purged. We obtained three composite samples from this well, each after different durations of pumping and found that this was indeed the case (April 2018: 37.5 ±8 pg/kg after 4.6 well vol. and 30.2 ±6 pg/kg after 6.5 well vol.; June 2016: 9.0 ±2 pg/kg after 8.3 well vol., Figure 4.4e).

So evidently the pumped flow regime was not chemically steady during our sampling. However, we avoided that problem, and the flow measurement problem, because the samples from the ambient flow regime actually provided more reliable information on native groundwater inflows. Figure 4.4e shows these depth-resolved aquifer concentrations compared to results from the adjacent nest of piezometers (described further below and in Figure 4.7) and the pumped composite samples taken from LHRP4.

4.5.2 WB11HD6001

A weak upward ambient flow regime was present in WB11HD6001 (Figures 4.5a and 4.5b), with small inflows over much of the well. Flow rates were indistinguishable from zero below 140 m, but a distinct inflow (0.3 l/min) was measured between 137–140 m, which was captured by the sample at 136 m (13.3 ±3 pg/kg CFC-12). Above, the samples were widely spaced and changes in concentration were negligible until 40 m depth, where a significant increase was measured (27.2 ±5 pg/kg). If we take the overall change in flow and concentration between the samples from 70–40 m then the average inflow concentration would be 83.8 ±16 pg/kg. The upward ambient flow (totalling 1 L/min) then invaded the aquifer at the very top of the screen (40–

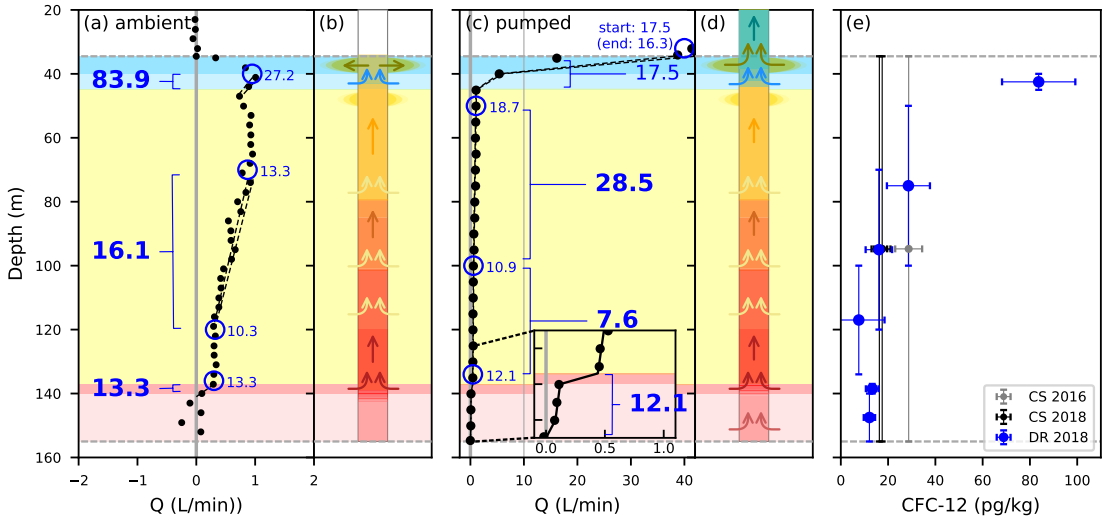

Figure 4.5: WB11HD6001 (see Figure 4.5 caption for description).

34.5 m), with the outflowing concentration identified by the sample at 40 m (27.2 ±5 pg/kg).

When the well was pumped (Figure 4.5c and 4.5d), similar inflows continued below 45 m and nearly all discharge (98%) came from between 34.5–45 m. While pumping, CFC-12 concentrations at depth remained near the lower limit of resolution, but an increase was measured in the well at 50 m (18.7 ±4 pg/kg). A mass balance with the underlying 100 m sample indicates an average inflow concentration of 28.5 ±9 pg/kg over that rather large interval. Above this, the major aquifer zone was calculated to contribute inflow with an average concentration of 17.5 pg/kg, which is lower than expected. But on closer inspection, the measured flows indicate that while some of the discharge (11%) would be native groundwater from the 40–45 m interval, most (87%) was from the 34.5–40 m interval and likely to have anomalously low CFCs due to the presence of the intraborehole flow plume. If we assume the concentration of the plume (27.2 pg/kg) and inflowing native groundwater (83.8 pg/kg) identified from the ambient regime and use the in-well concentration from below (18.7 pg/kg), a mass balance indicates that the sample above the screen should contain 34 pg/kg CFC-12. However, it actually had a lower concentration (17.5 ±4 pg/kg). This mass balance is most sensitive to the concentration of the intraborehole flow plume because that was the majority of discharge. If we consider that perhaps the 40–45 m zone does not always contribute to ambient flows (apparent in the flow profile measured in June 2016, within the generally similar flow pattern), then the concentration of intraborehole flow would actually be more similar to that measured from below (e.g. 13.3 pg/kg, ambient regime). In that case it is possible to account for the low concentration in the pumped sample above the screen while maintaining the higher concentration of native groundwater in the main aquifer zone.

There was little change in the CFC-12 concentration of the composite samples

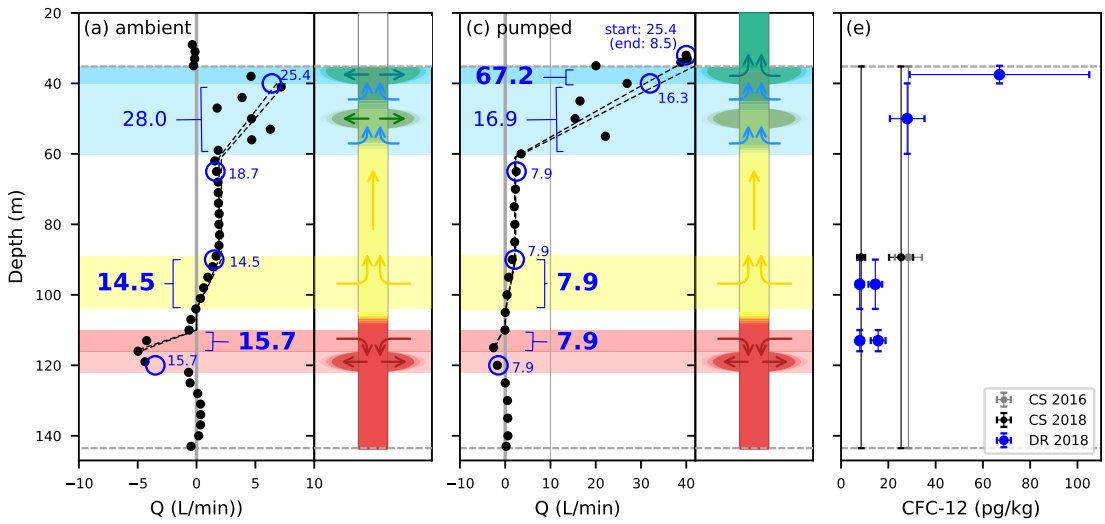

Figure 4.6: WB11AH001 (see Figure 4.5 caption for description).

taken at the start and end of the depth-specific sampling (17.5 ±4 and 16.3 ±3 pg/kg after purging 2.8 and 4.1 well vol. respectively). But a sample taken on a previous occasion, after significantly more pumping (June 2016, 9.9 well vol.), showed a higher CFC-12 concentration (28.7 ±6 pg/kg), as would be expected with a reduced fraction of intraborehole flow in the sample (i.e. intraborehole flow plume had lower CFC-12 concentration). Figure 4.5e compares these composite samples for the entire well screen with the depth-specific interpretations of aquifer concentrations from the ambient and pumped flow regimes.

4.5.3 WB11AH001

The ambient flow regime in WB11AH001 (Figure 4.6a and 4.6b) reflects a hydrogeological situation complicated by a fault zone in the Hamersley Group geology. The transition from Hamersley Group (fault gouge) to overlying Tertiary Detritals at 102 m (Figure 4.3) coincides with a split in the flow regime. Downward flow in the Hamersley of up to 5 l/min occurred in a relatively discrete interval (110–122 m), with CFC-12 concentration of inflowing native groundwater measured at 15.7 ±3 pg/kg. While in the Detritals, 2 l/min of upward flow was sourced between 104–90 m, with a measured concentration of 14.5 ±3 pg/kg. The flow profile then showed further inflow between 60–55 m, nearly all of which left the well between 110–122 m m, before inflowing again between 47–41 m, with an overall addition of 5.2 l/min. These aquifer-well interactions between 55–47 m increased the CFC-12 concentration in the well, so the aquifer concentration must be higher than that of water already in the well from below. The mass balance gives an average of the inflow concentrations (28.0 ±7 pg/kg) using the overall change of flow and concentration in the well across this interval. The intraborehole flow (7.2 l/min, 25.4 ±5 pg/kg) then invaded the aquifer surrounding the uppermost part of the well (35–40 m).

Source depth interval (m)	^{14}C (pmC)	CFC-12 (pg/kg)	He (ccSTP/g)	TDS (mg/l)
38-40	27.3	139.1	1.45e-6	578
58-60	24.4	81.0	4.23e-6	588
78-80	25.4	37.5	4.40e-6	590
108-110	26.0	54.4	4.42e-6	591
138-140	19.3	31.4	5.14e-6	597

Table 4.3: Tracers sampled from nested piezometers adjacent to LHRP4.

In the pumped regime (Figure 4.6c and 4.6d) inflow was mainly from the upper aquifer zone (35–60 m, 91%). Below this, the ambient regime continued, but with slightly enhanced upward flow above 75 m and half the rate of downward flow at depth (110–122 m). CFC-12 concentrations in these inflows (7.9 ±2 pg/kg) were even closer to zero than in the fully ambient condition. A lower concentration was also estimated for the 40–60 m interval (16.9 ±3 pg/kg), while the topmost zone produced water that was estimated to have higher than expected concentration (67.0 ±38 pg/kg) given that it had received the intraborehole flow (25.4 ±5 pg/kg). However, it is possible that the sample was a mixture with even higher concentration native groundwater. Although the two composite samples taken at the start and end of the depth-specific sampling procedure contrarily showed a decrease in concentration with pumping (25.4 ±5 and 8.5 ±2 pg/kg after purging 3 and 5 well vol. respectively), a previous composite sample taken after more pumping at a higher rate (May 2016: 180 l/min, 9.6 well vol.) did show a small increase in CFC-12 (28.5 ±6 pg/kg, Figure 4.6e). When considered as a whole, the interpreted concentrations from both the ambient and pumped regimes (Figure 4.6e) indicate appreciable CFC-12 concentrations in the upper aquifer zone, and near zero below.

4.5.4 Aquifer Concentration Profiles

Figure 4.7 shows aquifer concentration profiles for each of the four tracers. There was evidence of appreciable CFC concentrations at shallower depths in the groundwater systems intersected by all three long-screened wells (65-84 pg/kg, Figure 4.7a), indicating a fraction was recharged less than 60 years ago. The piezometers (Table 4.3 and Figure 4.7) showed generally good agreement with LHRP4, and although CFC-12 concentrations were slightly more elevated at depth, this was within the error of the estimate from LHRP4.

Interpreted aquifer ^{14}C activities equated to values in the range 17-30 pmC for all samples (Figure 4.7b), without correction for exchange with carbonate minerals. The youngest (30 pmC) is similar to the minimum pmC (i.e. oldest) measured in nearby mine dewatering (long-screened wells, mixed samples), which Cook et al. (2017) estimated to be 9900 years without corrections and ∼5000–7000 years with corrections. Corrections aside, this indicates a fraction of old (>5000 years) groundwater at all depths. LHRP4 and the adjacent piezometers showed decreasing values

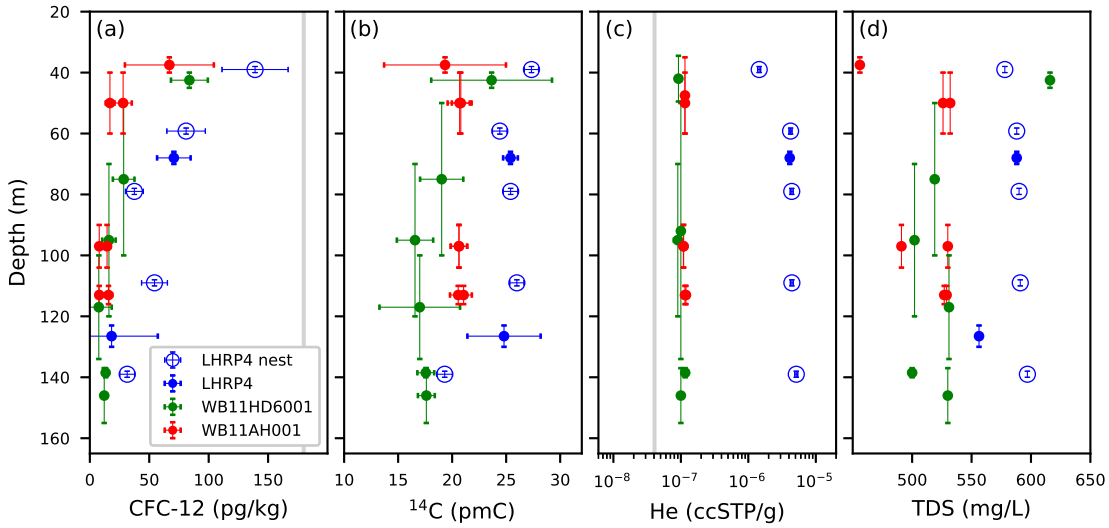

Figure 4.7: All depth-resolved aquifer concentrations interpreted from the three long-screened wells and those measured from a nest of piezometers (for direct comparison with LHRP4 only): (a) CFC-12 (grey line: max. atmospheric concentration), (b) ^{14}C, (c) He (grey line: water in equilibrium with the atmosphere at 25 °C), and (d) TDS. Vertical bars represent the inflow interval (less than symbol size for piezometers). Horizontal bars represent combined uncertainty of in-well flow and concentration measurement (less than symbol size for He, not shown for TDS). There are a different number of values for each well because the flow regimes in each offered different opportunities to sample aquifer concentrations. There are fewer data points for He because fewer samples were analysed.

with depth (27-19 pmC), consistent with the CFCs and the downward head gradient, all pointing to the occurrence of groundwater recharge. WB11HD6001 showed a slight decrease with depth (22-17 pmC) but this was within the uncertainty of the estimates. While WB11AH001 potentially indicated a slight increase with depth (19-21 pmC), in keeping with groundwater discharge driven by the observed upward head gradient, but again this variation was within the uncertainty.

There was measureable enrichment of helium in all samples, with distinctly different characteristics between the two sites (Figure 4.7c). At WB11HD6001 and WB11AH001 He was enriched by about half an order of magnitude above the atmospheric equilibrium concentration expected in recharge, and concentrations were essentially constant with depth ($\sim 1.1 \times 10^{-7}$ ccSTP/g). While at the LHRP4 site the long-screened well and piezometers showed He enrichment by two orders of magnitude, with evidence of concentrations increasing with depth ($1.5 - 5.1 \times 10^{-6}$ ccSTP/g). At both sites these data suggest a fraction of the water is at least in the order of 10^3 years old, and the lower concentrations at shallower depths at LHRP4 could be due to enhanced recharge from Pebble Mouse Creek.

The TDS concentrations (Figure 4.7d) give an overall representation of the major water chemistry. There were variations of all ions with depth within a limited range of concentrations, but without distinct stratification. Bicarbonate was the major component of TDS (46-86%) and sulphate the second most abundant (7-17%).

Previous work on groundwater ages in this type of environment Darling et al. (2012); Underwood et al. (2018) suggests that the simultaneous occurrence of young and old groundwater is probably explained by dual porosity in the aquifer. Specifically that relatively rapid flow within fractures and other preferential pathways mixes with water that infiltrates the primary porosity of the aquifer material over much longer timescales.

4.6 Discussion

A normal sampling approach is adequate if a well intersects just one discrete aquifer interval. In contrast, the approach described in this paper provides depth-resolved data from specific inflow zones within a well that intersects two or more permeable intervals or has a long screen in an otherwise homogeneous aquifer. Even in the latter case, it has been shown that small differences in head can drive vertical flow through the well, redistributing solutes between depths and causing significant bias in a pumped sample (e.g. Poulsen et al., 2018). The method presented here avoids or minimises in-well mixing of inflows and better indicates concentrations of a solute of interest for at least some of the aquifer intervals intersected by a well. In this study, the aquifer concentrations of environmental tracers interpreted from the ambient flow regime in LHRP4 are in good agreement with the depth-discrete samples from the adjacent piezometers (Figure 4.7), supporting the utility of the method. It appears unlikely that the intraborehole flow plume from LHRP4 has affected the chemistry sampled from any of the piezometers. That is, interpretation of available blended hydraulic heads indicates that groundwater flows eastwards with Pebble Mouse Creek (Figure 4.2c) and, assuming that this prevails at all depths intersected by LHRP4, the intraborehole flow plume most likely extends to the east as indicated by the flow line in Figure 4.2d, at a depth of approximately 130–140 m (i.e. the outflowing zone in Figure 4.4a). So the piezometers nearest to LHRP4 are much shallower than the plume and the deeper ones are positioned away from the plume.

Although this approach does not replace the need for piezometers at multiple depths in a groundwater investigation, it does provide a way to obtain more reliable data from certain depths in existing wells, allowing any new (properly designed) sampling installations to target depth intervals that remain un-sampled. Intervals that are typically not sampled with this method are those in which the head is lower than the blended head in the well (because they receive ambient flow), and those that contribute very little inflow. This paper focusses on the sampling method, and as such the principle concern is measuring the prevailing vertical flow regime in the well. However, we do recognise that additional borehole geophysical information helps to resolve the main hydraulically active zones

(e.g. Paillet and Pedler, 1996; Paillet and Crowder, 1996; Paillet and Reese, 2000). The broader hydrogeological situation of a well is also important for interpeting the sample results in the context of an investigation, but it is not germane to the sampling or deconvolution method itself. Conversely, one key benefit of measuring the ambient flow regime in a well is that the direction and relative magnitude of the vertical hydraulic gradient is identified, which helps to assess the position of a well in a flow system (e.g. recharge or discharge area), the influence of location specific heterogeneity, and/or hydraulic stresses (e.g. groundwater abstraction, irrigation drainage).

When a pumped sample is said to be an inflow-weighted mixture, it is implicitly assumed that the well has been pumped long enough for the inflow located furthest from the pump to reach the pump intake and contribute to the discharge. To illustrate the time involved in this, we calculated the travel times for the wells used in this study by integrating the velocities indicated by the measured flow profiles. That is, the well was discretised into finite elements sized equivalent to the spacing between the flow measurements, and each measured flow rate was applied to each element. The travel times for each element were then summed to give the total time taken for tracer to move with the flow of water in the well from the injection point to the pump. Prior to pumping, the ambient flow regime in LHRP4 was downwards and the in-well chemistry was mainly that of the highest head zone at 66–70 m (Figure 4.4b). Pumping reversed the flow direction (Figure 4.4d) and, with a large fraction of inflow from the bottom, it took 2-3 hours for the most distant inflow to reach the pump. In contrast, both WB11HD6001 and WB11AH001 had upward ambient flow regimes (Figure 4.5b and Figure 4.6b) and when pumped, nearly all discharge was sourced from a main aquifer zone near the top of the screen (Figure 4.5d and Figure 4.6d). Below, flow velocities remained very slow so inflows would take a long time to reach the pump (e.g. 80 hr from 137 m in WB11HD6001). However, given that pumping hardly altered the ambient flows, except in the main producing zones near the top of these wells, an approximately chemically steady regime occurred once inflow from the base of the main aquifer zone reached the pump (<1 hr). Clearly it is necessary to know the flow profile at the pumping rate used for sampling in order to identify the inflow zones and to determine when the sample can indeed be considered inflow-weighted. Alternatively, this problem can be avoided by depth-specific longitudinal sampling in the ambient flow regime, which is already chemically steady.

In this work, the ambient flow regime in all three wells provided equal or better sampling opportunities as the pumped regime. Zones that receive intraborehole flow do not provide useful data in either flow regime unless they are fully purged, which is usually unrealistic. An everted liner (e.g. Cherry et al., 2007) could be used to prevent ambient intraborehole flow if the need for sampling is known in advance

and such resources are available. In general, a key advantage of the ambient flow regime is that the chemically steady flow in the well is not disrupted (as it is with pumping), so it is not necessary to wait for a new one to establish. Sampling in the ambient regime is also simpler and more efficient because it does not require a discharge pump in addition to the sampling pump or device (e.g. grab sampler). Even for an active pumping well, stopping the pump and allowing the ambient flow regime to establish enbles a discrete unmixed sample to be obtained from the highest head zone. Although one caveat is that a well must have a clearly defined ambient flow regime so that samples are attributable to specific inflow zones. But given that vertical head gradients, and hence ambient vertical flows, are ubiquitous in groundwater systems (Elçi et al., 2003), this is likely to be common. The main reasons to sample in a pumped flow regime are if the ambient flow regime is inadequate, or to induce inflow from zones of intermediate head, which were inactive in the ambient regime (although we did not see these cases in this study). Another caveat, which applies to sampling in all wells, is that only the major flowing zones are elucidated, in both ambient and pumped conditions. Without using packers (or depth-discrete piezometers) to specifically sample low permeability zones, it is generally only possible to resolve inflows from zones that are within two orders of magnitude of the most permeable zone (e.g. Paillet, 1998, 2001).

The most certain estimate of aquifer chemistry is that from a single inflowing zone of a clearly defined ambient flow regime, which is only subject to analytical error. As a worst case, this was ±20% of the measured value for CFC-12 (66–70 m in LHRP4, CFC-12: 70.7 ±14 pg/kg, Figure 4.4e). If a well is always pumped then the same applies to the inflow zone most distant from the pump (e.g. A3 sample, Figure 4.1b). It is important to note here that most solutes can be measured much more accurately than dissolved gases like CFCs, so the resulting error would be considerably less. Greater uncertainty arises where in-well flow and concentration measurements are combined in a mass balance (e.g. Eq. (1)) to estimate inflowing aquifer concentration. A statistical analysis, like the Monte Carlo approach used here, helps to quantify the error on calculated tracer concentrations, as shown by the larger error bars in Figure 4.7. As a worst case this was ±200% of the measured value for CFC-12 (123–130 m in LHRP4, 18.5 ±39 pg/kg, Figure 4.4e). But again, most of this was analytical error in CFC-12 measurement. If the analytical error is removed, the mass balance error due to ±5% in flow measurement is ±30% for the CFC-12 concentration.

Clearly, accurate flow measurements are critical for accurate calculation of inflow concentrations using a mass balance. An inherent limitation with long-screened wells is the potential for vertical flow in the gravel pack (or void) in the borehole annulus to enter the well at a point downstream of where it was released from the aquifer. This can reduce resolution of flow zone boundaries and increase the appar-

ent inflow from downstream low conductivity zones (Ruud and Kabala, 1997), and it can potentially enhance apparent inflow from the top part of the screen, where the deficit of a pumped discharge rate must be met (e.g. Boman et al., 1997). The use of a flow diverter on a borehole flowmeter increases resistance to flow within the well, potentially exacerbating the above issues and causing flows to be under-measured until near the top of the screen. However, it is important to remember that these uncertainties exist within the limits of zero flow at one end of the screen and the pumping rate at the other end (usually the top), or zero at both ends in ambient conditions. A further limit on uncertainty is that flow rate changes occur incrementally in the direction of flow, so there is only so much error that can be tolerated whilst honouring the overall shape of the flow profile. We believe our use of ±5% error on flows reasonably captures uncertainty in our imperfect field data for flow rates below the 10 l/min head-loss threshold. Defining the pumped flow regime in LHRP4 was problematic because the flowmeters head-loss threshold was exceeded over much of the well (Figure 4.4c). Thus it is likely that the lack of apparent inflows from the intermediate zone (70–123 m) is because discharge was preferentially sourced from the much more productive zone at the top of the well, or it bypassed the flowmeter in the gravel pack. If the proportion of inflow from that intermediate zone is less than that required to explain the in-well concentrations (red line in Figure 4.4c) then it would be necessary to invoke well-aquifer exchanges that change concentration without changing the flow rate. As such, the mass balance may be insufficient to resolve specific aquifer concentrations where the spacing between samples incorporates multiple aquifer-well fluxes. This was apparent for the 60–40 m interval in WB11AH001, although the out fluxes could simply be flow bypassing the flowmeter. We have highlighted challenges with using a borehole flowmeter to measure a wide range of flow rates, and strongly encourage careful consideration to the flow measuring methodology for future work. As suggested by Ruud et al. (1999), with a borehole flowmeter this could include an undersized flow diverter to manage the flow rate through the sensor, and/or measuring low and high flow intervals in separate profiles in the same well. Despite the obvious difficulties with in-well flow measurement, with careful interpretation the practitioner can still obtain a clear picture of the distribution of inflows. Depth-resolved estimates of solute concentrations derived from these inflows can provide valuable evidence for many groundwater studies.

We measured flow logs on multiple occasions over several years (Figure 4.8), so the consistency of the ambient flow regimes is fairly well defined. But in the absence of repeat logs, it could be relevant to assess the likelihood that the inflowing zones ($h_z > h_{av}$) are in fact producing native groundwater, rather than potentially being contaminated with intraborehole flow. This could occur where transient conditions result in the head of a zone dropping below the blended head in the well at some

times. Heads in the individual aquifer zones can be estimated by combined analysis of ambient and pumped flow logs with an analytical solution (Day-Lewis et al., 2011; Sawdey and Reeve, 2012). The amount of change required to reverse the prevailing head gradient and hence direction of intraborehole flow could then be assessed. This would be best done in combination with groundwater level hydrographs showing the range of seasonal fluctuations expected for a study area. Clearly, if a zone is likely to be impacted by intraborehole flow at some times, then it will not necessarily provide a representative sample of native groundwater from that zone, even if it is inflowing in ambient conditions at the time of sampling.

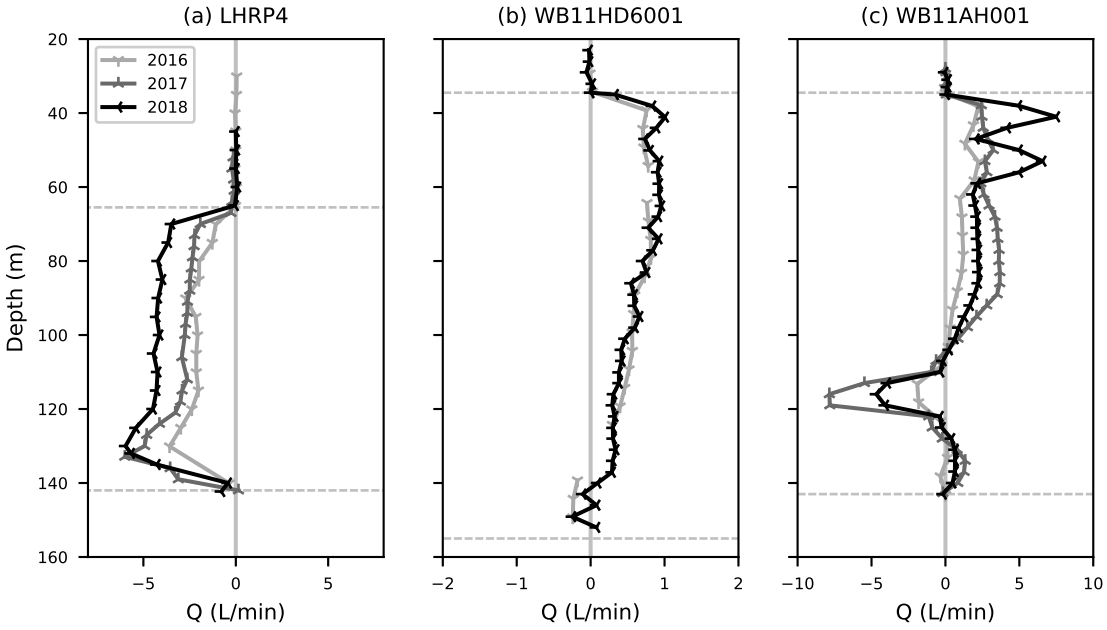

Figure 4.8: Ambient (un-pumped) vertical flow profiles measured in the three long-screened wells in June 2016, June 2017, and April 2018. Symbols represent depth and flow rate measured with an EM flowmeter held stationary in the well with a flow diverter fitted.

4.7 Conclusion

The chemistry of specific groundwater inflows to long-screened and open borehole wells can be estimated by measuring and sampling the in-well vertical flow regime. By conceptualising the well-aquifer exchanges in ambient or pumped conditions, inflowing zones can be targeted with depth-specific sampling (low flow rate or grab sampler). Ambient vertical flows within the well, driven by a natural head gradient, provide particularly compelling sampling conditions. In a clearly defined ambient flow regime, sampling of the inflowing zones ($h_z > h_{av}$) does not require pumping or purging in the normal sense. The highest head zone is subject only to analytical error on a single sample, while mixtures can be deconvolved with a simple mass balance, incorporating errors of flow and concentration measurements before and

after the inflow. Native groundwater from ambient outflowing zones ($h_z < h_{av}$) in wells that are not routinely pumped cannot be sampled (even with pumping) because it is displaced by large volumes of intraborehole flow. For wells that are routinely pumped, also sampling in the ambient flow regime (i.e. when the pump is off) can add value by enabling a discrete sample from the highest head zone, rather than having it mixed with other inflows. At our field site, clear ambient flow regimes in all three wells (1–7 l/min) provided multiple opportunities for sampling inflowing native groundwater. Interpreted aquifer concentrations were consistent with discrete samples from a nest of piezometers adjacent to one well. Appreciable CFCs at shallower depths indicate the occurrence of modern recharge (<60 years) particularly at a site along a watercourse. The simultaneous occurrence of consistent levels of ^{14}C in all samples suggests that old groundwater (>5000 years) is present at all depths. Compared to a normal pumped sample, this targeted sampling approach minimises the effect of in-well mixing of water from different depths, enables sample bias caused by intraborehole flow to be avoided, and is particularly relevant where the integrity of packers is compromised. We do not recommend long-screened or long open borehole wells as sampling devices by design, but rather that the method described in this paper enables more reliable depth-resolved estimates of groundwater chemistry to be obtained from such wells where they already exist.

Chapter 5

Conclusion

This thesis brings into clear focus the opportunity offered by working with the flow regime within a well to resolve the depth and chemistry of specific inflows, in addition to characterising the intersected aquifer heterogeneity and distribution of hydraulic heads. This approach greatly improves the value of the derived information compared to the common practice of measuring the standing water level, the drawdown induced by pumping and sampling pumped discharge.

5.1 Summary of findings

The key findings from the three studies presented in this thesis are:

1. **Modelling intraborehole flow**
   Vertical head gradients are very common in aquifer systems, so head driven vertical flow in wells is equally common. Three dimensional numerical modelling of a hypothetical but realistic situation (Chapter 2) showed that purging an intraborehole flow plume invading an aquifer requires pumping a volume much larger than that of the plume itself because only a fraction of discharge is sourced from the interval containing the plume. Although a plume volume is readily estimated based on measured flow rates in a well and the un-pumped history, the required purge volume is usually prohibitively large. However, the plume is only ever in the lower head zone(s) intersected by a well, so even if purging is not feasible, native groundwater samples can be obtained from inflowing high to intermediate head zones. This work highlights both the challenge and the opportunity of working with long-screened wells that have been left un-pumped, like those in our Pilbara study area.

2. **Quantifying the pumped flow regime using a tracer**
   The profile of vertical flow rates within a pumped well can be quantified with the novel constant rate tracer test presented in Chapter 3. The test involves simultaneous pumping and tracer injection while repeatedly measuring tracer

profiles in the well. Once a model is set up to convert tracer dilution into flow rate, which we did with the advection-dispersion equation, a Laplace transform, and a graphical user interface, the test is readily analysed. Flowing features are visually identified and the model is manually fit to the pre-injection, transient and steady-state tracer profiles. The uniqueness of the solution was optimised by simultaneously fitting the model to all profiles. Results compare favourably to borehole electromagnetic flowmeter data, particularly if tracer density effects are correctly interpreted and head-loss in the flowmeter is avoided. Although the flowmeter is easy to use, it must be set up for a limited dynamic range of sensitivity (to avoid head loss problems) so separate profiles would be needed to accurately measure both slow flow rates and fast flow rates in a well. In contrast, our tracer approach does not suffer this issue because it does not impede flow in the well and, providing that dilutions remain measureable, it can simultaneously resolve a greater range of flow rates. Although the salt tracer was cheap and easy to use, there were buoyancy problems at slow flow rates and high concentrations, and it has a high limit of detectability, particularly because of naturally occurring salinity in groundwater. To help interpret the salt tracer, we also developed a novel method to assess the role of mixed convection. This can be used to identify and avoid buoyancy issues at the planning stage of any single-well tracer test involving a density contrast with inflowing groundwater.

3. **Depth-resolved sampling of groundwater chemistry**
   In Chapter 4, two existing but largely independent areas of knowledge are combined to achieve a concept that was highlighted in the first study presented in this thesis, and which has not previously been reported in the literature. Specifically, the vertical flow regime within long-screened wells is measured and sampled to target zones that produce native groundwater and avoid those impacted by head-driven intraborehole flow. The in-well samples are interpreted either as native groundwater from a discrete source or a mixture to be deconvolved with a mass balance using samples taken before and after the inflow. The head-driven ambient flow regime is shown to be particularly useful for sampling groundwater native to defined inflow depths, and this can be sampled without even needing to purge or pump the well. Ambient vertical flow in wells is very common so this approach is widely applicable wherever stratified aquifer chemistry intersected by a well needs to be better resolved. For the Pilbara field site we showed that old groundwater (>5,000 years) occurred at all sampled depths, while young groundwater (<60 years) and evidence of recharge occurred only at shallower sampled depths, particularly near a watercourse. A key finding of this study is that pumped sampling of wells impacted by intraborehole flow is not necessarily justified, unless the plume of

head-driven intraborehole is first purged, which is often not feasible. Without pumped sampling, some intersected depths remain un-sampled, but at least the samples that are obtained are free of bias and can be related to defined depth intervals. This approach enables valuable data to be derived from existing groundwater infrastructure, and the cost of obtaining an ambient borehole flow profile is at least partially offset by waiving the usual requirement of purging a well prior to sampling.

Measuring the flow regime within a well does not seem to fall into the regular practice of many hydrogeologists, probably because the required tools or expertise are not readily available. But it also requires a conceptual shift from thinking of a well as a single entity, to considering the well as a vertical conduit, which interacts with the intersected aquifer system in a predictable and measurable way. Although there is a cost of measuring the vertical flow regime in ambient and/or pumped conditions, the benefit is that reliable information is obtained from wells that are otherwise of limited use in many groundwater studies. This contributes to meeting the data needs of an investigation and enables investment in new purpose-built installations to better target remaining knowledge gaps and uncertainties.

5.2 Limitations

The utility of long-screened and long open borehole wells for quantitative groundwater investigation is improved by working with the in-well vertical flows (flow logs) in ambient and pumped conditions. However, careful consideration needs to be given to how the in-well flows measured as a function of depth relate to flowing features in the surrounding aquifer.

The "window" provided by a well (regardless of screen length or open interval) must be considered in the context of the type of heterogeneity in the aquifer system being studied. For example, in homogeneous or layered type systems, the hydraulically active features observed in the well may be reasonably extrapolated to aquifer characteristics at the intersected depth(s) in the local area. However, in highly heterogeneous environments like fractured rock, water entering the well at a certain depth might actually originate from a deeper or shallower interval (e.g. where the well intersects an inclined fracture). Fractured rock boreholes are often stable, so the depth(s) and orientation of intersected fractures can be mapped in the open hole with tools like borehole camera, acoustic televiewer and caliper (e.g. Maliva, 2016). This improves the interpretation of how flows measured in a well relate to flow in the surrounding aquifer. However, in such environments it is also often necessary to do cross-well testing to more reliably characterise the spatial patterns of actual groundwater flow (e.g. Le Borgne et al., 2007; Paillet, 1993; Paillet et al., 2012).

If a well is constructed with a screen, the gravel pack (or void) in the annulus

between the screen and the borehole wall is a largely unmeasurable and uncontrollable pathway for vertical flow. This feature makes it possible for flow to enter the well at a point downstream of where it was released from the aquifer. The use of a flow diverter with a borehole flowmeter can be problematic in such situations, because some flow can bypass the meter, and it can cause bias in the inflow profile (as discussed in Chapter 3 and Chapter 4). In addition, a vertical flow component can be induced near pumping wells that are partially penetrating. For these reasons, attempts to characterise the hydraulic conductivity distribution from the apparent distribution of inflows may need to explicitly include these processes (e.g. Garcia et al., 2010; Halford, 2009).

Although in some special cases a blended sample from a large vertical interval can be useful (e.g. to assess the range of ages present in a groundwater system, McCallum et al. (2017)), usually such a mixture is not helpful, and can even be misleading. In particular, if a well is not always pumped then some of the intersected zones are not represented in a sample, due to the invasion of ambient intraborehole flow (as detailed in Chapter 2 and Chapter 4). The depth-resolved sampling approach described in Chapter 4 provides a solution to this problem by targetting specific inflow zones. However, the practitioner must be mindful that changes of in-well flow rate in a screened well might not be exactly related to the intersected permeable features of the aquifer (for the reasons described in the previous paragraphs). Even so, there are limits to that uncertainty, as discussed in Chapter 4, so if flow profiles are collected and interpreted with care, a depth-resolved sampling approach can still provide valuable information compared to a standard pumped sample.

5.3 Future work

The numerical model presented in Chapter 2 was a hypothetical situation based on a previous study of intraborehole flow that did not include pumping (Reilly et al., 1989; Konikow and Hornberger, 2006). As such, our model could have been better designed to avoid any boundary effects caused by pumping. However, there are as many possible scenarios to model as there are real-world situations, so we do not necessarily envisage further hypothetical modelling is required. However, simplified block models like ours can be exceptionally useful for exploring specific real-world situations where the physical processes and interactions need to be visualised and tested.

The tracer method of determining the pumped borehole flow profile (Chapter 3) could be improved primarily by exploring the use of a fluorescent dye tracer. The main benefit compared to the salt tracer would be that a dye has neutral buoyancy and is far more detectable. This would be best achieved with a borehole

fluorometer, or similar optical sensor, that can be deployed remotely or operated on a wireline, logging tracer concentration at high resolution throughout the well (e.g. logging every 1-2 seconds). Although we achieved good fits of our model to the measured data with the advection-dispersion equation, which is generally appropriate for laminar flow conditions, our inversion model could potentially be improved by revising the theoretical basis to better deal with pipe flow conditions. In particular the mixing of inflows with flow already in the well, and the effects of dispersion in turbulent flow condition could be better represented.

The pumped borehole flow profile is most relevant to assess aquifer heterogeneity (i.e. hydraulic conductivity and head distribution) intersected by a well, and to obtain samples where the ambient flow regime is insufficient or can be purged. For wells that have been left un-pumped, it is often more practical and accurate to measure and sample the ambient flow regime. We intend to do this in a wider range of wells in the Pilbara study area to derive more information on the stratification of groundwater ages. It would also be good to see this ambient flow sampling method (Chapter 4) applied in a range of other situations, with the results being compared to composite samples from the wells. Some other examples of where long-screened or open borehole wells are often available (and sometimes sampled) include a range of mining operations, seawater intrusion monitoring, and monitoring of nutrient pollution in agricultural areas.

References

Anderson, M.P. and Woessner, W.W. (2002). *Applied groundwater modeling - simulation of flow and advective transport*. Academic Press, San Diego, California.

Aquaterra (2007). Lang Hancock Railway construction water supply bore completion report. Consultancy report (ref: 652/C5/402a) prepared for Calibre Engenium. Technical report, Aquaterra Consulting Pty Ltd.

Aquaterra (2011). Hope Downs 4 rail construction water supply investigations. Consultancy report (ref: 1187D/101a) prepared for Calibre Engenium. Technical report, RPS Aquaterra Pty Ltd.

Arnold, K.B. and Molz, F.J. (2000). In-Well Hydraulics of the Electromagnetic Borehole Flowmeter: Further Studies. *Groundwater Monitoring & Remediation*, 20(1):52–55. doi:10.1111/j.1745-6592.2000.tb00251.x.

Ataie-Ashtiani, B., Simmons, C.T., and Irvine, D.J. (2018). Confusion About "Convection"! *Groundwater*, 56(5):683–687. doi:10.1111/gwat.12790.

Avila, K., Moxey, D., de Lozar, A., Avila, M., Barkley, D., and Hof, B. (2011). The onset of turbulence in pipe flow. *Science*, 333(6039):192–196. doi:10.1126/science.1203223.

Bakker, M., Post, V., Langevin, C.D., Hughes, J.D., White, J.T., Starn, J.J., and Fienen, M.N. (2016). Scripting MODFLOW model development using python and FloPy. *Groundwater*, 54(5):733–739. doi:10.1111/gwat.12413.

Banks, E.W., Shanafield, M.A., and Cook, P.G. (2014). Induced temperature gradients to examine groundwater flowpaths in open boreholes. *Groundwater*, 52(6):943–951. ISSN 17456584. doi:10.1111/gwat.12157.

Batlle-Aguilar, J., Harrington, G.A., Leblanc, M., Welch, C., and Cook, P.G. (2014). Chemistry of groundwater discharge inferred from longitudinal river sampling. *Water Resources Research*, 50(2):1550–1568. doi:10.1002/2013WR013591.

Behroozmand, A.A., Keating, K., and Auken, E. (2015). A Review of the Principles and Applications of the NMR Technique for Near-Surface Characterization. *Surveys in Geophysics*, 36(1):27–85. doi:10.1007/s10712-014-9304-0.

Bexfield, L.M. and Jurgens, B.C. (2014). Effects of seasonal operation on the quality of water produced by public-supply wells. *Ground water*, 52(S1):10–24. ISSN 17456584. doi:10.1111/gwat.12174.

Boman, G.K., Molz, F.J., and Boone, K.D. (1997). Borehole flowmeter application in fluvial sediment: methodology, results and assessment. *Ground Water*, 35(3):443–450. doi:10.1111/j.1745-6584.1997.tb00104.x.

Brainerd, R.J. and Robbins, G.A. (2004). A tracer dilution method for fracture characterization in bedrock wells. *Ground water*, 42(5):774–780. doi:10.1111/j.1745-6584.2004.tb02731.x.

Brassington, F. (1992). Measurements of head variations within observation boreholes and their implications for groundwater monitoring. *Water and Environment Journal*, 6(3):91–100. doi:10.1111/j.1747-6593.1992.tb00742.x.

Brouyère, S., Batlle-Aguilar, J., Goderniaux, P., and Dassargues, A. (2008). A new tracer technique for monitoring groundwater fluxes: The Finite Volume Point Dilution Method. *Journal of Contaminant Hydrology*, 95(3-4):121–140. doi:10.1016/j.jconhyd.2007.09.001.

Cartwright, I., Cendón, D., Currell, M., and Meredith, K. (2017). A review of radioactive isotopes and other residence time tracers in understanding groundwater recharge: possibilities, challenges, and limitations. *Journal of Hydrology*, 555:797–811. doi:10.1016/j.jhydrol.2017.10.053.

Cherry, J.A., Parker, B.L., and Keller, C. (2007). A new depth-discrete multilevel monitoring approach for fractured rock. *Ground Water Monitoring and Remediation*, 27(2):57–70. ISSN 10693629. doi:10.1111/j.1745-6592.2007.00137.x.

Chlebica, D.W. and Robbins, G.A. (2013). Altering dissolved oxygen to determine flow conditions in fractured bedrock wells. *Groundwater Monitoring and Remediation*, 33(4):100–107. doi:10.1111/gwmr.12019.

Church, P. and Granato, G. (1996). Bias in ground-water data caused by well-bore flow in long-screen wells. doi:10.1111/j.1745-6584.1996.tb01886.x.

Claasen, H.C. (1982). Guidelines and techniques for obtaining water samples that accurately represent the water chemistry of an aquifer. Open-File Report 82-1024. Technical report, U.S. Geological Survey.

Clemo, T., Barrash, W., Reboulet, E.C., Johnson, T.C., and Leven, C. (2009). The influence of wellbore inflow on electromagnetic borehole flowmeter measurements. *Ground Water*, 47(4):515–525. doi:10.1111/j.1745-6584.2008.00559.x.

Collar, R.J. and Mock, P.A. (1997). Using water-supply wells to investigate vertical ground-water quality. *Ground Water*, 35(5):743–750. doi:10.1111/j.1745-6584.1997.tb00142.x.

Colombani, N., Volta, G., Osti, A., and Mastrocicco, M. (2016). Misleading reconstruction of seawater intrusion via integral depth sampling. *Journal of Hydrology*, 536:320–326. doi:10.1016/j.jhydrol.2016.03.011.

Cook, P.G., Dogramaci, S., McCallum, J.L., and Hedley, J. (2017). Groundwater age, mixing and flow rates in the vicinity of large open pit mines, Pilbara region, northwestern Australia. *Hydrogeology Journal*, 25:39–53. doi:10.1007/s10040-016-1467-y.

Cook, P.G. and Herczeg, A.L. (2000). *Environmental tracers in subsurface hydrology*. Springer Science+Business Media, LLC, New York. doi:10.1007/978-1-4615-4557-6.

Cook, P.G., Solomon, D.K., Plummer, L.N., Busenberg, E., and Schiff, S.L. (1995). Chlorofluorocarbons as tracers of groundwater transport processes in a shallow, silty sand aquifer. *Water Resources Research*, 31(3):425–434. doi: 10.1029/94WR02528.

Corcho Alvarado, J.A., Barbecot, F., and Purtschert, R. (2009). Ambient vertical flow in long-screen wells: a case study in the Fontainebleau Sands Aquifer (France). *Hydrogeology Journal*, 17:425–431. doi:10.1007/s10040-008-0383-1.

Darling, W., Gooddy, D., MacDonald, A., and Morris, B. (2012). The practicalities of using CFCs and SF6 for groundwater dating and tracing. *Applied Geochemistry*, 27(9):1688–1697. doi:10.1016/j.apgeochem.2012.02.005.

Day-Lewis, F.D., Johnson, C.D., Paillet, F.L., and Halford, K.J. (2011). A computer program for flow-log analysis of single holes (FLASH). *Ground Water*, 49(6):926–931. doi:10.1111/j.1745-6584.2011.00798.x.

de Hoog, F.R., Knight, J.H., and Stokes, A.N. (1982). An improved method for numerical inversion of Laplace transforms. *SIAM Journal on Scientific and Statistical Computing*, 3(3):357–366. doi:10.1137/0903022.

Dlubac, K., Knight, R., Song, Y.Q., Bachman, N., Grau, B., Cannia, J., and Williams, J. (2013). Use of NMR logging to obtain estimates of hydraulic conductivity in the High Plains aquifer, Nebraska, USA. *Water Resources Research*, 49(4):1871–1886. doi:10.1002/wrcr.20151.

Dogramaci, S. and Skrzypek, G. (2015). Unravelling sources of solutes in groundwater of an ancient landscape in NW Australia using stable Sr, H and O isotopes. *Chemical Geology*, 393-394:67–78. doi:10.1016/j.chemgeo.2014.11.021.

Dogramaci, S., Skrzypek, G., Dodson, W., and Grierson, P.F. (2012). Stable isotope and hydrochemical evolution of groundwater in the semi-arid Hamersley Basin of subtropical northwest Australia. *Journal of Hydrology*, 475:281–293. doi:10.1016/j.jhydrol.2012.10.004.

Doughty, C. and Tsang, C.F. (2005). Signatures in flowing fluid electric conductivity logs. *Journal of Hydrology*, 310(1-4):157–180. doi:10.1016/j.jhydrol.2004.12.003.

Einarson, M. (2006). Multilevel ground-water monitoring. In D.M. Nielsen, editor, *Practical handbook of environmental site characterization and ground-water monitoring*, volume 11, chapter Chapter 11, pages 808–845. CRC Press, Taylor & Francis Group, Boca Raton, Florida, second edition.

Elçi, A., Flach, G.P., and Molz, F.J. (2003). Detrimental effects of natural vertical head gradients on chemical and water level measurements in observation wells: Identification and control. *Journal of Hydrology*, 281(1-2):70–81. doi:10.1016/S0022-1694(03)00201-4.

Elçi, A., Molz, F.J., and Waldrop, W.R. (2001). Implications of observed and simulated ambient flow in monitoring wells. *Groundwater*, 39(6):853–862. doi: 10.1111/j.1745-6584.2001.tb02473.x.

Freeze, R.A. and Cherry, J.A. (1979). *Groundwater*. Prentice Hall, Inc., Englewood Cliffs, New Jersey. ISBN 9780133653120.

Gailey, R.M. (2017). Inactive supply wells as conduits for flow and contaminant migration: conditions of occurrence and suggestions for management. *Hydrogeology Journal*, 25(7):2163–2183. doi:10.1007/s10040-017-1588-y.

Garcia, C., Halford, K., and Laczniak, R. (2010). Interpretation of flow logs from Nevada test site boreholes to estimate hydraulic conductivity using numerical simulations constrained by single-well aquifer tests. Technical report, U.S. Geological Survey, Reston, Virginia.

Gelhar, L.W., Welty, C., and Rehfeldt, K.R. (1992). A critical review of data on field-scale dispersion in aquifers. *Water Resources Research*, 28(7):1955–1974. doi:10.1029/92WR00607.

Gloss, D. and Herwig, H. (2010). Wall roughness effects in laminar flows: An often ignored though significant issue. *Experiments in Fluids*, 49(2):461–470. doi:10.1007/s00348-009-0811-6.

Goldrath, D.A., Izbicki, J.A., and Thorbjarnarson, K.W. (2015). Simulating arsenic mitigation strategies in a production well. *Journal of Geology & Geophysics*, 4(5). doi:10.4172/jgg.1000218.

Gossell, M., Nishikawa, T., Hanson, R., Izbicki, J.A., Tabidian, M., and Bertine, K. (1999). Application of Flowmeter and Depth-Dependent Water Quality Data for Improved Production Well Construction. *Ground Water*, 37(5):729–735. doi:10.1111/j.1745-6584.1999.tb01165.x.

Halford, K.J. (2009). AnalyzeHOLE - An integrated wellbore flow analysis tool: U.S. Geological Survey Techniques and Methods 4-F2. Technical report, U.S. Geological Survey, Reston, Virginia. doi:10.2172/965975.
URL: *http://www.osti.gov/servlets/purl/965975-1C8k3C/*

Halford, K.J. and Hanson, R.T. (2002). User guide for the drawdown-limited, multi-node well (MNW) package for the U.S. Geological Survey's Modular Three-Dimensional Finite-Difference Ground-Water Flow Model, Versions MODFLOW-96 and MODFLOW-2000. Open-File Report 02-293. Technical report, U.S. Geological Survey.

Halford, K.J., Stamos, C.L., Nishikawa, T., and Martin, P. (2010). Arsenic management through well modification and simulation. *Ground Water*, 48(4):526–537. doi:10.1111/j.1745-6584.2009.00670.x.

Harbaugh, A.W. (2005). MODFLOW-2005 , The U . S . Geological Survey Modular Ground-Water Model — the Ground-Water Flow Process. Techniques and Methods 6-A16. Technical report, U.S. Geological Survey, Reston, Virginia.

Harrington, G.A., James-smith, J.M., Wohling, D., and van den Akker, J. (2004). Hydrogeological investigation of the Mount Lofty Ranges, progress report 5: Drilling phases 2.1 to 2.3: research and monitoring wells at Scott Creek, Balhannah, Willunga Fault, Lobethal, Eden Valley and Ashbourne. Report DWLBC 2004/04. Technical report, Department for Water Land and Biodiversity Conservation, Government of South Australia.

Hart, J., Guymer, I., Jones, A., and Stovin, V. (2013). Longitudinal Dispersion Coefficients Within Turbulent and Transitional Pipe Flow. In P. Rowiński, editor, *GeoPlanet: Earth and Planetary Sciences*, volume 11, chapter Experiment, pages 133–145. Springer, Berlin, Heidelberg. doi:10.1007/978-3-642-30209-1_8.

Harte, P.T. (2013). Hydraulically controlled discrete sampling from open boreholes. *Groundwater*, 51(6):822–827. doi:10.1111/gwat.12120.

Holloway, O.G. and Waddell, J.P. (2008). Design and operation of a borehole straddle packer for ground-water sampling and hydraulic testing of discrete intervals at U.S. Air Force Plant 6, Marietta, Georgia. Open-File Report 2008–1349. Technical report, U.S. Geological Survey.

Hutchins, S.R. and Acree, S.D. (2000). Ground water sampling bias observed in shallow, conventional wells. *Ground Water Monitoring & Remediation*, 20(1):86–93. doi:10.1111/j.1745-6592.2000.tb00255.x.

Izbicki, J.A. (2004). A small-diameter sample pump for collection of depth-dependent samples from production wells under pumping conditions. Fact Sheet 2004-3096. Technical report, U.S. Geological Survey.

Izbicki, J.A., Christensen, A., and Hanson, R. (1999). U.S. Geological Survey combined well-bore flow and depth-dependent water sampler. U.S. Fact Sheet 196-99. Technical report, U.S. Geological Survey.

Izbicki, J.A., Christensen, A.H., Newhouse, M.W., Smith, G.A., and Hanson, R.T. (2005). Temporal changes in the vertical distribution of flow and chloride in deep wells. *Ground Water*, 43(4):531–544. doi:10.1111/j.1745-6584.2005.0032.x.

Izbicki, J.A., Metzger, L.F., Mcpherson, K.R., Everett, R.R., and Bennett V, G.L. (2006). Sources of high-chloride water to wells, eastern San Joaquin groundwater subbasin, California. Open File Report 2006-1309. Technical report, U.S Geological Survey.

Izbicki, J.A., Petersen, C.E., Glotzbach, K.J., Metzger, L.F., Christensen, A.H., Smith, G.A., O'Leary, D., Fram, M.S., Joseph, T., and Shannon, H. (2010). Aquifer Storage Recovery (ASR) of chlorinated municipal drinking water in a confined aquifer. *Applied Geochemistry*, 25(8):1133–1152. doi:10.1016/j.apgeochem.2010.04.017.

Izbicki, J.A., Stamos, C., Metzger, L.F., Kulp, T., McPherson, K.R., Halford, K., and Bennett, G.L. (2008). Sources, distribution, and management of arsenic in water from wells, Eastern San Joaquin Ground-Water Subbasin, California. Open File Report 2008-1272. Technical report, U.S. Geological Survey.

Jackson, J., Cotton, M., and Axcell, B. (1989). Studies of mixed convection in vertical tubes. *International Journal of Heat and Fluid Flow*, 10(1):2–15. doi:10.1016/0142-727X(89)90049-0.

Jones, I. and Lerner, D.N. (1995). Level-determined sampling in an uncased borehole. *Journal of Hydrology*, 171:291–317. doi:10.1016/0022-1694(95)06015-B.

Jurgens, B.C., Bexfield, L.M., and Eberts, S.M. (2014). A ternary age-mixing model to explain contaminant occurrence in a deep supply well. *Ground water*, 52:25–39. doi:10.1111/gwat.12170.

Keller, C.E., Cherry, J.A., and Parker, B.L. (2014). New method for continuous transmissivity profiling in fractured rock. *Groundwater*, 52(3):352–367. doi:10.1111/gwat.12064.

Kendall, C. and Aravena, R. (2000). Nitrate isotopes in groundwater systems. In P.G. Cook and A.L. Herczeg, editors, *Environmental tracers in subsurface hydrology*, chapter Chapter 9, pages 261–297. Science+Business Media, LLC, New York. doi:10.1007/978-1-4615-4557-6.

Klepikova, M.V., Le Borgne, T., Bour, O., and Davy, P. (2011). A methodology for using borehole temperature-depth profiles under ambient, single and cross-borehole pumping conditions to estimate fracture hydraulic properties. *Journal of Hydrology*, 407(1-4):145–152. doi:10.1016/j.jhydrol.2011.07.018.

Knight, R., Walsh, D.O., Butler, J.J., Grunewald, E., Liu, G., Parsekian, A.D., Reboulet, E.C., Knobbe, S., and Barrows, M. (2016). NMR Logging to Estimate Hydraulic Conductivity in Unconsolidated Aquifers. *Groundwater*, 54(1):104–114. doi:10.1111/gwat.12324.

Kobr, M., Mares, S., and Paillet, F. (2005). Geophysical well logging: Borehole geophysics for hydrogeological studies: principles and applications. In Y. Rubin and S.S. Hubbard, editors, *Hydrogeophysics*, Water Science and Technology Library, chapter 10, pages 291–331. Springer, Dordrecht, The Netherlands. doi:10.1007/1-4020-3102-5.

Konikow, L.F. and Hornberger, G.Z. (2006). Modeling effects of multinode wells on solute transport. *Ground Water*, 44(5):648–660. doi:10.1111/j.1745-6584.2006.00231.x.

Konikow, L.F., Hornberger, G.Z., Halford, K.J., and Hanson, R.T. (2009). Revised multi-node well (MNW2) package for MODFLOW ground-water flow model. Techniques and Methods 6-A30. Technical report, U.S. Geological Survey.

Kruseman, G.P. and de Ridder, N. (2000). *Analysis and evaluation of pumping test data*. Publication 47, International Institute for Land Reclamation and Improvement, Wageningen, The Netherlands, 2nd edition. ISBN 9070754207.

Lacombe, S., Sudicky, E.A., Frape, S.K., and Unger, A.J.A. (1995). Influence of leaky boreholes on cross-formational groundwater flow and contaminant transport. *Water Resources Research*, 31(8):1871–1882. doi:10.1029/95WR00661.

Lakshmi, V., Fayne, J., and Bolten, J. (2018). A comparative study of available water in the major river basins of the world. *Journal of Hydrology*, 567:510–532. doi:10.1016/j.jhydrol.2018.10.038.

Landon, M.K., Jurgens, B.C., Katz, B.G., Eberts, S.M., Burow, K.R., and Crandall, C.A. (2010). Depth-dependent sampling to identify short-circuit pathways to public-supply wells in multiple aquifer settings in the United States. *Hydrogeology Journal*, 18(3):577–593. doi:10.1007/s10040-009-0531-2.

Le Borgne, T., Bour, O., Riley, M.S., Gouze, P., Pezard, P.A., Belghoul, A., Lods, G., Le Provost, R., Greswell, R.B., Ellis, P.A., Isakov, E., and Last, B.J. (2007). Comparison of alternative methodologies for identifying and characterizing preferential flow paths in heterogeneous aquifers. *Journal of Hydrology*, 345(3-4):134–148. ISSN 00221694. doi:10.1016/j.jhydrol.2007.07.007.

Leaf, A.T., Hart, D.J., and Bahr, J.M. (2012). Active Thermal Tracer Tests for Improved Hydrostratigraphic Characterization. *Ground Water*, 50(5):726–735. ISSN 0017467X. doi:10.1111/j.1745-6584.2012.00913.x.

Lerner, D.N. and Teutsch, G. (1995). Recommendations for level-determined sampling in wells. *Journal of Hydrology*, 171(3-4):355–377. doi:10.1016/0022-1694(95)06016-C.

Libby, J.L. and Robbins, G.A. (2014). An unsteady state tracer method for characterizing fractures in bedrock wells. *Groundwater*, 52(1):136–144. doi:10.1111/gwat.12045.

Ma, R., Zheng, C., Tonkin, M., and Zachara, J.M. (2011). Importance of considering intraborehole flow in solute transport modeling under highly dynamic flow conditions. *Journal of Contaminant Hydrology*, 123(1-2):11–19. doi:10.1016/j.jconhyd.2010.12.001.

Maliva, R.G. (2016). *Borehole Geophysical Techniques*, chapter 10, pages 273–330. Springer International Publishing, Cham. doi:10.1007/978-3-319-32137-0_10.

Martin-Hayden, J.M. (2000). Sample concentration response to laminar wellbore flow: Implications to ground water data variability. *Ground Water*, 38(1):12–19.

Martin-Hayden, J.M., Plummer, M., and Britt, S.L. (2014). Controls of wellbore flow regimes on pump effluent composition. *Groundwater*, 52(1):96–104. doi:10.1111/gwat.12036.

Martin-Hayden, J.M. and Wolfe, N. (2000). A novel view of wellbore flow and partial mixing: digital image analysis. *Ground Water Monitoring & Remediation*, 20(4):96–103. doi:10.1111/j.1745-6592.2000.tb00294.x.

Massmann, G., Simmons, C., Love, A., Ward, J., and James-Smith, J. (2006). On variable density surface water-groundwater interaction: A theoretical analysis of mixed convection in a stably-stratified fresh surface water - saline groundwater discharge zone. *Journal of Hydrology*, 329(3-4):390–402. doi:10.1016/j.jhydrol.2006.02.024.

Maurice, L., Barker, J.A., Atkinson, T.C., Williams, A.T., and Smart, P.L. (2011). A tracer methodology for identifying ambient flows in boreholes. *Ground Water*, 49(2):227–238. doi:10.1111/j.1745-6584.2010.00708.x.

Mayo, A.L. (2010). Ambient well-bore mixing, aquifer cross-contamination, pumping stress, and water quality from long-screened wells: what is sampled and what is not? *Hydrogeology Journal*, 18(4):823–837. doi:10.1007/s10040-009-0568-2.

McCallum, J.L., Cook, P.G., Dogramaci, S., Purtschert, R., Simmons, C.T., and Burk, L. (2017). Identifying modern and historic recharge events from tracer-derived groundwater age distributions. *Water Resources Research*, 53(2):1039–1056. doi:10.1002/2016WR019839.

McCallum, J.L., Cook, P.G., and Simmons, C.T. (2015). Limitations of the use of environmental tracers to infer groundwater age. *Groundwater*, 53(S1):56–70. doi:10.1111/gwat.12237.

McCallum, J.L., Cook, P.G., Simmons, C.T., and Werner, A.D. (2014). Bias of apparent tracer ages in heterogeneous environments. *Groundwater*, 52(2):239–250. doi:10.1111/gwat.12052.

McDonald, J.P. and Smith, R.M. (2009). Concentration profiles in screened wells under static and pumped conditions. *Ground Water Monitoring and Remediation*, 29(2):78–86. doi:10.1111/j.1745-6592.2009.01232.x.

McIlvride, W.A. and Rector, B.M. (1988). Comparison of short- and long-screen monitoring wells in alluvial sediments. In *Proceedings of the Second National Outdoor Action Conference on Aquifer Restoration, Ground Water Monitoring and Geophysical Methods*, pages 375–390. Las Vegas, Nevada.

McMillan, L.A., Rivett, M.O., Tellam, J.H., Dumble, P., and Sharp, H. (2014). Influence of vertical flows in wells on groundwater sampling. *Journal of Contaminant Hydrology*, 169:50–61. doi:10.1016/j.jconhyd.2014.05.005.

Molz, F.J., Boman, G.K., Young, S.C., and Waldrop, W.R. (1994). Borehole flowmeters: field application and data analysis. *Journal of Hydrology*, 163(3-4):347–371. doi:10.1016/0022-1694(94)90148-1.

Müller, T., Osenbrück, K., Strauch, G., Pavetich, S., Al-Mashaikhi, K.S., Herb, C., Merchel, S., Rugel, G., Aeschbach, W., and Sanford, W. (2016). Use of multiple age tracers to estimate groundwater residence times and long-term recharge rates in arid southern Oman. *Applied Geochemistry*, 74:67–83. doi:10.1016/j.apgeochem.2016.08.012.

Neilsen, D.M. and Neilsen, G.L. (2007). *The essential handbook of ground-water sampling*, volume 1. CRC Press, Taylor & Francis Group, Boca Raton, Florida. doi:10.1017/CBO9781107415324.004.

Newhouse, M.W., Izbicki, J.A., and Smith, G.A. (2005). Comparison of velocity-log data collected using impeller and electromagnetic flowmeters. *Ground Water*, 43(3):434–438. doi:10.1111/j.1745-6584.2005.0030.x.

Nield, D.A. and Bejan, A. (2017). *Convection in porous media*. Springer International Publishing AG, Cham, Switzerland, 5th edition. ISBN 9783319495613.

Nilsson, B., Jakobsen, R., and Andersent, L.J. (1995a). Development and testing of active groundwater samplers. *Journal of Hydrology*, 171:223–238. doi:10.1016/0022-1694(94)06011-S.

Nilsson, B., Luckner, L., and Schirmer, M. (1995b). Field trials of active and multiport sock samplers in gravel-packed wells. *Journal of Hydrology*, 171(3-4):259–289. doi:10.1016/0022-1694(94)06013-U.

O'Leary, D.R., Izbicki, J.A., and Metzger, L.F. (2015). Sources of high-chloride water and managed aquifer recharge in an alluvial aquifer in California, USA. *Hydrogeology Journal*, 23(7):1515–1533. doi:10.1007/s10040-015-1277-7.

O'Leary, D.R., Izbicki, J.A., Moran, J.E., Meeth, T., Nakagawa, B., Metzger, L., Bonds, C., and Singleton, M.J. (2012). Movement of water infiltrated from a recharge basin to wells. *Ground Water*, 50(2):242–255. doi:10.1111/j.1745-6584.2011.00838.x.

Paillet, F. (2012). A mass-balance code for the quantitative interpretation of fluid column profiles in ground-water studies. *Computers and Geosciences*, 45:221–228. doi:10.1016/j.cageo.2011.11.016.

Paillet, F.L. (1993). Using borehole geophysics and cross-borehole flow testing to define hydraulic connections between fracture zones in bedrock aquifers. *Journal of Applied Geophysics*, 30(4):261–279. ISSN 09269851. doi:10.1016/0926-9851(93)90036-X.

Paillet, F.L. (1998). Flow modeling and permeability estimation using borehole flow logs in heterogeneous fractured formations. *Water Resources Research*, 34(5):997. doi:10.1029/98WR00268.

Paillet, F.L. (2000). A field technique for estimating aquifer parameters using flow log data. *Ground Water*, 38(4):510–521. doi:10.1111/j.1745-6584.2000.tb00243.x.

Paillet, F.L. (2001). Hydraulic head applications of flow logs in the study of heterogeneous aquifers. *Ground Water*, 39(5):667–675. doi:10.1111/j.1745-6584.2001.tb02356.x.

Paillet, F.L. (2004a). Borehole flowmeter applications in irregular and large-diameter boreholes. *Journal of Applied Geophysics*, 55(1-2):39–59. doi:10.1016/j.jappgeo.2003.06.004.

Paillet, F.L. (2004b). Discussion of "Elçi et al (2001), Implications of observed and simulated ambient flow in monitoring wells, Ground Water 39(6), 853–862". *Ground Water*, 42:137–138. doi:doi:10.1111/j.1745-6584.2004.tb02461.x.

Paillet, F.L. and Crowder, R.E. (1996). A generalized approach for the interpretation of geophysical well logs in ground-water studies—theory and application. *Ground Water*, 34(5):883–898. doi:10.1111/j.1745-6584.1996.tb02083.x.

Paillet, F.L. and Pedler, W. (1996). Integrated borehole logging methods for wellhead protection applications. *Engineering Geology*, 42(2-3):155–165. doi:10.1016/0013-7952(95)00077-1.

Paillet, F.L. and Reese, R.S. (2000). Integrating borehole logs and aquifer tests in aquifer characterization. *Ground Water*, 38(5):713–725. doi:10.1111/j.1745-6584.2000.tb02707.x.

Paillet, F.L. and Thomas, D. (1996). Hydrogeology of the Hawaii Scientific Drilling Project borehole KP-1: 1. Hydraulic conditions adjacent to the well bore. *Journal of Geophysical Research: Solid Earth*, 101(B5):11675–11682. doi:10.1029/95jb03445.

Paillet, F.L., Williams, J.H., Urik, J., Lukes, J., Kobr, M., and Mares, S. (2012). Cross-borehole flow analysis to characterize fracture connections in the Melechov Granite, Bohemian-Moravian Highland, Czech Republic. *Hydrogeology Journal*, 20(1):143–154. ISSN 14350157. doi:10.1007/s10040-011-0787-1.

Pitrak, M., Mares, S., and Kobr, M. (2007). A simple borehole dilution technique in measuring horizontal ground water flow. *Ground Water*, 45(1):89–92. doi:10.1111/j.1745-6584.2006.00258.x.

Pizzi, N.G. (2009). *Principles and practices of water supply operations: Water Treatment*. American Water Works Association, Denver, Colorado, 4th edition. ISBN 1583217770.

Poulsen, D.L., Cook, P.G., Simmons, C.T., McCallum, J.L., and Dogramaci, S. (2018). Effects of Intraborehole Flow on Purging and Sampling Long-Screened or Open Wells. *Groundwater*, 57(2):269–278. doi:10.1111/gwat.12797.

Poulsen, D.L., Cook, P.G., Simmons, C.T., McCallum, J.M., Noorduijn, S.L., and Dogramaci, S. (2019). A constant rate salt tracer injection method to quantify pumped flows in long-screened or open borehole wells. *Journal of Hydrology*, 574:408–420. doi:10.1016/j.jhydrol.2019.04.051.

Quinn, P., Cherry, J.A., and Parker, B.L. (2012). Hydraulic testing using a versatile straddle packer system for improved transmissivity estimation in fractured-rock boreholes. *Hydrogeology Journal*, 20(8):1529–1547. doi:10.1007/s10040-012-0893-8.

Quinn, P., Parker, B.L., and Cherry, J.A. (2015). Blended head analyses to reduce uncertainty in packer testing in fractured-rock boreholes. *Hydrogeology Journal*, 24(1):59–77. doi:10.1007/s10040-015-1326-2.

Read, T., Bour, O., Selker, J.S., Bense, V.F., Le Borgne, T., Hochreutener, R., and Lavenant, N. (2014). Active-distributed temperature sensing to continuously quantify vertical flow in boreholes. *Water Resources Research*, 50(5):3706–3713. doi:10.1002/2014WR015273.

Reilly, T.E., Franke, O.L., and Bennett, G.D. (1989). Bias in groundwater samples caused by wellbore flow. *Journal of Hydraulic Engineering*, 115(2):270–276. doi:10.1061/(ASCE)0733-9429(1989)115:2(270).

Reilly, T.E. and LeBlanc, D. (1998). Experimental evaluation of factors affecting temporal variability of water samples obtained from long-screened wells. *Ground Water*, 36(4):566–576. doi:10.1111/j.1745-6584.1998.tb02830.x.

Robinson, D.A., Binley, A., Crook, N., Day-Lewis, F.D., Ferré, T.P.A., Grauch, V.J.S., Knight, R., Knoll, M., Lakshmi, V., Miller, R., Nyquist, J., Pellerin, L., Singha, K., and Slater, L. (2008). Advancing process-based watershed hydrological research using near-surface geophysics: a vision for, and review of, electrical and magnetic geophysical methods. *Hydrological Processes*, 22(18):3604–3635. doi:10.1002/hyp.6963.

Rojas, R., Commander, P., McFarlane, D., Ali, R., Dawes, W., Barron, O., Hodgson, G., and Charles, S. (2018). Groundwater resource assessment and conceptualization in the Pilbara Region, Western Australia. *Earth Systems and Environment*. doi:10.1007/s41748-018-0051-0.

Ruud, N.C. and Kabala, Z.J. (1997). Numerical evaluation of the flowmeter test in a layered aquifer with a skin zone. *Journal of Hydrology*, 203(1-4):101–108. ISSN 00221694. doi:10.1016/S0022-1694(97)00091-7.

Ruud, N.C., Kabala, Z.J., and Molz, F.J. (1999). Evaluation of flowmeter-head loss effects in the flowmeter test. *Journal of Hydrology*, 224(1-2):55–63. ISSN 00221694. doi:10.1016/S0022-1694(99)00119-5.

Sawdey, J.R. and Reeve, A.S. (2012). Automated inverse computer modeling of borehole flow data in heterogeneous aquifers. *Computers and Geosciences*, 46:219–228. doi:10.1016/j.cageo.2011.12.010.

Sellwood, S.M., Hart, D.J., and Bahr, J.M. (2015). Evaluating the use of in-well heat tracer tests to measure borehole flow rates. *Groundwater Monitoring and Remediation*, 35(4):85–94. ISSN 17456592. doi:10.1111/gwmr.12134.

Shapiro, A.M. (2002). Cautions and suggestions for geochemical sampling in fractured rock. *Ground Water Monitoring & Remediation*, 22(3):151–164. doi:10.1111/j.1745-6592.2002.tb00764.x.

Silliman, S. and Higgins, D. (1990). An analytical solution for steady-state flow between aquifers through an open well. *Ground Water*, 28(2):184–190. doi:10.1111/j.1745-6584.1990.tb02245.x.

Smith, S.J. (2005). Naturally occurring arsenic in ground water, Norman, Oklahoma, 2004, and remediation options for produced water. Fact Sheet 2005-3111. Technical report, U.S. Geological Survey.

Solomon, D.K. (2000). 4He in groundwater. In P.G. Cook and A.L. Herczeg, editors, *Environmental tracers in subsurface hydrology*, chapter Chapter 14, pages 425–439. Science+Business Media, LLC, New York. doi:10.1007/978-1-4615-4557-6.

Stuiver, M. and Polach, H. (1977). Discussion: reporting of carbon-14 data. *Radiocarbon*, 19(3):355–363. doi:10.1017/S0033822200033154.

Sudicky, E.A. (1989). The Laplace Transform Galerkin Technique for Large-Scale: A Time-Continuous Finite Element Theory and Application to Mass Transport in Groundwater. *Water Resources Research*, 25(8):1833–1846. doi:10.1029/WR025i008p01833.

Sukop, M.C. (2000). Estimation of vertical concentration profiles from existing wells. *Ground Water*, 38(6):836–841. doi:10.1111/j.1745-6584.2000.tb00681.x.

Taylor, K., Wheatcraft, S., Hess, J., Hayworth, J., and Molz, F. (1990). Evaluation of methods for determining the vertical distribution of hydraulic conductivity. *Ground Water*, 28(1):88–98. doi:10.1111/j.1745-6584.1990.tb02232.x.

Tsang, C., Hufschmied, P., and Hale, F.V. (1990). Determination of fracture inflow parameters with a borehole fluid conductivity logging method. *Water Resources Research*, 26(4):561–578. doi:10.1029/WR026i004p00561.

Underwood, S.C., McCallum, J.L., Cook, P.G., Simmons, C.T., Dogramaci, S., Purtschert, R., Siade, A.J., and Prommer, H. (2018). Physical and chemical controls on the simultaneous occurrence of young and old groundwater inferred from multiple age tracers. *Water Resources Research*, 54(11):9514–9532. doi:10.1029/2018WR022800.

van Sommeren, D.D.J.A., Caulfield, C.P., and Woods, A.W. (2013). Advection and buoyancy-induced turbulent mixing in a narrow vertical tank. *Journal of Fluid Mechanics*, 724:450–479. doi:10.1017/jfm.2013.164.

Walsh, D., Turner, P., Grunewald, E., Zhang, H., Butler, J.J., Reboulet, E., Knobbe, S., Christy, T., Lane, J.W., Johnson, C.D., Munday, T., and Fitzpatrick, A. (2013). A small-diameter NMR logging tool for groundwater investigations. *Groundwater*, 51(6):914–926. doi:10.1111/gwat.12024.

Widory, D., Petelet-Giraud, E., Négrel, P., and Ladouche, B. (2005). Tracking the sources of nitrate in groundwater using coupled nitrogen and boron isotopes: a synthesis. *Environmental Science and Technology*, 39(2):539–548. doi:10.1021/es0493897.

Wilson, J.T., Mandell, W.A., Paillet, F.L., Bayless, E.R., Hanson, R.T., Kearl, P.M., Kerfoot, W.B., Newhouse, M.W., and Pedler, W.H. (2001). An evaluation of borehole flowmeters used to measure horizontal ground-water flow in limestones of Indiana, Kentucky, and Tennessee, 1999. Water-Resources Investigations Report 01-4139. Technical report, US Geological Survey.

Young, S.C. and Pearson, H.S. (1995). The electromagnetic borehole flowmeter: description and application. *Groundwater Monitoring & Remediation*, 15(4):138–147. doi:10.1111/j.1745-6592.1995.tb00561.x.

Zheng, C. (2010). MT3DMS v5.3: Supplemental User's Guide. Technical report, Department of Geological Sciences, The University of Alabama, Tuscaloosa, Alabama.

Zheng, C. and Wang, P.P. (1999). MT3DMS: A modular three-dimensional multispecies transport model for simulation of advection, dispersion, and chemical reactions of contaminants in groundwater systems. Strategic Environmental Research and Development Program, Contract Report SERDP-99-1. Technical report, U.S. Army Corps of Engineers, Vicksburg, Mississippi.

Zinn, B.A. and Konikow, L.F. (2007). Effects of intraborehole flow on groundwater age distribution. *Hydrogeology Journal*, 15(4):633–643. doi:10.1007/s10040-006-0139-8.

Zlotnik, V.A. and Zurbuchen, B.R. (2003). Estimation of hydraulic conductivity from borehole flowmeter tests considering head losses. *Journal of Hydrology*, 281(1-2):115–128. doi:10.1016/S0022-1694(03)00204-X.

Appendix A: Conference abstracts

Effects of intraborehole flow on purging and sampling long-screened or open wells

Oral presentation at the Australasian Groundwater Conference
11-13 July 2017, Sydney, Australia

David L. Poulsen[1], Peter G. Cook[1], James L. McCallum[1], Craig T. Simmons[1] and Shawan Dogramaci[2,1]

[1]National Centre for Groundwater Research and Training, Flinders University, Adelaide, Australia
[2]Rio Tinto Iron Ore, Perth, Australia

Wells with long screens or open intervals are common and in some cases they are all that is available to investigate a groundwater system. However, such wells create a shortcut for vertical flow of water, driven by hydraulic head gradients. In a recharge area, water moves vertically down through the borehole and, over time, a plume of 'contaminating' water develops in zones with lower head. When the well is pumped, yield from zones with lower head will actually be water originating from zones with higher head. This process requires special consideration if groundwater samples are to be accurately interpreted. This modelling study investigates mixtures of groundwater sampled from a long-screened well and the time needed to purge a plume of intraborehole flow as a function of preceding un-pumped duration. An unconfined regional groundwater system (dimensions of 3000 x 77 x 75 m) was simulated using MODFLOW, with recharge applied across the surface and discharge via a constant head boundary on one side. A long-screened well was represented using the Multi-Node Well Package (MNW2) and water was traced by simulating groundwater age in MT3DMS. Un-pumped and pumped stress periods were applied in uniform, layered and heterogeneous systems. Results show that the volume of intraborehole flow can exceed the common practice of purging three casing volumes, even under small vertical head gradients and short times. Pumping a well draws water from all permeable zones in the screened interval so, unless packers are used to target specific intraborehole flow receiving zones, total pumped volume must greatly exceed the volume of intraborehole flow if it is to be fully removed. Complete purging may not be feasible, so identifying which depths a sample actually represents avoids misleading interpretations and provides representative data for at least some depths in a wells screened interval.

The importance of measuring flows in long-screened or open wells

Oral presentation at the Australian Geological Council Convention
14-18 October 2018, Adelaide, Australia

David L. Poulsen[1], Peter G. Cook[1], James L. McCallum[1], Saskia Noorduijn[1], Craig T. Simmons[1] and Shawan Dogramaci[3,1]

[1]National Centre for Groundwater Research and Training, Flinders University, Adelaide, Australia
[2]School of Earth Sciences, University of Western Australia, Australia [3]Rio Tinto Iron Ore, Perth, Australia

Effective groundwater management depends on understanding heterogeneity at a relevant scale both vertically and spatially in an aquifer system. Studies usually rely on data from wells, which are expensive to install, so use of available infrastructure is the economical approach. Despite potential complications, long-screened or open wells can provide valuable data and insight, if used correctly. Quantifying the in-well flow regime is essential. In un-pumped conditions, a flow profile shows the producing and receiving zones of vertical flow, the relative vertical head gradient in the aquifer system, and potential bias in water chemistry samples. A flow profile while pumping can be used to quantify aquifer heterogeneity and the sampled water mixture. This presentation describes a new tracer dilution method to determine the pumped flow regime in a well that can be used instead of, or complementary to, a wireline borehole flowmeter. A steady-state EC tracer dilution profile is established under constant injection and pumping. A 1D solution of the advection-dispersion equation for solute transport is fitted to the data by visually identifying producing zones and assigning a fraction of yield to each zone. This test is distinct from transient "moving front" tracer dilution methods because there is no concern about the rate of fluid column wash-out, the analysis is independent of time and the effect of dispersion is minimised. Like the borehole flowmeter, the method is particularly suited to high yield long-screened wells, where other methods such as packers or liners are not effective.

Making the most of long-screened wells in groundwater investigations

Oral presentation at the NZ Hydrological Society & Meteorological Society of NZ Joint Conference
4-7 December 2018, Christchurch, New Zealand

David L. Poulsen[1], Peter G. Cook[1], Craig T. Simmons[1], James L. McCallum[1], Saskia Noorduijn[1], and Shawan Dogramaci[3,1]

[1]National Centre for Groundwater Research and Training, Flinders University, Adelaide, Australia
[2]School of Earth Sciences, University of Western Australia, Perth, Australia
[3]Rio Tinto Iron Ore, Perth, Australia

Introduction

Effective groundwater management depends on understanding aquifer characteristics, flow dynamics and water quality at a representative scale. Wells are expensive to install, so the economical approach is to use available infrastructure where possible. However, wells installed for other purposes (e.g. water production) often have much longer screened or open intervals than wells designed for collecting scientific data. This means that, with traditional methods, key data – like hydraulic properties, water level and water quality – are averaged over an unhelpfully large interval of the aquifer system. So, such wells tend to be underused or even misused in groundwater investigations. The aim of this talk is to show that, with a little extra work and appropriate methods of measurement and analysis, long-screened wells can in fact provide valuable scientific data and insight for groundwater investigations. In particular, it is possible to determine the intersected hydraulic conductivity and head distribution and obtain native groundwater samples from discrete zones.

Method

This talk draws on knowledge developed for a study that used environmental tracers to examine groundwater recharge processes and residences time in the complex geological setting of the Pilbara region of Western Australia. In this study we: (1) numerically modelled the effects of intraborehole flow on purging and sampling long-screened or open wells (Poulsen et al. 2018); (2) measured the in-well flow regime in ambient and pumped conditions with a borehole electromagnetic (EM) flowmeter; (3) developed and tested a new constant-rate tracer dilution method to determine the in-well flow regime in pumped conditions (Poulsen et al. in prep.); (4) developed a depth-specific sampling strategy, exploiting the ambient and pumped in-well flow regimes to target discrete zones that produce native groundwater (Poulsen et al. in prep.); and (5) sampled environmental tracers from long-screened wells and a multi-depth nest of piezometers to investigate groundwater residence times.

Results

The wells used in this work had been un-pumped for several years, so the intraborehole flow plumes were large and it was more practical to avoid sampling them, rather than attempt purging. While pumping, the in-well flow profiles measured with the EM flowmeter clearly showed the main inflow zones, and the proportion from each zone. We produced very similar flow profiles with the new constant-rate tracer dilution method. This involved constantly injecting a tracer at one end of the screen while constantly pumping from the other end. The tracer was drawn towards

the pump and diluted in proportion to each inflow. Tracer concentration profiles were collected at regular intervals, and at steady-state they were translated into flows by applying a solute mass balance model. Significant vertical heterogeneity was observed, with the majority of yield sourced from sub-intervals within the wells. Two had strong ambient flows (6-7 L/min) that could be sampled simply by placing the low-rate (0.5 L/min) sampling pump in the higher head zone. Purging was unnecessary because native groundwater was constantly flowing through the well. One well had weak upward ambient flow (<1 L/min), which was enhanced by pumping. Another had negligible ambient flow, so it would produce native groundwater after a modest purge. Preliminary results of sampling show no clear stratification of basic water chemistry, some significant differences of Radon, while Carbon-14 indicates consistently old (10-14k years) groundwater at all depths. CFC and Helium samples are being analysed at GNS Science Water Dating Lab and University of Utah respectively (at the time of writing).

References

Poulsen, D.L., Cook, P.G., Simmons, C.T., McCallum, J.L., Dogramaci, S., 2018. Effects of intraborehole flow on purging and sampling long-screened or open wells. Groundwater. doi: 10.1111/gwat.12797

Appendix B: Data

Data generated as part of this PhD research are included on the DVD inserted at the back of this thesis. This includes data that were analysed in Chapters 2, 3 and 4, and additional data that were not included in the thesis. The Python code developed for analysis of the pumped tracer dilution test (Chapter 3) is also provided, together with the tracer profiles from one well as an example.

These data are provided for anyone who may have a use for it in the future.

The files included on the DVD are summarised in the table and figure below.

Folder name	**Description of contents/data**
Borehole camera	This folder contains borehole video files from each of the long-screened wells in the Pilbara (LHRP4, WB11AH001 and WB11HD6001) and the open borehole well in the Adelaide Hills (6628-21204) used in this work.
Borehole flowmeter	This folder contains the borehole flowmeter data files from each of the wells used in this work (raw data in sub-folders, processed data in Excel files). Data from the long-screened wells in the Pilbara (LHRP4, WB11AH001 and WB11HD6001) was acquired by Rio Tinto's wireline service provider Kinetic. Data from the open borehole well at Balhannah in the Adelaide Hills (6628-21204) was provided by the South Australian Department of Environment and Water (formerly Dept. of Water Land and Biodiversity Conservation).

Folder name	**Description of contents/data**
Chemistry	This folder contains all chemical analyses completed on depth-specific samples from the long-screened wells in the Pilbara as part of this project, obtained in April 2018, as described in Chapter 4. The Excel file provides a summary of the data, including well details and sampling details. The sample ID indicates the well name, whether the sample was taken from an ambient flow regime (e.g. `LHRP4_amb_70m`) or pumped flow regime (e.g. `LHRP4_pum_70m`) and the depth of the sample intake in the well. The data are in sub-folders, with the folder name indicating the laboratory name and the analysis type (major ion chemistry, radon, CFC's and 14C, and noble gases). Sampling protocols are also included. The spreadsheet used for the depth-resolved analysis of aquifer concentrations presented in Table 4.2 is included (`DSS_analysis_190531.xlsx`) to show the procedure used to apply the mass balance with a Monte Carlo approach. For clarity, these samples are in addition to an earlier sampling campaign (May-June 2016), detailed in the fieldwork report included on the DVD (`Pilbara_fieldwork_report_160720.pdf`), but those data are not included here.
HD1 dilution test	This folder contains all field data from a salt dilution test that was done in a disused dewatering well 32.5 m from an active dewatering well at the Hope Downs 1 mine site on 27 May 2016. The test was not analysed as part of this PhD, so the data and details are provided for possible future analysis by anyone who feels so inclined. The concept was that transport and dilution of the salt tracer in the well, measured by EC profiles, should indicate the flow regime in the well, which was probably a combination of vertical and horizontal components, given the proximity to the dewatering well pumping at 75.5 L/s. The test is described more fully in the fieldwork report included on the DVD (`Pilbara_fieldwork_report_160720.pdf`).
Multi-piezo nest	This folder contains all chemical analyses completed on samples from the five piezometers adjacent to well LHRP4 in the Pilbara as part of this project. The field trip also included sampling four wells at West Angelas, so the files include those results but they are unrelated to this work. The Excel files provide a summary of the data, including well details and sampling details. The sample ID indicates the piezometer name. The data are in sub-folders, with the folder name indicating the laboratory name and the analysis type (major ion chemistry, CFC's, SF6 and 14C, and noble gases). Sampling protocols are also included. In addition, the Flinders University gas-stripper was used to fill cylinders for analysis of Kr85/Ar39 at the University of Bern, Switzerland, but these data were not used in this work, and are not included.

Folder name	**Description of contents/data**
Pumped tracer test	This folder includes Excel files containing the data derived from the pumped tracer dilution tests on two wells in the Pilbara (LHRP4 and WB11AH001) and one well in the Adelaide Hills (6628-21204), as described in Chapter 3. This includes all tracer profiles, tracer concentrations in pumped discharge, and pumping/injection rates.
Model	A sub-folder called "Model" contains the Python code and associated files for the one dimensional finite element model developed for the pumped tracer dilution test (Chapter 3). Jim McCallum developed the tracer dilution model to simulate borehole flow (`BHFM_class_180302.py`), which includes the De Hoog algorithm for the Laplace transform (`DeHoog.py`). Saskia Noorduijn developed the graphical user interface (`guiV8.py`), in discussion with me (David Poulsen). I have not removed the versioning of files lest I delete something important. The example data text files that were used for testing are also included to enable the script to run and produce an output. There is no user manual for the GUI yet, but it can be launched by running the Python script. It should be fairly intuitive to fill in the test details, load tracer profiles and specify the inflow zones visually identified in the tracer profiles. The model is manually optimised by fitting to the measured profiles taken during transient and/or steady state conditions, by changing for each inflow zone: top and bottom depth, fraction of total discharge and background tracer concentration. Tracer transport parameters (dispersion and diffusion) are also specified/fitted. In its current form the model is only designed for monotonically increasing pumped flow in a well (i.e. there can be no outflows back to the aquifer). There are still a few known bugs and probably unknown bugs too. Good luck!
	`Pilbara_fieldwork_report_160720.pdf` - This report summarises a two week field campaign completed for the Rio Tinto ARC Linkage project – of which this PhD was a part – in the Koodaideri and Hope Downs areas of the Pilbara, Western Australia. Data from disused supply wells in the Hope Downs (LHRP4) and Rhodes Ridge (WB11AH001 and WB11HD6001) areas were used in this PhD work. This report also describes the HD1 dilution test, as indicated above, which is also included on this data DVD.

Overview of DVD contents